

University of Mississippi

eGrove

---

Electronic Theses and Dissertations

Graduate School

---

1-1-2021

## Responses of Myxobacteria to Plant-Related Chemosignals Suggests Their Roles in the Rhizobiome

Barbara Iyare Adaikpoh  
*University of Mississippi*

Follow this and additional works at: <https://egrove.olemiss.edu/etd>



Part of the [Pharmacy and Pharmaceutical Sciences Commons](#)

---

### Recommended Citation

Adaikpoh, Barbara Iyare, "Responses of Myxobacteria to Plant-Related Chemosignals Suggests Their Roles in the Rhizobiome" (2021). *Electronic Theses and Dissertations*. 1979.  
<https://egrove.olemiss.edu/etd/1979>

This Dissertation is brought to you for free and open access by the Graduate School at eGrove. It has been accepted for inclusion in Electronic Theses and Dissertations by an authorized administrator of eGrove. For more information, please contact [egrove@olemiss.edu](mailto:egrove@olemiss.edu).

RESPONSES OF MYXOBACTERIA TO PLANT-RELATED CHEMOSIGNALS  
SUGGEST THEIR ROLES IN THE RHIZOBIOME

A Dissertation  
presented in partial fulfilment of requirements  
for the degree of Doctor of Philosophy  
in the Department of BioMolecular Sciences  
Division of Pharmacognosy  
The University of Mississippi

by

Barbara Iyare Adaikpoh

May 2021

Copyright Barbara I. Adaikpoh 2021

ALL RIGHTS RESERVED

## ABSTRACT

In the rhizosphere, plants curate and maintain distinct rhizobiome, some of which serve as secondary defense mechanisms against pathogenic microorganisms. Additionally, in response to biotic stress, plants generate phytohormones which regulate signaling pathways to activate systemic resistance. These phytohormones contribute to the chemical space within the rhizosphere in addition to other low-molecular-weight metabolites used for cell-to-cell communication within species and across kingdoms. However, little is known about the influences of stress-related phytohormones on beneficial bacteria even though biocontrol strategies abundantly explore plant-beneficial microorganisms to manage pathogens in agricultural systems. Myxobacteria are competent predators of plant pathogens and have demonstrated responses when exposed to exogenous quorum signals produced by prey bacteria. Our objective was to study the impacts of exogenous phytohormones and plant-related signals on myxobacterial motility, global transcriptome, and metabolism to reveal the potential roles of these bacteria in the rhizosphere. The plant-associated myxobacterium *Archangium* sp. strain Cb G35 exhibited a  $p < 0.05$  increase in motility on exposure to methyljasmonate (MeJA), salicylic acid (SA), and abscisic acid (ABA) while transcriptomic studies revealed a  $\geq$  four-fold change ( $p < 0.05$ ) in the transcription for 56 genes in response to MeJA exposure. Untargeted analysis of LC-MS/MS datasets of crude extracts from exposure experiments with Global Natural Products Social Molecular Networking (GNPS) and XCMS-MRM tools further highlighted the activation and deactivation of specialized metabolites in response to these signals. Antibacterial assays of fractions from active extracts against *E. coli* revealed active metabolites of the terpene, fatty acid, and polyketide molecular families. However, before our investigations, only the

bioactive roimantacene polyene, and *p*-hydroxyacetophenone amides have been associated with *A. sp.* While we have demonstrated the potential of observing signal-activated production of functional metabolites in the rhizosphere, our studies provide the condition-specific potential for discovering novel specialized metabolites that would contribute to natural product discovery.

## DEDICATION

This dissertation is dedicated to my dear parents, Prof. Edwin O. Adaikpoh and Prof. Mrs. Martina A. Adaikpoh, for the enormous inspiration and support I get, towards achieving my dreams. And to my siblings, Ogeonye and Sapphire, for their words of encouragement.

I dedicate this work to all my past and present teachers, advisors, friends, and family. They immensely contributed to my motivation and growth in this career path.

Finally, and most importantly, I dedicate this dissertation to God, the almighty, thankful for a healthy mind and body to complete this degree.

## LIST OF ABBREVIATIONS

ABA	Abscisic acid
ABC	ATP-binding cassette
AHL	<i>N</i> -Acylhomoserine lactone
ANOVA	Analysis of variance
antiSMASH	antibiotics & Secondary Metabolite Analysis Shell
ARTS	Antibiotic Resistant Target Seeker
AUX	Auxin
BGCs	Biosynthetic gene clusters
CAZymes	Carbohydrate active enzymes
CHAP	Cysteine, histidine-dependent amidohydrolases/peptidases
DUF	Domain of unknown function
DMSO	Dimethylsulfoxide
DSF	Diffusible signal factor
ET	Ethylene
EtOAc	Ethyl Acetate
FAD	Flavin adenine dinucleotide
GA	Giberellic acid

GNPS	Global Natural Products Social Molecular Networking
HET	4-methyl-5-( $\beta$ -hydroxyethyl) thiazole
HMP	4-amino-5-hydroxymethyl-2-methylpyrimidine
HMP-PP	4-amino-5-hydroxymethyl-2-methylpyrimidine pyrophosphate
HPLC	High performance liquid chromatography
HSL	Homoserine lactone
I-3-PA	Indole-3-propanoic acid
JA	Jasmonic acid
JA-Ile	Jasmonic acid-Isoleucine
LB	Luria-Bertani
LC-MS/MS	Liquid chromatography with tandem mass spectrometry
LCO	Lipo-chitinoligosaccharides
LIIC	Linoleic acid
LINN	Linolenic acid
LP	Lipopolysaccharide
MeJA	Methyljasmonate
MeOH	Methanol
MG	Methylglyoxal



MIBiG	Minimum information about a biosynthetic gene cluster
NAP	Network Annotation Propagation
NRPS	Nonribosomal peptide synthases
OD	Optical density
OMV	Outer membrane vesicles
PKS	Polyketide synthases
QS	Quorum signals
RiPPs	Ribosomally synthesized and post-translationally modified peptides
SA	Salicylic acid
t-11-DA	11-methyl-2 <i>E</i> -dodecenoic acid
TMP	Thiamine monophosphate
TOMM	Thiazole/oxazole modified microcin
XCMS-MRM	Various forms (X) of chromatography mass spectrometry-Multiple Reaction Monitoring

## ACKNOWLEDGEMENT

I would like to express my sincere gratitude to my Ph.D. advisor, Dr. D. Cole Stevens, for his support in facilitating my learning to be a better scientist, developing my research skills, and achieving this degree.

The assistance and support of my labmates Shukria Akbar, Hanan Albataineh, and Andrew Ahearne have been wonderful and greatly appreciated. I would also like to acknowledge Dr. Sandeep Misra for all his help with mass spectrometric analysis.

My deepest gratitude to my committee members: Dr. Dale C. Nagle, Dr. Sudeshna Roy, and Dr. Erik Hom for their constructive criticisms and feedbacks that enhanced my performance and critical thinking skills.

Dr. Nicole Ashpole and Dr. Robert J. Doerksen offered me great counsel when I needed help moving forward in my career choice; I appreciate them. I also appreciate Dr. Noa Valcarcel's contributions in improving my teaching skills. My appreciation goes to the administrative staff, Ms. Sherrie Gussow, Ms. Danielle Noonan, and Ms. Candace G. Lowstuter, for their assistance with departmental-related issues and paperwork.

The research is supported by grant number R15AI37996 from the National Institute of Allergy and Infectious Diseases (NIAID), part of the National Institute of Health (NIH).

Finally, I would like to acknowledge all the friends turned family that I met at the University of Mississippi, AyoOluwa Aderibigbe, Kola Adenekan, Evi Addoh, Angela Fasuyi, Elsie Udejaja, Amna Adam, and other friends too many to mention. Each of them made life in Oxford, MS, beautiful in many ways.

## TABLE OF CONTENTS

ABSTRACT.....	ii
DEDICATION.....	iv
LIST OF ABBREVIATIONS.....	v
ACKNOWLEDGEMENT.....	viii
LIST OF TABLES.....	xiii
LIST OF FIGURES.....	xiv
CHAPTER 1. INTRODUCTION.....	1
1.1 The Myxococcales (Myxobacteria).....	1
1.2 Plants and their Rhizobiome.....	3
1.2.1 Phytohormones and Root Exudates.....	5
1.2.2 Bacterial Chemotaxis Triggered by Plant Exudates and Phytohormones.....	7
1.2.3 Bacterial Enzymes and Transporters Involved in Plant-Microbe Interactions.....	9
1.2.4 Phytopathogenic Responses to Plant Exudates that Promotes Virulence.....	13
1.2.5 How Beneficial Bacteria Interact with Phytopathogens.....	19
1.2.5.1 Interference of Microbial Signaling Mechanisms.....	19
1.2.5.2 Specialized Metabolites that are Beneficial in the Rhizosphere.....	20
1.2.5.3 Microbial Predation.....	24
1.3 Myxobacteria and the Rhizobiome Structure.....	26
1.4 Significance of Study.....	27
CHAPTER 2. PROFILING THE BIOSYNTHETIC CAPACITY OF <i>ARCHANGIUM</i> SP. STRAIN CB G35.....	29
2.1 Aims.....	29
2.2 Draft Genome Sequence of <i>Archangium</i> sp. strain Cb G35.....	30
2.2.1 Abstract.....	31
2.2.2 Introduction.....	31
2.2.3 Materials and Methods.....	31
2.2.4 Results and Discussion.....	32

2.3 Analysis of the Metabolic Capacity of <i>Archangium</i> sp. strain Cb G35 .....	33
2.3.1 Abstract.....	33
2.3.2 Introduction .....	33
2.3.3 Materials and Methods .....	34
2.3.3.1 Medias and Strains.....	34
2.3.3.2 Analysis with antiSMASH and Antibiotics Resistance Target seeker (ARTS).....	35
2.3.4 Results and Discussion .....	35
2.4 Conclusions .....	39
<b>CHAPTER 3. ASSESSING RESPONSES OF ARCHANGIUM SP. STRAIN CB G35 TO</b>	
<b>PHYTOHORMONES AND PLANT-RELATED SIGNALS .....</b>	<b>40</b>
3.1 Aims .....	40
3.2 Myxobacterial Response to Methyljasmonate Exposure Indicates Contribution to Plant Recruitment of Micropredators .....	42
3.2.1 Abstract.....	43
3.2.2 Introduction .....	44
3.2.3 Materials and Methods .....	45
3.2.3.1 Medias and Strains.....	45
3.2.3.2 MeJA Exposure Experiments .....	46
3.2.3.3 Metabolite Extraction and Analysis.....	46
3.2.3.4 GNPS, NAP, and XCMS-MRM Analysis .....	47
3.2.3.5 Motility Assays .....	47
3.2.3.6 RNaseq Analysis.....	48
3.2.4 Results .....	49
3.2.4.1 MeJA Exposure Impacts Myxobacterial Metabolism.....	49
3.2.4.2 MeJA Exposure Influences <i>A. sp.</i> Motility .....	51
3.3 Selective Responses of <i>Archangium</i> sp. Cb G35 to Phytohormones and Plant-Related Signals .....	61
3.3.1 Abstract.....	61
3.3.2 Introduction .....	62
3.3.3 Materials and Methods .....	63
3.3.3.1 Medias and Strains.....	63

3.3.3.2	Phytohormones and plant-related signals .....	63
3.3.3.3	Motility Assays .....	64
3.3.3.4	Exposure to Signals, Metabolite Extraction and Analysis.....	64
3.3.3.5	GNPS, Cytoscape and XCMS-MRM Analysis .....	65
3.3.4	Results .....	66
3.3.4.1	Exposures to SA, ABA and DSF Differentially Influences <i>A. sp.</i> Motility .....	66
3.3.5	Discussion.....	72
3.4	Conclusion.....	74
CHAPTER 4. EVALUATING THE IMPACTS OF PHYTOHORMONES AND PLANT-RELATED SIGNALS EXPOSURE ON ANTIBACTERIAL PRODUCTION BY <i>ARCHANGIUM SP.</i> STRAIN CB G35 CULTURES.....		
4.1	Aims .....	75
4.2	Abstract.....	76
4.3	Introduction .....	76
4.4	Materials and Methods .....	78
4.4.1	Medias and Strains.....	78
4.4.2	Phytohormones and plant-related signals .....	78
4.4.3	Exposure to Phytohormones and Plant-Related Signals Experiments .....	78
4.4.4	Metabolite Extraction, Antibacterial testing and Fractionation.....	79
4.4.5	GNPS, Cytoscape and Analysis.....	80
4.5	Results .....	81
4.6	Discussion .....	84
4.7	Conclusion.....	87
CHAPTER 5. FUTURE DIRECTIONS .....		
LIST OF REFERENCES .....		
LIST OF APPENDICES.....		
Appendix A.	Antibiotic resistant target seeker (ARTS) rendered analysis of <i>Archangium sp.</i> genome.....	115

Appendix B. Links to Global Natural Products Social Molecular Networking (GNPS) jobs .....	124
Appendix C. Antimicrobial assays .....	125
VITA.....	126

## LIST OF TABLES

Table 1.1: Roles of defense-related phytohormones and how they are exploited by phytopathogens during invasion of plant hosts.....	14
Table 2.1. Summary of identified biosynthetic gene clusters (BGCs) and other potential targets from the analysis of the genome of <i>A. sp. Cb G35</i> .....	36
Table 2.2. Proximity hits of resistance markers to biosynthetic gene clusters from ARTS analysis.....	38
Table 2.3. Sensitivity testing of <i>A. sp.</i> strain <i>Cb G35</i> to antibiotics. - (negative) - sensitive, + (positive) - resistant, SG (slight growth).....	38
Table 3.1. Associated gene products and fold change for genes with increased transcription during MeJA exposure conditions <sup>a</sup> .....	54
Table 3.2. Associated gene products and fold change for genes with decreased transcription during MeJA exposure conditions <sup>a</sup> .....	55
Table A.1. Hits to fifty-three known resistance models (targets) observed in the <i>A. sp.</i> genome.....	115
Table A.2. Twenty-two biosynthetic gene clusters with proximity to housekeeping (core) genes, duplicated genes and resistant models. ....	118
Table A.3. Thirty-six housekeeping (core) genes observed to be duplicated.....	122

## LIST OF FIGURES

Figure 1.1. The order of Myxococcales with suborders and families (as of March 2021). Blue outline represents known saprophytic nutritional behaviour and red outline represents known predatory nutritional behaviour.....	2
Figure 1.2. Representative antimicrobials identified from myxobacteria.....	4
Figure 1.3. Phytohormones involved in plant defense mechanisms .....	6
Figure 1.4. Venn diagram of lytic enzymes from beneficial bacteria and selective effects on either plant or fungi based on the cell wall components.....	11
Figure 1.5. Examples of polyketides from phytopathogenic bacteria .....	16
Figure 1.6. Examples of peptides from phytopathogenic bacteria.....	18
Figure 1.7. Examples of other structural classes of phytotoxins .....	19
Figure 1.8. <i>Bacillus</i> species derived antimicrobials.....	23
Figure 1.9. Examples of antimicrobials from rhizospheric <i>Pseudomonads</i> .....	25
Figure 1.10. Examples of antimicrobials from plant-beneficial <i>Burkholderia</i> .....	25
Figure 2.1. antiSMASH v6.0 predicted biosynthetic gene clusters from the genome of <i>Archangium</i> sp. strain Cb G35. The number of identified BGCs is indicated.....	36
Figure 2.2. ARTS rendered hits to known resistance models and targets grouped according to the mechanism of resistance. Complete lists of models and targets are available in Table A.1, Appendix.....	37
Figure 3.1. MeJA-impacted features provided by XCMS analysis of LC-MS/MS data after filtering feature tables for those with a $\geq$ five-fold change and $p \leq 0.05$ with (A) depicting increased metabolites and (B) depicting decreased metabolites .....	51



Figure 3.2. (A) Molecular network of MeJA and associated metabolites including nodes labeled with detected parent ions and edges labeled with cosine values. Predicted metabolites provided by NAP analysis of the GNPS-rendered cluster. \*Multiple fatty acids and prenol lipids with identical exact masses predicted by NAP analysis. (B) Metabolites identified by GNPS analysis (cosine > 0.8) impacted by MeJA exposure.....52

Figure 3.3. Motility assays depicting cumulative change in swarm diameter post MeJA exposure. The symbol “\*” indicates  $p < 0.05$ . .....53

Figure 3.4. (A) Fold change data observed from *A. sp.* MeJA exposure experiments with increased transcription indicated with red and positive fold change values and decreased transcription indicated with blue and negative fold change values. Data represented for all genes with  $\geq$  four-fold change ( $p < 0.05$ ;  $n = 3$  per condition). (B) General categories and classes associated with *A. sp.* genes with observed  $\geq$  four-fold increases in transcription during MeJA exposure. (C) General categories associated with *A. sp.* genes with observed  $\geq$  four-fold decreases in transcription during MeJA exposure. ....56

Figure 3.5. Motility assays showing cumulative change in swarm diameters after exposure to (A) phytohormones and (B) plant-related signals. “\*” indicates  $p < 0.05$ . DMSO = no signal control, ABA = abscisic acid, GA = gibberellic acid, LIIC = linoleic acid, LINN = linolenic acid, MG = methylglyoxal, SA = salicylic acid, I-3-PA = indole-3-propionic acid, JA-Ile = jasmonic acid-isoleucine and t-11-DA = 11-methyl-2E-dodecenoic acid.....67

Figure 3.6. Signal-impacted features reported from XCMS analysis of LC-MS/MS datasets showing decreased and increased features compared to the no-exposure control. Feature tables were filtered to provide those with a  $\geq$  five-fold change and  $p \leq 0.05$ . ABA = abscisic acid, GA = gibberellic acid, LIIC = linoleic acid, LINN = linolenic acid, MG = methylglyoxal, SA = salicylic acid, I-3-PA = indole-3-propionic acid, JA-Ile = jasmonic acid-isoleucine and t-11-DA = 11-methyl-2E-dodecenoic acid.....68

Figure 3.7. Metabolomics analysis of extracts from SA, ABA, GA, LINN, MG, and no-signal control culture conditions. (A) Molecular network annotated with compound classes based on library hits. Singletons are excluded from the network. (B) Venn diagram of features contributed by SA, ABA, GA, and control culture conditions. (C) Venn diagram of features contributed by MG compared to control. Node counts based on ion distribution are shown. Link to network file is available in Appendix B.1. DMSO = no signal control, ABA = abscisic acid, GA = gibberellic acid, SA = salicylic acid and MG = methylglyoxal .....69

Figure 3.8. Metabolomics analysis of extracts from JA-Ile, I-3-PA, t-11-DA, and no-signal control culture conditions. (A) Molecular network annotated with compound classes based on library hits. Singletons are excluded from the network. (B) Venn diagram of features contributed by SA, ABA, GA, and control culture conditions. Node counts based on ion distribution are shown. Link to network file is available in Appendix B.2. I-3-PA = indole-3-propionic acid, JA-Ile = jasmonic acid-isoleucine, t-11-DA = 11-methyl-2E-dodecenoic acid and DMSO = no signal control. ....71

Figure 4.1 Minimum concentration of crude extracts that impacted antibacterial activities at  $p \leq 0.005$  against *R. radiobacter* and  $p \leq 0.0001$  against *E. coli*. ABA= Abscisic acid, GA= Gibberellic acid, I-3-PA= Indole-3-propionic acid, JA-Ile= Jasmonic acid-isoleucine, LIIC= Linoleic acid, LINN= Linolenic acid, MG= Methylglyoxal, SA = Salicylic acid exposure. ....83

Figure 4.2. Results from antibacterial activity testing showing the effects of active fractions against *E. coli*. ....84

Figure 4.3. Euler plot of features contributed by ASPfr-4, ASPfr-10, SAfr-3, SAfr-6, MGfr-2, and MGfr-3. Node counts based on ion distribution are shown. Link to network file is available in Appendix B.3. ....85

Figure 4.4. Dereplicated and mined molecular network of features from ASPfr-4, ASPfr-10, SAfr-3, SAfr-6, MGfr-2, and MGfr-3 based on GNPS library hits. The pie chart represents the number of spectra observed for each feature. Link to complete network file is available in Appendix B.3.....86

Figure C-1. Antibacterial effects of phytohormones and plant-related signals used in the study shows no growth inhibiting activities. 1\_control = media control (no bacteria) and 2\_control = bacteria control (no signal). .... 125

## CHAPTER 1. INTRODUCTION

### 1.1 The Myxococcales (Myxobacteria)

Distinguished by their organized social behavior and coordinated predation strategies, these ubiquitous Gram-negative bacteria exhibit gliding motility with the secretion of slime and are capable of feeding on a wide range of soil bacteria and fungi as most members are generalist predators.<sup>1-5</sup> The myxococcales, comprising of 4 suborders with 13 families (Figure 1.1) belong to  $\delta$ -proteobacteria and based on their feeding habits, can be grouped as either cellulose decomposers or predators.<sup>6-8</sup> They are usually observed in habitats rich in microbial and organic life but because these slow-growing bacteria are generally difficult to cultivate, most studies have focused on genome-mining approaches for identification of specialized metabolites therefore the chances for chemical novelty discovery remains high with these bacteria.<sup>4,9,10</sup> Myxobacteria are an under-explored group of organisms especially for the beneficial roles that they may play in promoting plant health. Having a wide range of target pathogens is a desirable trait when searching for plant-beneficial bacteria<sup>2,5,11</sup> but even more important is the ability of such bacteria to survive and colonize the rhizosphere. The success of a biocontrol strategy in agricultural systems, for microbial and insect pest management, depends on the fitness of microbial supplements including the ability to achieve high cell density levels within the rhizosphere, enough to accumulate antimicrobials or other traits that will ensure competitive advantages against pathogens and establishment of niches.<sup>12-19</sup> Maintaining significant cell densities has been a limitation for currently utilized biocontrol agents,<sup>20</sup> but most myxobacteria, through cooperative morphogenesis are capable

of forming fruiting bodies resulting in heat-, drought- and UV-resistant spores favoring their survival in unfavorable environments;<sup>1,21-23</sup> thereby demonstrating the capability of retaining high cell densities in the rhizosphere.

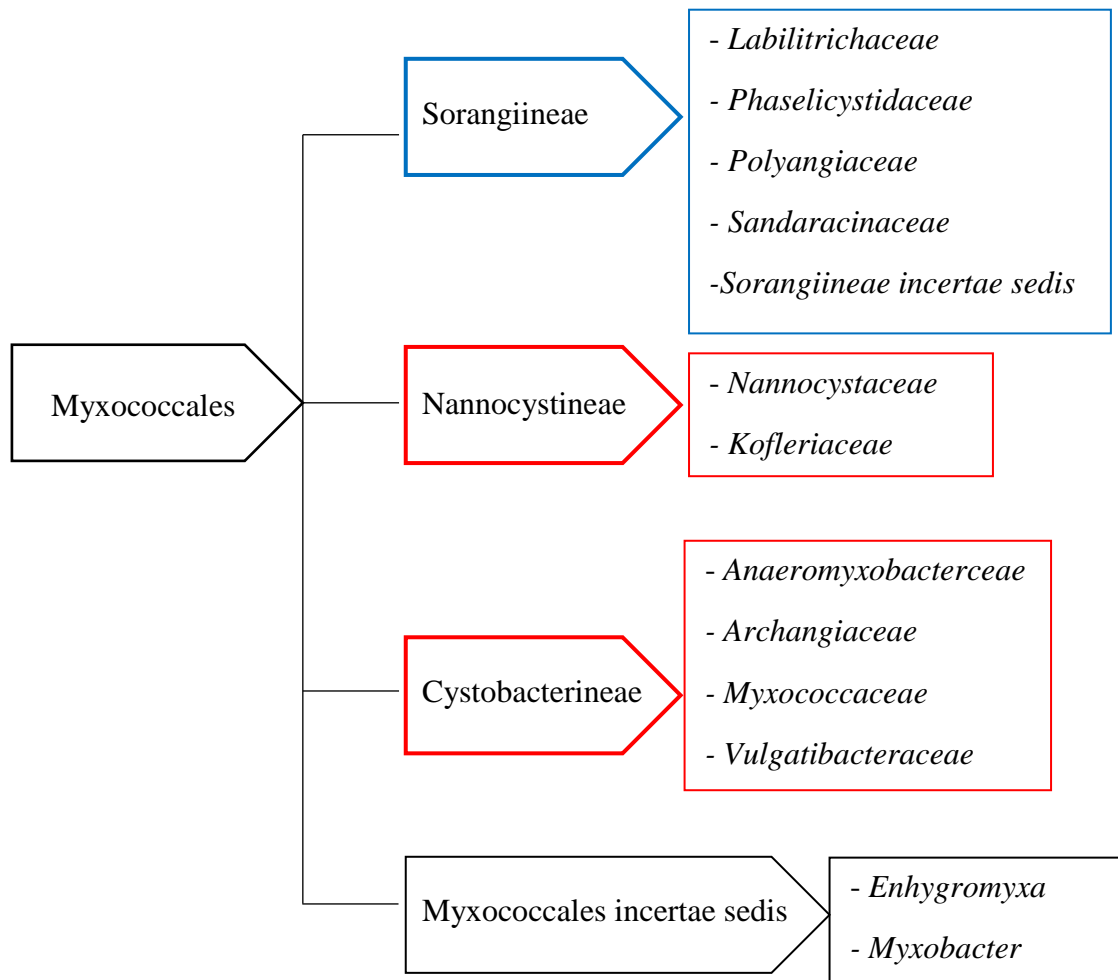


Figure 1.1. The order of Myxococcales with suborders and families (as of March 2021). Blue outline represents known saprophytic nutritional behaviour and red outline represents known predatory nutritional behaviour.

Myxobacteria also possess biosynthetic gene clusters (BGCs) capable of encoding numerous polyketides, peptides and other structural classes of compounds that demonstrate a wide range of activities including those that are antibacterial and antifungal (Figure 1.2).<sup>7,22,24-26</sup> However, little is known about the metabolic changes in myxobacteria, triggered by fluctuations in the chemical cues of the rhizosphere, that may lead to a disease-suppressive soil especially during pathogenic invasions. The theory is that antimicrobials along with lytic

enzymes in the outer membrane vesicles (OMVs) of myxobacteria, assists with predation,<sup>27,28</sup> henceforth studies that record chemical responses of these bacteria to phytopathogens are necessary. To investigate the roles that myxobacteria play in the rhizosphere, an understanding of the dynamics of plant-microbe interactions in the rhizosphere is essential.

## 1.2 Plants and their Rhizobiome

Biological control of diseases and pests, with its complications, has gathered substantial attention in the search for alternatives to chemical control options. In the rhizosphere, plants must continually adapt to diverse microbial populations in addition to surrounding abiotic pressures in order to survive. Exploration of roles that each microbial class plays in the rhizosphere reveals why unique microbial communities are particularly curated to suit specific plant species. Current knowledge categorizes microbial roles based on positive, negative or neutral influences on plant health, identifiable through disease progression or suppression activities<sup>29-31</sup> further suggesting that “specific traits” are required from microbes to achieve desired disease-suppressive soil. Studies to identify and characterize these traits, especially of interest to the agricultural industry, highlights groups of specialized metabolites, enzymes, and effector proteins with the purpose to probe the rhizobiome for their beneficial prospects.<sup>12,32</sup> However, beneficial bacteria are not impervious to competition from phytopathogens and it is challenging to supplement the rhizosphere with a selection of microbes possessing desired characteristics, capable of a wide range of suppressive effects against diverse pathogens while also maintaining effective population density because the rhizosphere brims with complex chemical interactions that are still not yet well-understood.<sup>20,31</sup> In fact, some traits attributed to beneficial bacteria are shared characteristics also observed in phytopathogens, such as secretion of lytic enzymes, which

can either promote pathogenesis or facilitate endophyte symbiosis with the plant host.<sup>33-35</sup>

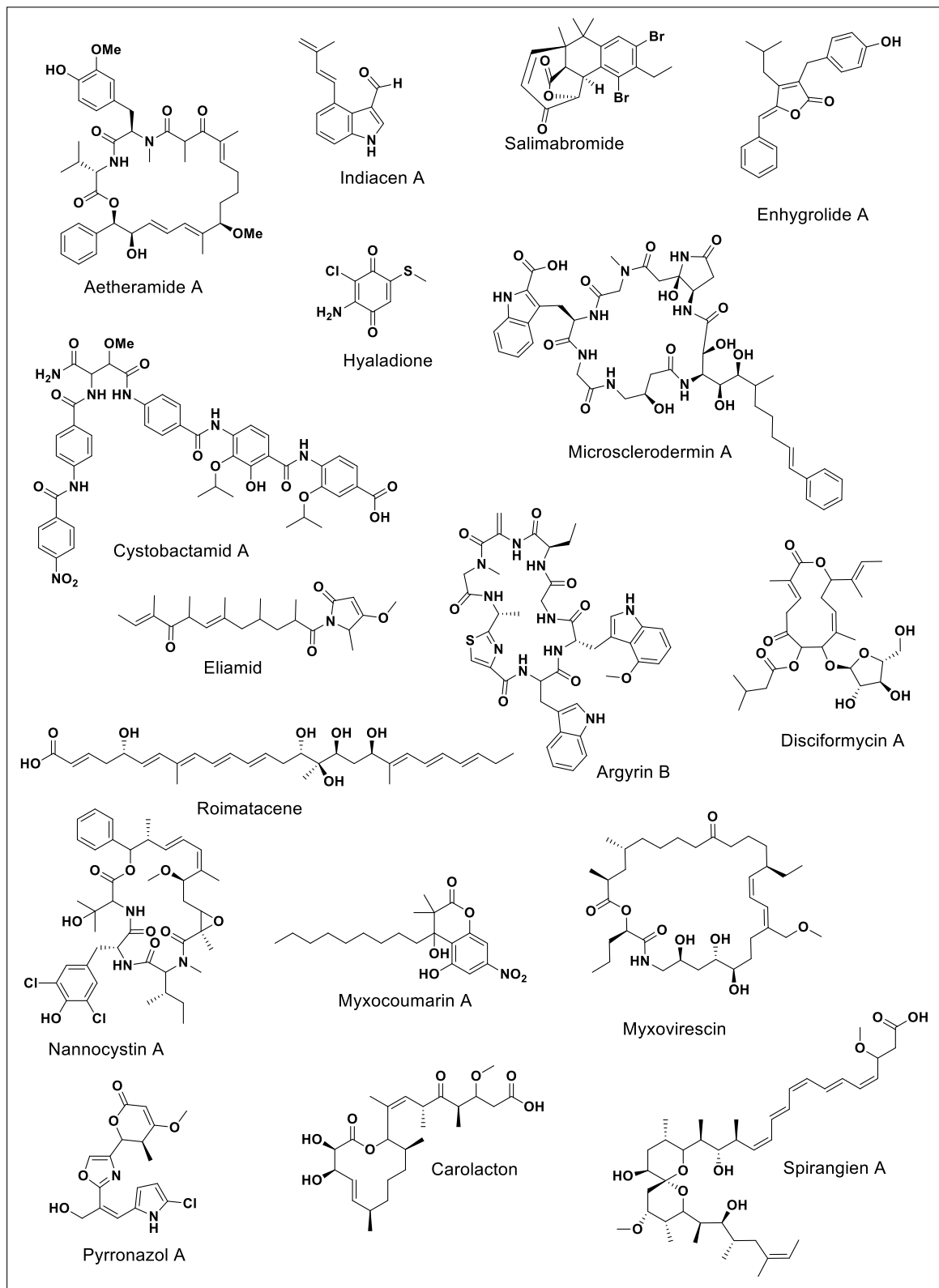


Figure 1.2. Representative antimicrobials identified from myxobacteria

This section will highlight the shared chemical ecology associated with the rhizosphere including phytohormones, phytotoxins, and antimicrobials, and how these metabolites influence traits associated with beneficial bacteria.

### 1.2.1 Phytohormones and Root Exudates

Phytohormones play important roles in the adaptation and survival of plants during adverse conditions resulting from either abiotic stress, such as unfavorable environmental conditions including drought, changes in temperatures, salinity, or biotic stress arising from microorganisms, nematodes, and insects. The defense-related hormones regulate complex signaling mechanisms in plants, with interconnecting pathways to provide with efficiency, various stress responses. Among the different groups of defense-related hormones, including the jasmonates (JA), abscisic acid (ABA), auxins (AUX), cytokinins (CK), ethylene (ET), gibberellins (GA), salicylic acid (SA), brassinosteroids (BR) and strigolactones (SL), most studies associate crosstalks between JA, ABA, ET and SA signaling pathways (Figure 1.3) in mediating systemic resistance to phytopathogenic insult.<sup>36,37</sup> It is usually expected that the chemical presence of the majority of these phytohormones should be secluded only to the plant internal system but in fact, current reports suggest possible micro-titer leakages as root exudates that contribute to the shared chemical space of root microbiomes.<sup>38-40</sup> Generally, root exudation (also commonly referred to as ‘rhizodeposition’) is viewed as a major process in which the plant interacts with the rhizosphere via a wide range of low- and high-molecular-weight organic compounds generated from both primary and specialized metabolism.<sup>41</sup> Exudates including organic acids, sugars, sugar alcohols, phenolic glycosides, amino acids, flavonoids, and polysaccharides (usually present in root mucilage) are believed to be passively lost from roots through diffusion further suggesting a longstanding



establishment of nutrient gradients in the soil. <sup>42,43</sup> As expected, exudation can be supported by rhizobiome metabolism of these compounds, where microbes act as a soil sink to increase the flux of exudates into the rhizosphere, a process similar to rhizosphere priming effect. <sup>44</sup> It should be noted that bioactive specialized metabolites are also generated by plants to combat pathogens and are exuded via energy-dependent mechanisms. <sup>45-48</sup> Current knowledge indicates that exudates are utilized by plants to attract beneficial microbes for the purpose of promoting nutrient acquisition and facilitating pathogen resistance, supported by studies which highlight distinct community structures specific to various plant species with less diverse microbes than is observed in bulk soil. <sup>49,50</sup>

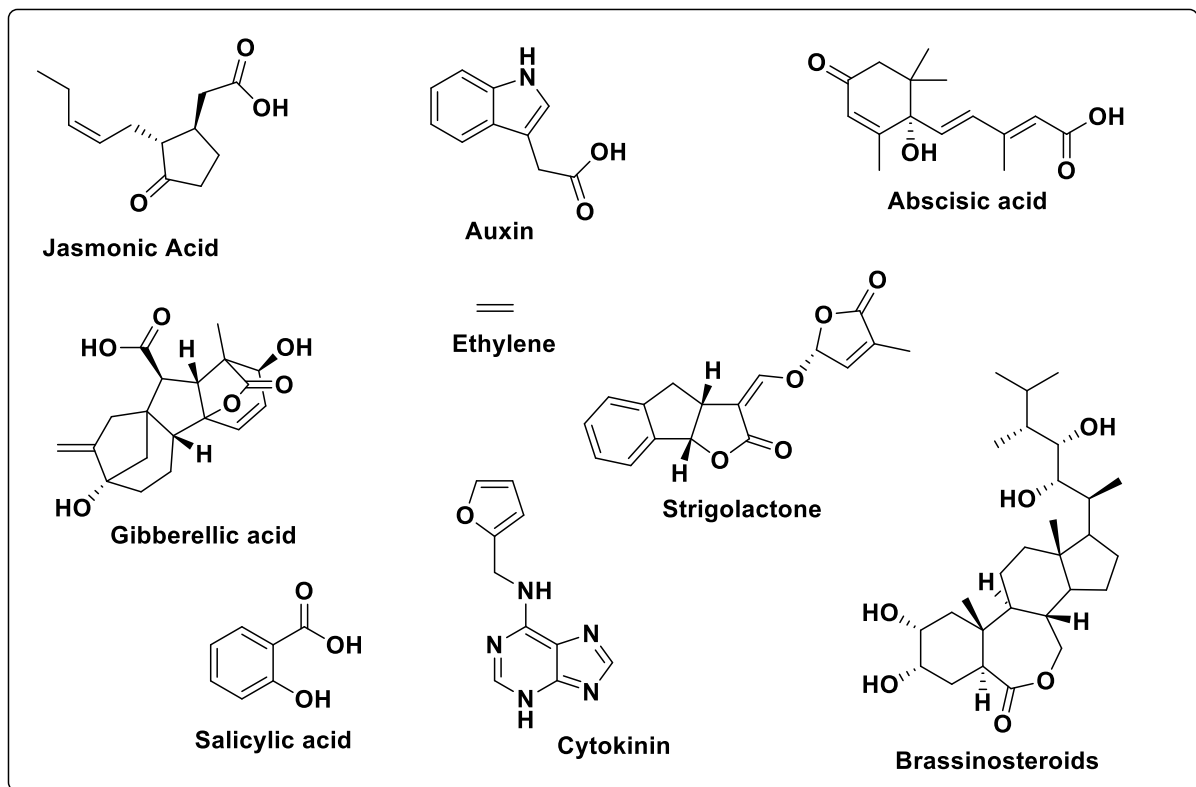


Figure 1.3. Phytohormones involved in plant defense mechanisms

### 1.2.2 Bacterial Chemotaxis Triggered by Plant Exudates and Phytohormones

It is generally thought that low-molecular-weight compounds play an important role in propagating communication within species and across kingdoms. In the rhizosphere, plants continuously monitor the fluctuating activities of the microbial population and make appropriate responses to maintain good health as earlier mentioned via exudates and phytohormones. At the same time, bacteria also display several responses to these exudates and systemic changes in plants, usually initiated with chemotaxis. Important for survival and gaining selective advantages in unfavorable environments, chemotactic signaling enables motile soil bacteria to follow nutrient gradients created by plant roots in the soil.<sup>41,51</sup> The chemical attraction of bacteria towards plants is a well-documented occurrence often leading to the development of plant-microbe relationships, either pathogenic or symbiotic. This is evident in the enrichment of rhizobiomes with chemotaxis encoding genes compared to microbes in bulk soil.<sup>35</sup>

In bacteria, complex chemosensory systems control several biological functions including chemotaxis and expression of genes relevant for complementing changes in the microenvironment. Mechanisms of chemotaxis can be understood using the well-studied *Escherichia coli*, where chemotactic responses to stimuli are initiated by changes in the conformation of the methyl-accepting chemotaxis proteins (MCPs) which promote the autophosphorylation of histidine kinase, CheA. Activated CheA then phosphorylates CheY, a response regulator that in turn interacts with the flagellar switch protein FliM, altering the direction of flagellar rotation.<sup>52-55</sup> Most studies of bacterial chemotaxis to plant-related signals often present with changes in motility and cell cycle progression, induction of virulence factors, activation of specialized metabolites, and production of lytic enzymes.<sup>56,57</sup> One possible explanation for these observations is that regulatory systems are coupled to

provide dynamic and efficient control of cellular processes important for interacting with hosts. For example, the McpU and McpA chemoreceptors in *Pseudomonas pudita* contribute to mediating motility and biofilm formation;<sup>58</sup> similar observation has also been reported in *Comamonas testosteroni* CNB-1.<sup>52</sup> Moreover, crosstalk between chemotaxis and adhesion regulation has been observed in endophytic *rhizobia* which is significant for successful nodulation of plant roots and seeds.<sup>55</sup> Furthermore, the hypersensitive responses and pathogenicity (*hrp*) genes regulate chemotaxis and pathogenicity of *Xanthomonas oryzae* pv. *Oryzae*.<sup>59,60</sup>

Nutrient gradients are formed in the soil by root exudates and rhizodeposition and provide an effective mechanism to attract diverse microbes to the rhizosphere.<sup>51</sup> Because plant species determine the composition of exudates, it is evident that plants may contribute selective pressure to recruit and maintain a distinct microbial community in their rhizosphere.<sup>38,50,61</sup> Organic acids, present in exudates, represent a major attractant for several plant-related bacteria. These compounds also function as catabolite repressors to the nitrogen-fixing *Rhizobium meliloti*, *Rhizobium leguminosarum*, and *Azospirillum brasilense*.<sup>62–64</sup> Other root exudates are recorded to activate chemotaxis and various gene expressions. In fact, amino acids in exudates are especially attractive to *R. meliloti* and *R. leguminosarum* as nitrogen sources because these bacteria only fix nitrogen when in established symbiosis with plant hosts.<sup>51</sup> Phytopathogens are also included in the attracted microbial population, which may seem counterintuitive, but it is important to note that most of these low-molecular-weight compounds in exudates generally serve as carbon and nitrogen sources for microbes.<sup>41</sup>

### 1.2.3 Bacterial Enzymes and Transporters Involved in Plant-Microbe Interactions

To adapt to the rhizosphere, bacteria are known to alter the expression of multiple genes in response to plant exudates and other chemical signals in the microenvironment. Altered gene expressions are likely to enable bacteria to aggressively compete with resident microbes and colonize the rhizosphere<sup>35,49</sup> because both beneficial and pathogenic bacteria need to access carbon and nitrogen from organic matter, detoxify potential toxins and where necessary, gain entry into the plants as well as evade resulting systemic defense mechanisms. So far, what is known about the roles that each unique enzymatic repertoire for individual bacterial species play in the soil is centered on evidence that portrays the selection of organisms to the rhizosphere. However, studies have either looked at the usefulness of specific enzymes possessed by the bacteria in establishing symbiotic relationships or a general snapshot of all overexpressed enzymes present in a specific rhizosphere at a defined disease state. We will now highlight known enzymes and transporters that are responsive to rhizospheric pressure.

Eukaryotic cell walls consist of polysaccharides that provide support to the cell which have been strategically targeted during microbial interactions. A metagenomics study of the endophytic microbiome of a disease-suppressive compared to a disease-conducive soil revealed the overexpression of protein domains encoding for carbohydrate-active enzymes (CAZymes) during *Rhizoctonia solani* infection.<sup>29</sup> Certain bacteria, through the type 2 secretion system (T2SS), release chitinolytic enzymes and chitin-binding proteins when establishing a competitive or symbiotic relationship with fungi. This is important because fungal cell walls are structurally supported by chitin and chitosan, which provide an obvious target for chitinase and chitosanase respectively, thereby promoting the entry of the bacteria into the host.<sup>65</sup> As a result, chitinolytic enzymes have been explored for agricultural purposes

as antifungals against plant pathogens as well as biocontrol agents against insect pests known to possess chitin-rich exoskeletons.<sup>66,67</sup> T2SS gene clusters are well conserved among related species and are often highly expressed in the rhizospheric environment because they play a vital role in the secretion of various extracellular degradative enzymes that important in bypassing the physical barriers of competing or host organisms.<sup>68</sup> Lytic enzymes secreted via this system are functionally and structurally diverse, each playing unique roles in specific circumstances (Figure 1.4). In bacteria-plant interactions, cellulases, pectinases, and xylanases are employed to break down the structural molecules of plant cell wall propagating tissue necrosis and serving to provide carbon sources to the bacteria.<sup>31,38</sup> Oftentimes, given the complexity of polysaccharides that may be encountered and the hydrolytic capacities of specific CAZymes, it is not uncommon to find that a variety of enzymes are deployed at a time to achieve complete degradation and helper enzymes including polysaccharide lyases, glucanase, glycosyl hydrolases, debranching enzymes, and carbohydrate esterases are necessary.<sup>69</sup> An alternate role played by CAZymes can be seen with certain glycosyltransferases identified to contribute to the virulence of *Pseudomonas syringae* where it was hypothesized that these enzymes decorate lipopolysaccharides (LPS), known to induce systemic resistance in plants, with O-antigen so as to disguise their cellular presence from potential defense mechanisms.<sup>70,71</sup>

Another group of enzymes implicated in the necrosis of plant tissues is extracellular proteases. Endophytes utilize exoproteases in addition to CAZymes to facilitate entry into host cells and to metabolize soil polymer substrates, therefore, releasing low molecular weight organic nitrogen, a process commonly referred to as nitrogen mineralization.<sup>72</sup> On the other hand, studies of *Pseudomonas fluorescens* CHA0 as a biocontrol agent attributed their antagonistic activity against phytopathogenic nematodes to the activities of the extracellular protease, AprA that is regulated by the GacS/GacA signal transduction pathway. Under

greenhouse conditions, mutant strains when compared to *Pseudomonas fluorescens* CHA0 strains were unable to suppress *Meloidogyne incognita* induced root-knot disease.<sup>73</sup>

Similarly, plant-beneficial *Bacillus* species have been suggested to secrete cuticle-degrading and nematicidal proteases.<sup>74</sup> Although there are limited studies focused on extracellular proteases of the rhizobiome, protease production counts among traits used to characterize plant growth-promoting rhizobacteria.<sup>75-77</sup>

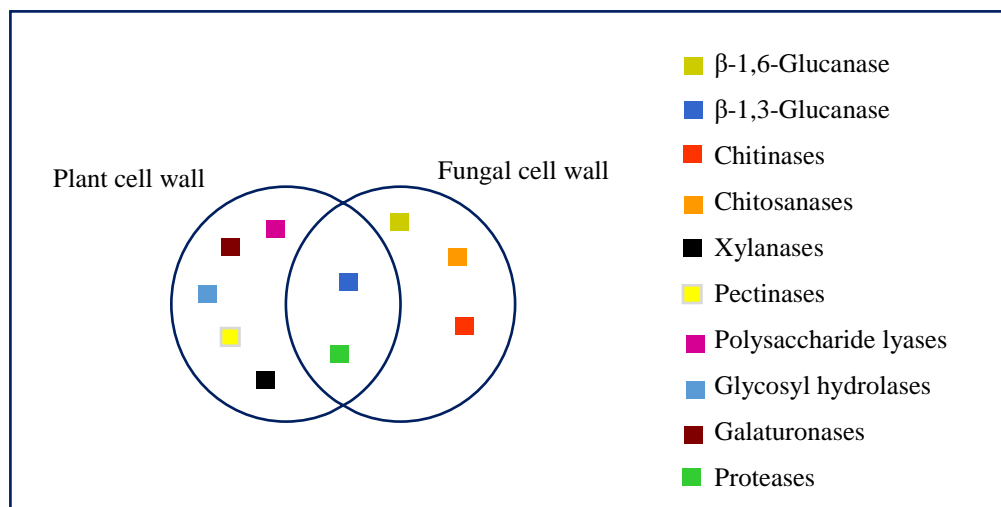


Figure 1.4. Venn diagram of lytic enzymes from beneficial bacteria and selective effects on either plant or fungi based on the cell wall components.

Genes encoding for oxidoreductases in the rhizosphere are found to be varied given that they come from a more diverse microbiome compared to other microbial communities<sup>78</sup> and were observed to be enriched in a fungal disease-suppressive soil<sup>29</sup> which suggests that they may have important roles in benefiting plants. Recently, GmcA, a glucose-methanol-choline oxidase, was seen to be vital in the extracellular detoxification of hydrogen peroxide, iron homeostasis, and nitrogen fixation activities of *Rhizobium leguminosarum* bv. *Viciae*. The adaptation of *gmcA* mutants in the rhizosphere was greatly diminished with the observation of poor nodulation and ineffective establishment of symbiosis.<sup>79</sup> Taken together, it is apparent that more studies are needed to explore the potential benefits of bacterial redox traits in the microenvironment of plants. An alternative contribution that certain bacterial

enzymes may offer in promoting colonization in the rhizosphere is exemplified via biotransformation or biodegradation of compounds encountered in the rhizosphere. In polycyclic aromatic hydrocarbon contamination, plant-related bacteria adapt by regulating the expression of biodegradation-related genes explaining why a high expression of phenol monooxygenase gene and other aromatic oxygenase genes were observed in the microenvironment.<sup>80</sup> Consequently, microorganisms capable of expressing these biodegrading oxygenases have been explored for their use in biological remediation. Studies of *Bacillus* sp. BPR7 and *Pseudomonas fluorescens* CHA0 as biocontrol agents against *Rhizoctonia solani* in rice sheath blight disease suggested the benefits of oxalate oxidases because oxalic acids produced during mycelial growth renders plant tissues susceptible to enzymatic degradation by the phytopathogenic fungi and experimental data showed successful suppression of the disease.<sup>66,81</sup>

ATP-binding cassette (ABC) transporters, with diverse functions, are also involved in maintaining interactions in the rhizosphere through nutrient absorption and amino acid recycling during nodulation and nitrogen fixation.<sup>82</sup> Early stages of rhizobium symbiosis revealed high amounts of ABC transport proteins consistent with data for these proteins as the most important class for intercellular transportation.<sup>82</sup> During adaptation in the rhizosphere, extracellular packages of lytic enzymes and specialized metabolites are expected to be delivered across membranes to facilitate reaching plant tissues or microbial targets. Transcriptomic analysis of *Bacillus sonorensis* showed that in addition to ABC transport proteins, the overexpression of other transporters could also be observed concomitantly with the overexpression of bacterial enzymes in the rhizosphere. The multidrug transporter, AcrB, permeases, sugar transporters, and outer membrane porins were highly expressed to facilitate the efflux of antimicrobial peptides, uptake of sugars, and diffusion of hydrophilic compounds in the rhizosphere.<sup>83,84</sup>

#### 1.2.4 Phytopathogenic Responses to Plant Exudates that Promotes Virulence

The responsiveness of phytopathogens to the rhizosphere is central to infection. Navigating community-level signaling and utilizing environmental cues to find suitable hosts, coupled with overcoming the plant's physical and chemical barriers, would require activating chemotaxis pathways, motility, and specialized metabolites. Plant-associated bacteria have been found to possess a subgroup of LuxR solos that have evolved to eavesdrop on and bind to low molecular weight compounds produced by plants rather than to acylhomoserine lactones (AHLs).<sup>30,85</sup> Phytopathogens exploit these plant exudates to activate virulence and induce the biosynthesis of phytotoxins. In addition, some phytopathogens like *Pseudomonas syringae* and *Dickeya dadantii* have evolved to also sense and hijack phytohormones important in regulating systemic resistance mechanisms of the plant (Table 1.1), via the generation of mimics to improve their chances of host invasion.<sup>86,102</sup> Various molecular classes of phytotoxins, from phytopathogens possessing different mechanisms of action, have been reported.

**Polyketides:** During biotic stress when plants are attacked by necrotrophic pathogens or herbivorous insects, defense responses mediated by the jasmonic acid (JA) pathway are activated.<sup>88,103</sup> However on sensing the secretion of the phytohormone during the systemic resistance event, coronafacoyl phytotoxins, initially isolated from *Pseudomonas coronafaciens*, usurps this resistance process resulting in chlorosis of developing tissues.<sup>86</sup> Coronafacoyl phytotoxins are viewed as JA-isoleucine mimics (Figure 1.5a) and contain a bicyclic hydrindane ring-based polyketide, coronafacic acid (CFA), linked via an amide bond to either an amino acid or amino acid derivatives (Figure 1.5b).



Table 1.1: Roles of defense-related phytohormones and how they are exploited by phytopathogens during invasion of plant hosts.

Phytohormones	Roles in systemic resistance	Manipulation by Phytopathogens	Present in root exudates?
Jasmonates (JA) <sup>86-88</sup>	<ul style="list-style-type: none"> <li>▪ Activation of systemic acquired resistance</li> <li>▪ Involved in defense against necrotrophic pathogens</li> <li>▪ Mediates defense synergistically with ET</li> </ul>	Generation of JA and jasmonate-mimics such as the coronafacoyl phytotoxins to hijack and stop the JA-pathway	Yes
Abscisic acid (ABA) <sup>89,90</sup>	<ul style="list-style-type: none"> <li>▪ High levels interfere with SA, JA, CK and ET signaling, therefore, promoting susceptibility to disease</li> <li>▪ Stimulates root colonization and establishment of symbiosis with endophytes</li> <li>▪ Involved in defense against abiotic stress</li> </ul>	Generation of ABA and ABA-mimics to achieve high concentrations and promote colonization	Yes
Auxins (AUX) <sup>91</sup>	<ul style="list-style-type: none"> <li>▪ The major type is indole-3-acetic acid (IAA)</li> <li>▪ Promotes microbial colonization</li> <li>▪ Suppression of signaling improves physical barrier in restricting pathogens</li> </ul>	Generation of IAA and other auxin precursors to achieve high concentrations of auxins	Yes
Cytokinins (CK) <sup>92</sup>	<ul style="list-style-type: none"> <li>▪ Important in developing resistance against necrotrophs</li> <li>▪ Acts synergistically with SA to mediate resistance</li> </ul>	Generation of CK analogs to interfere with plant immunity	Yes
Ethylene (ET) <sup>93,94</sup>	<ul style="list-style-type: none"> <li>▪ Important in plant signaling</li> <li>▪ Involved in defense against necrotrophic pathogens</li> <li>▪ Acts synergistically with JA</li> </ul>	Generation of ET to interfere with systemic resistance	Yes
Gibberellins (GA) <sup>95,96</sup>	<ul style="list-style-type: none"> <li>▪ Promotes resistance to biotrophs but increases susceptibility to necrotrophs</li> <li>▪ Antagonistic to ABA</li> </ul>	Necrotrophs secrete GA as part of their virulence mechanisms	Yes
Salicylic acid (SA) <sup>88,97</sup>	<ul style="list-style-type: none"> <li>▪ Promotes antioxidant activities</li> <li>▪ Defense against biotrophic pathogens</li> <li>▪ Antagonistic to JA, ET, and AUX signaling pathways</li> <li>▪ Activation of systemic acquired resistance</li> </ul>	Biotrophs produce effector proteins like Cmu1 to interrupt the biosynthesis of SA	Yes
Brassinosteroids (BR) <sup>98,99</sup>	<ul style="list-style-type: none"> <li>▪ Negatively regulates ET and GA</li> <li>▪ Play important roles in trade-offs between plant growth and defense mechanisms</li> </ul>	Generation of effector proteins to hijack BR signaling and promote disease susceptibility of plant hosts	Unknown
Strigolactones (SL) <sup>100,101</sup>	<ul style="list-style-type: none"> <li>▪ Positive crosstalk with ABA and AUX but negative crosstalk with GA</li> <li>▪ Promotes microbial colonization</li> </ul>	Unknown	Yes

Biosynthesis of this toxin has been identified in various *Pseudomonas* and *Pectobacterium* sp. as well as in *Brenneria* EniD312 sp., *Dickeya dadantii*, *Lonsdalea quercina*, *Streptomyces scabies*, and *Xanthomonas campestris*.<sup>104-106</sup> Concanamycins, (Figure 1.5c) which were first isolated from *S. diastatochromogenes* S-45 in 1984, contain an 18-membered tetraenic macrolide ring with a methyl enol ether and a  $\beta$ -hydroxyhemiacetal side chain. These metabolites together with other phytotoxins from *Streptomyces* including the 18-membered macrolide borrelidin, 16-membered macrolide labeled FD-891, and the type II polyketides desmethylmensacarcin and Fridamycin E (Figure 1.5d-g) have been implicated in causing deep necrotic lesions associated with scab disease of potato tubers and taproot crops.<sup>107</sup>

Peptides: A phytotoxic family of cyclic dipeptides, the thaxtomins (Figure 1.6a), known for inducing scab-like lesions on tubers by inhibiting cellulose synthesis, were the first to be associated with the plant-pathogenicity of *Streptomyces*. Thaxomin A, the most prevalent analog isolated from *Streptomyces scabies*, *Streptomyces turgidiscabies*, and *Streptomyces acidiscabies*, is a nitrated 2,5-diketopiperazine derived from L-phenylalanine and L-4-nitrotryptophan.<sup>105,107</sup> As specialized metabolites representing the main virulence factor, the thaxomin biosynthetic gene clusters are highly conserved in plant-pathogenic *Streptomyces*, and biosynthesis of the toxin is exclusive to these species.<sup>108</sup> *Pseudomonas syringae* (and other phytopathogenic *Pseudomonas* species) employ lipodepsipeptide toxins, such as syringomycin, syringopeptin, corpeptin, and the hybrid non-ribosomal/polyketide toxin, syringolins (Figure 1.6b-e) in addition to the mentioned coronafacoyl phytotoxins to gain entry and invade the plant host. The pathogen locates the plant host by sensing phenolic glycosides and sugars from the root exudates which in turn activates the biosynthesis of syringomycin.<sup>70</sup> Syringomycin compound often contains non-proteinogenic amino acids such as 2,3-dehydroaminobutyric acid, 3-hydroxyaspartic acid, and 4-chlorothreonine, along

with serine D-isomers and 2,4-diaminobutyric acid. Lipodepsipeptide toxins induce direct cellular damage to plants by forming pores within the membrane resulting in loss of integrity and tissue necrosis,<sup>109</sup> a mechanism different from how the syringolins act. Syringolin A is a tripeptide proteasome inhibitor that suppresses the JA-pathway and other plant hormones involved in mediating defense responses.<sup>110,111</sup>

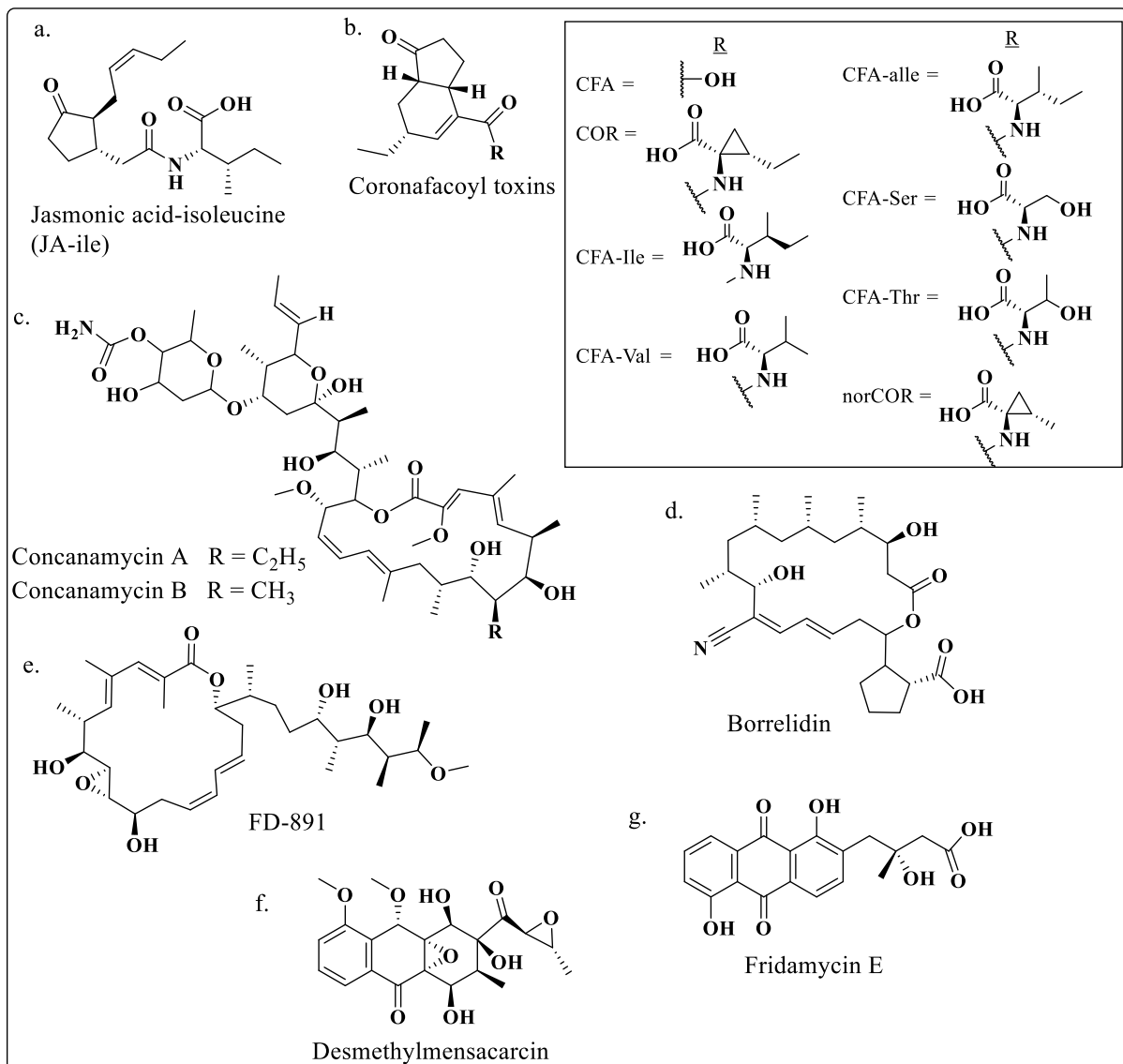


Figure 1.5. Examples of polyketides from phytopathogenic bacteria

Other phytotoxic peptides from *Pseudomonas* like phaseolotoxin, mangotoxin, and tabtoxin (Figure 1.6f-g) target enzymes involved in amino acid biosynthesis resulting in nitrogen metabolism interference in the host.<sup>108</sup> *Ralstonia solanacearum* also senses plant

sugars and is identified as one of the causes of bacterial wilt disease via the production of ralstonins (Figure 1.6h) which are cyclic lipodesipeptides from the hybrid non-ribosomal/polyketide synthase biosynthetic gene cluster.<sup>112,113</sup>

Other structural classes: Although not directly toxic to plants, the ralfuranones (Figure 1.7a) have been reported to aid in the virulence of *Ralstonia solanacearum*. Biosynthesis of these aryl-furanone metabolites, triggered when the pathogen senses plant sugars, activates the quorum sensing (QS) circuit that controls the expression of the gene clusters encoding the ralstonins with mutant strains reportedly also losing their aggregation and swimming motility.<sup>114</sup> Wilting in rice and other field crops can be caused by toxoflavin (Figure 1.7b), a pyrimidotriazine secreted by the phytopathogenic *Burkholderia gladioli*.<sup>115,116</sup> Other rare phytotoxins such as tropolone (Figure 1.7c) from *Burkholderia plantarii* containing a 7-membered aromatic ring and pyridazocodin (Figure 1.7d) from *Streptomyces* have been identified to negatively affect plant health while promoting virulence of phytopathogens.<sup>117,118</sup>

### 1.2.5 How Beneficial Bacteria Interact with Phytopathogens

Plants exude numerous compounds and phytohormones that attract a variety of microorganisms to the rhizosphere including phytopathogens. Although most plants generate specialized metabolites (not covered in this review) to defend against pathogenic invasion, a number of rhizospheric bacteria, dubbed as “beneficial” also act as an additional defense barrier for pathogens to overcome.<sup>61</sup> Certain bacterial traits shared among known plant-beneficial bacteria are documented as “selection criteria” by plants, as a result, many studies have focused on identifying beneficial bacteria from the rhizosphere that could improve the

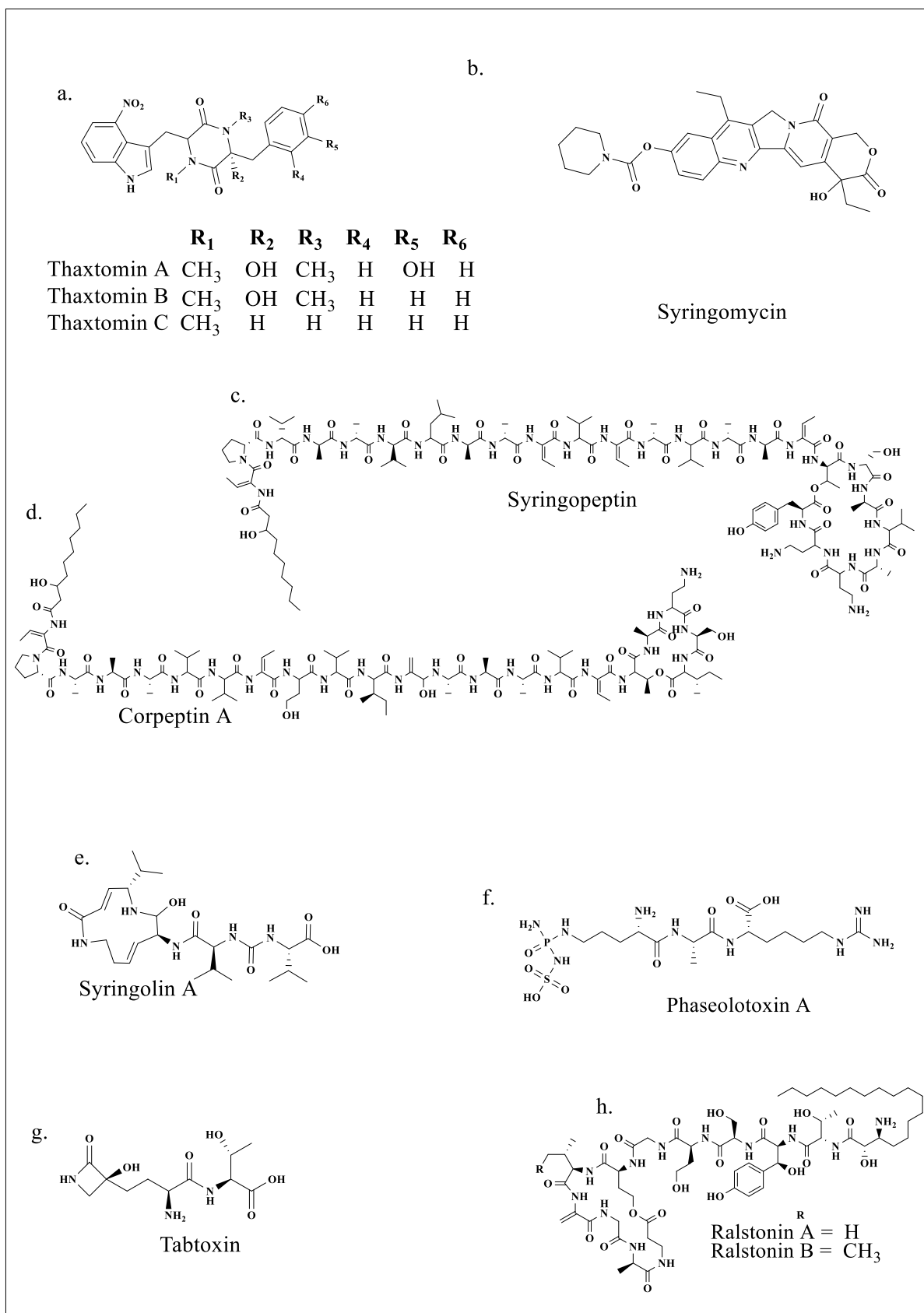


Figure 1.6. Examples of peptides from phytopathogenic bacteria

health of plants and promote stress resistance although only a few strains have been developed commercially.<sup>19,119</sup>

Plant-beneficial bacteria interact with other microbes in the environment through complex chemical interactions either to kill the pathogen or inhibit the activation of virulence mechanisms. The production of lytic enzymes has already been covered in previous sections but it is important to mention that these enzymes are often observed to be utilized synergistically with mechanisms discuss here.

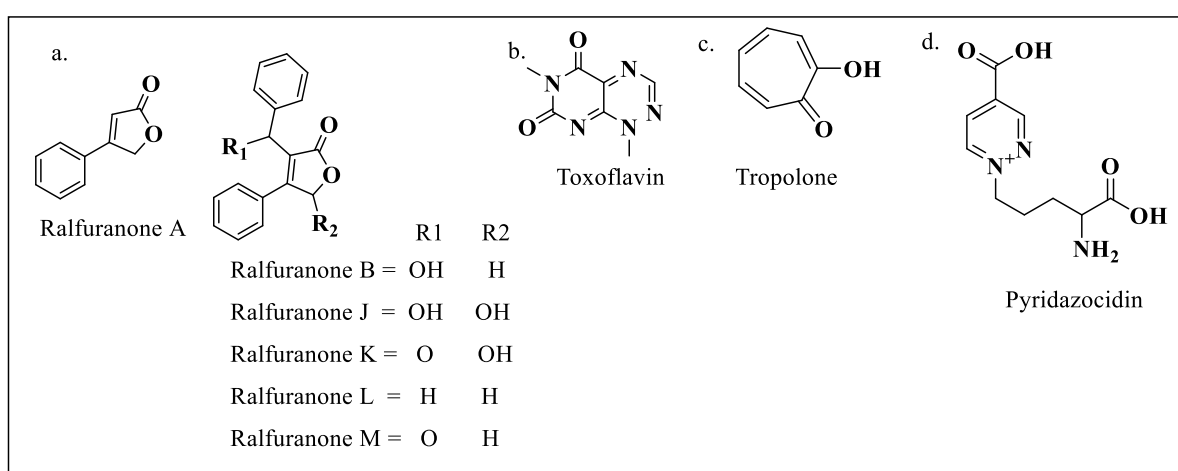


Figure 1.7. Examples of other structural classes of phytotoxins

### 1.2.5.1 Interference of Microbial Signaling Mechanisms

Microbes perform coordinated activities and intercellular communications through quorum signaling (QS) mediated by small molecules and auto-inducers.<sup>72</sup> Quorum signaling has been observed to be enriched in the rhizosphere consistent with high densities of microbial cells and it contributes to microbial survival in this highly competitive and nutrient-restricted environment, particularly shown by QS-activation of virulence factors.<sup>31,120</sup> Signaling among phytopathogens via molecules including *N*-acyl-homoserine lactones (AHLs), butyrolactones, small peptides, unsaturated fatty acids (such as 3-hydroxy palmitic

acid methyl ester), furan derivatives (Autoinducer-2) and quinolones serve as proposed targets for some ways beneficial bacteria can be used to thwart pathogenic attacks in biocontrol research. Strategies that involve the inhibition of biosynthesis, receptor-binding, or biotransformation of signaling molecules to inactive forms are usually referred to as quorum quenching.<sup>121</sup> Biological quorum quenching of signals have been recorded but more attention has been given to the degradation of AHLs revealing multiple enzymes like amidases, lactonases, reductases, and oxidases being involved in ring-opening and chain cleaving.<sup>17,121</sup> QS in *Pectobacterium carotovorum*, a known cause of blackleg and soft-rot diseases in plants was interrupted by secreted lactonase, reductase, and acylase enzymes from *Rhodococcus erythropolis* and *Bacillus* species.<sup>122,123</sup> *Bacillus* species and several Gram-positive bacteria are identified to show sensitivity to *N*-(3-Oxododecanoyl)-L-homoserine lactone (OC12-HSL) and the tetramic acid, 3-(1-hydroxydecylidene)-5-(2-hydroxyethyl) pyrrolidine-2,4-dione obtained from the spontaneous degradation product of OC12-HSL.<sup>124,125</sup> But the presence of an AHL lactonase, AiiA, protects the *Bacillus* genus by opening the lactone ring, therefore, bypassing the formation of the tetramic acid.<sup>121</sup> Expectedly, quorum quenching is not exclusive to beneficial bacteria as *Agrobacterium tumefaciens*, and some phytopathogens, also express AHL-lactonase genes.<sup>126</sup> Quorum quenching techniques are explored in the control of phytopathogenic expressions of virulence genes, which does not necessarily result in growth inhibition; instead, additional generation of toxic specialized metabolites detrimental to phytopathogens can synergistically act to curb pathogenic populations.

#### 1.2.5.2 Specialized Metabolites that are Beneficial in the Rhizosphere

Recent metagenomic exploration of biosynthetic gene clusters (BGCs) capable of encoding specialized metabolites in a selected soil ecosystem, revealed profuse PKS, NRPS,

and hybrid NRPS/PKS BGCs in the rhizobiome suspected to contribute to the disease-suppressive status of the rhizosphere.<sup>127</sup> The ability to generate antimicrobials provides competitive advantages to survive in the rhizosphere. Few bacteria species have been identified and studied for their ability to generate toxic compounds in addition to other traits that make them suitable biocontrol agents.<sup>12</sup>

*Bacillus* species: Over time, these Gram-positive bacteria ignited interest as agents for the biocontrol of plant pathogens because of the ease of genetic manipulation, extensive characterization of expression systems, and numerous antimicrobial compounds (Figure 1.8) generated by the organisms.<sup>15,128–130</sup> Numerous bioactive compounds belonging to the polyketide and peptide classes have been identified to be effective in controlling various phytopathogens. *Bacillus amyloliquefaciens* FZB42 and *B. subtilis* strains possess BGCs that encode difficidin (Figure 1.8f), a macrocyclic polyene lactone with broad-spectrum antibacterial activities especially against *Xanthomonas* species, *Pseudomonas syringe* pv. *Tabaci* and *Rhizobium radiobacter*.<sup>32</sup> Difficidin together with bacilysin (Figure 1.8c) efficiently controlled the blight disease pathogen, *Erwinia amylovora*<sup>131</sup> further suggesting synergistic effects of these metabolites. On the other hand, plantazolicin (Figure 1.8i) from *B. amyloliquefaciens* exerted a nematocidal effect<sup>132</sup> consequently broadening the spectrum of activities of compounds from this species. Similarly, *B. subtilis* are known for biosynthesizing complex membrane acting cyclic lipopeptides (cyclic LPs) which are effective against certain Gram-positive bacteria but more potent against fungal pathogens like *Rhizoctonia solani* and *Paecilomyces variot*;<sup>15,129</sup> but it has been observed that cyclic LPs, except for the fengycins (Figure 1.8e), may have some toxicity to plants.<sup>128</sup>

*Pseudomonas* species: Many cyclic LPs from these genera constitute virulence via the formation of pores in the plant cell membrane but beneficial species utilize these surface-



acting compounds for antimicrobial activities as well. For instance, massetolide A (Figure 1.9a) from *Pseudomonas fluorescens* exhibits zoosporicidal activities against *Pythium*, *Phytophthora* species, and other oomycete pathogens.<sup>133,134</sup> Viscosinamide (Figure 1.9b), another cyclic LP from this bacteria acts antagonistically against fungal pathogens by altering the growth, cellular activities, and morphology of the mycelium.<sup>135</sup> Veering off from antimicrobial peptides, pseudomonads are also known to biosynthesize phenazines, 2,4-diacetylphloroglucinol (DAPG), and pyrrolnitrin (Figure 1.9e-g) in the rhizosphere which are antifungal and have been studied for the management of plant pathogens.<sup>136,137</sup> The blend of toxins which included pyrrolnitrin and DAPG have been observed to give protective activities to *Pseudomonas fluorescens* CHA0 from protozoan grazing.<sup>138</sup> A study of the interactions between *Pseudomonas chlororaphis* PCL1606 and *Rosellinia necatrix* revealed an aggressive competition for the establishment of niches in the avocado rhizosphere.

However, the generation of 2-hexyl, 5-propyl resorcinol (Figure 1.9h) by the beneficial *Pseudomonas* inhibited the pathogenic *R. necatrix*<sup>139</sup> which resulted in the low incidence of white root rot disease, caused by the pathogenic fungi during permeation of mycelial aggregates during colonization.<sup>84</sup>

*Burkholderia* species: Consistent with the enrichment of *Burkholderia* species in a fungal pathogen-induced disease-suppressive soil,<sup>29</sup> previous studies of the activities of *Collimonas fungivorans* against *Aspergillus niger* observed the upregulation of genes encoding for PKS and NRPS which were attributed to generating compounds that resulted in zones of inhibition of microbial growth.<sup>140</sup> Latter reports characterized the polyene metabolite, the collimonins (Figure 1.10) notable for antifungal and hyphae pigmentation activities.<sup>141</sup>

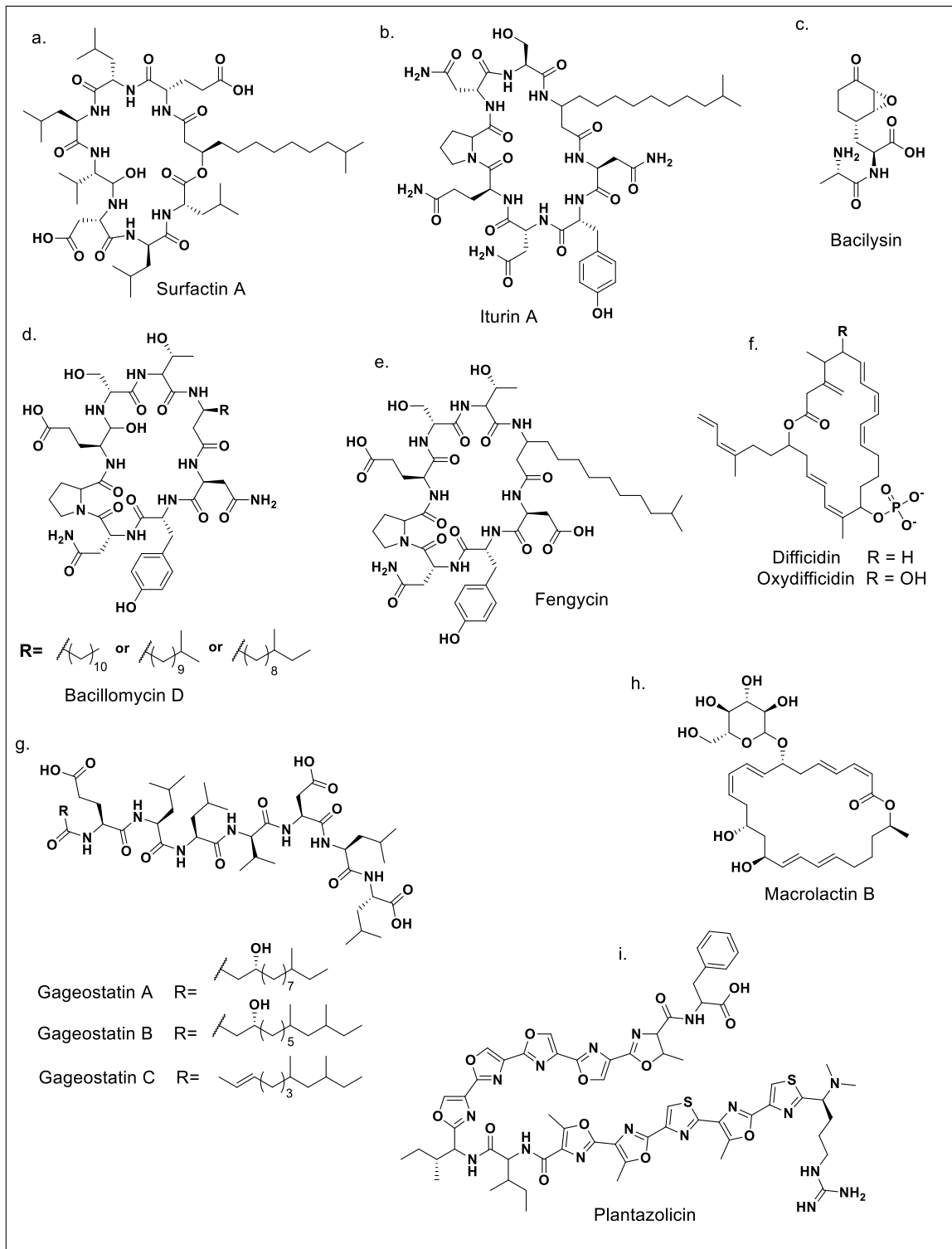


Figure 1.8. *Bacillus* species derived antimicrobials

### 1.2.5.3 Microbial Predation

There is a deficit of evidence for the beneficial effects of inter-bacterial predation in the rhizosphere. Predation is an important component of food webs therefore, it is essential to investigate the contributions of micro-predators to plant health. Overexpression of proteins encoding lytic enzymes, observed in disease-suppressive soils,<sup>29</sup> shows the potential benefits of this trait because feeding usually occurs after prey are killed by a plethora of lytic enzymes and toxic metabolites deployed to target cells by the micro-predators<sup>2</sup>. *Bdellovibrio* strains have been suggested for various biocontrol strategies because these ubiquitous motile bacteria are predators of Gram-negative organisms.<sup>13</sup> Various strains of *Bdellovibrio* species have been isolated from the rhizosphere when baited with phytopathogens like *Pseudomonas corrugate*, *Erwinia carotovora* subsp. *carotovora* and *Agrobacterium tumefaciens*<sup>11</sup> giving evidence for their ability to control plant pathogens.

Recently, this potential was tested against *Pectobacterium carotovorum* subsp. *Brasilense*, a highly virulent soft rot bacterial strain with *Bdellovibrio bacteriovorus* effectively reducing the cell density thereby inhibiting pathogenesis.<sup>13</sup> Yet, these bacteria are obligate predators thus they have a limit to prey options. Normally, prey preferences of micro-predators can determine their selection for biocontrol functions within specific rhizospheres as microbial communities are unique across plant species.<sup>50</sup> In a controlled study where <sup>13</sup>C-labelled *Pseudomonas pudita* and *Arthrobacter globiformis* cells represented both Gram-negative and Gram-positive bacteria respectively and designated as rhizobiome population, most test predators preferentially consumed *Pseudomonas pudita*. However, some myxobacteria also predated on *A. globiformis* revealing that a more relaxed feeding

preference, such as observed with generalist micro-predators,<sup>4</sup> could be more advantageous than the restrictive obligate predation.

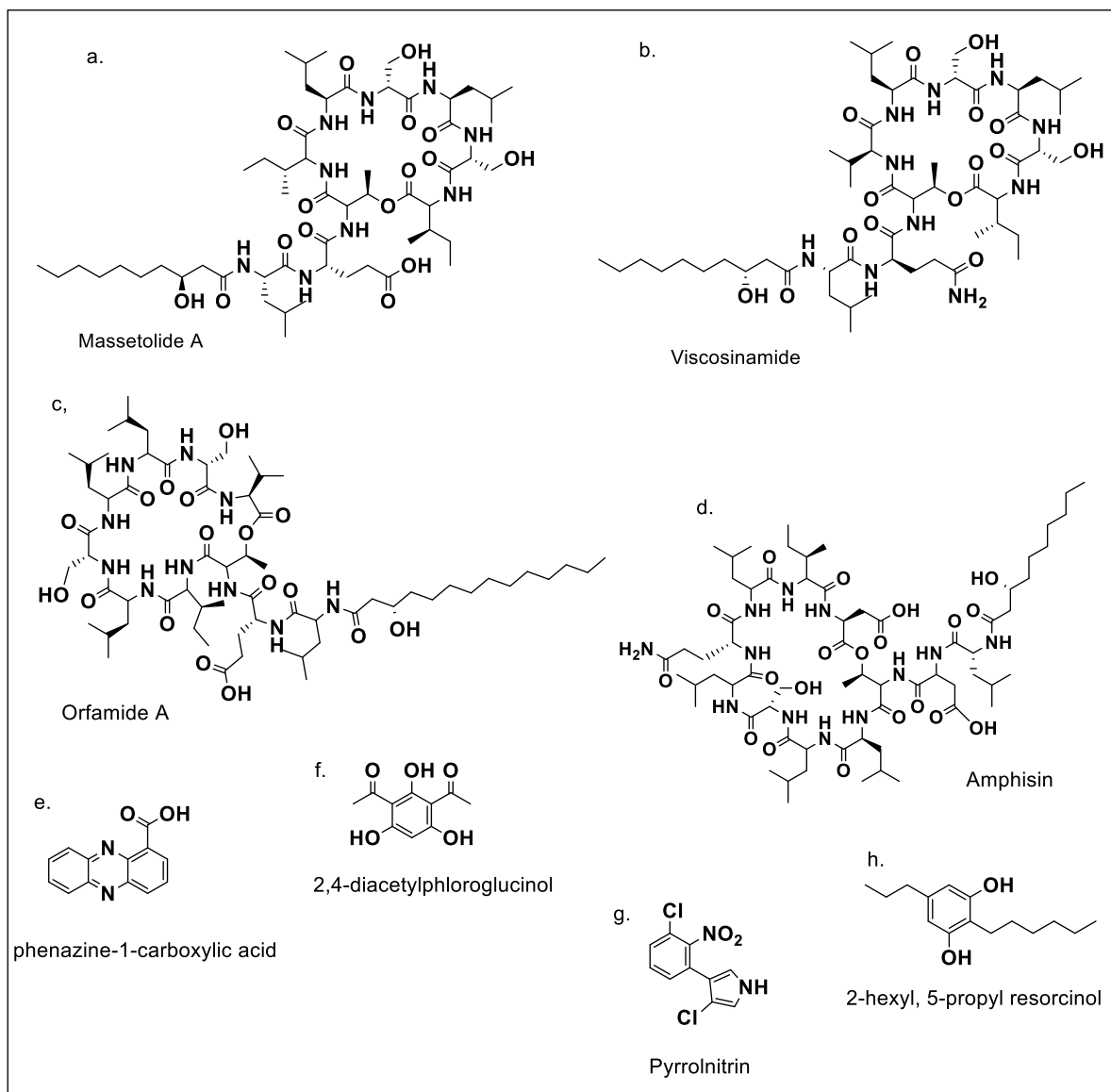


Figure 1.9. Examples of antimicrobials from rhizospheric *Pseudomonads*.

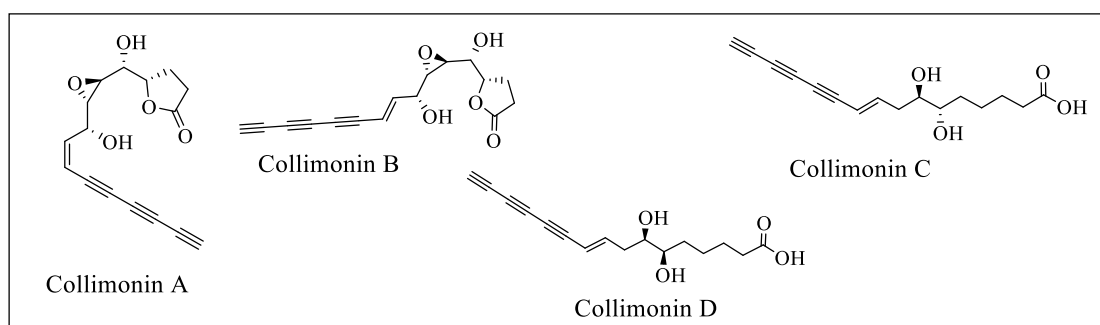


Figure 1.10. Examples of antimicrobials from plant-beneficial *Burkholderia*

### 1.3 Myxobacteria and the Rhizobiome Structure

Although there is a limited understanding of key factors that influence microbial community structures, the ability to control the members of a rhizobiome could improve biocontrol strategies currently employed in agricultural systems. Terrestrial myxobacteria have been sourced from various natural sources which are distributed across numerous climatic zones around the world and have a dependence on dead cells for their source of carbon and nitrogen.<sup>1,7,10,28</sup> These order of bacteria greatly contribute to nutrient cycling and carbon turnover in the soil via two nutritional behaviors that group them into predators or saprophytes.<sup>2-4,6,142,143</sup> Accordingly, it is expected that they could play important roles in influencing microbial structure. The chemo-attraction of *Corallococcus* sp. strain EGB towards low concentrations of maltose and maltitol in the exudates of cucumber<sup>20</sup> illustrates plants potential recruitment of these myxobacteria. However, because predatory myxobacterial isolations are usually conducted via baiting with prey organisms including *Pseudomonas* species and *E. coli*<sup>5</sup> from soil and environmental samples, a second potential for attraction of these bacteria to the microbial rich rhizosphere of plants exists. Furthermore, recent studies illustrating the eavesdropping of prey signaling by *Myxococcus xanthus*, resulting in the activation of predatory features on exposure to exogenous AHLs,<sup>144</sup> supports the idea that these bacteria can play a role in restructuring the microbial community of the rhizosphere.

Myxobacteria use outer membrane vesicles (OMV), from the cell envelope, to deliver lytic enzymes to prey during predation,<sup>27,145,146</sup> to break down prey cells and consume the released biomass. Earlier studies of myxobacteria identified *Polyangium* species that lyse the hyphae of the pathogenic fungi, *Rhizoctonia solani* through the perforation of the cell walls.<sup>147</sup> And more recently, an outer membrane  $\beta$ -1,6-glucanase was discovered in the

OMVs of *Corallococcus* sp. strain EGB which provided a cell wall-lysing selectivity for the control of fungal pathogens<sup>146</sup> because  $\beta$ -1,6-glucan is unique only to cell walls of fungi and some oomycetes but not plants.<sup>148</sup> Additionally, when compared to other biocontrol agents that instead generate enzymes targeting the mutable  $\beta$ -1,3-glucan<sup>149</sup> of fungal cell walls, the ability to generate the  $\beta$ -1,6-glucanases could provide a potent advantage for myxobacteria.

Biocontrol mechanisms aim at the competitive struggle for resources with phytopathogens,<sup>12</sup> however, myxobacteria can also decrease the population of their prey thereby altering the community structure of the rhizosphere. Consider that in a greenhouse setting and a 2-year field study, there was a consistent observation of the ability of *Corallococcus* sp. strain EGB to significantly reduce fungal diversity that resulted in the establishment of a disease-suppressive soil. This was achieved through increased predation of *Fusarium oxysporum* Schlecht. and a potential ability of the myxobacteria to support the proliferation of some identified plant growth-promoting bacteria.<sup>20</sup>

#### 1.4 Significance of Study

To date, literature has focused primarily on the impacts of the bacterial population on plant health<sup>30,31,38</sup> and how plants can benefit from a group of beneficial microbes.<sup>19,150,151</sup> Similarly, biocontrol studies have explored the generation of antimicrobials and lytic enzymes by these beneficial organisms and their potential supplementation to the soil.<sup>13,19,67</sup> While these studies certainly highlight the apparent cooperation between plants and beneficial microbes from the perspective of plants, an imbalance exists where there are limited data on how plant signals impact microbes on the molecular level. Such data are vital in giving a complete picture of plant-microbial interactions in the rhizosphere. This research

focuses on exploring the general responses, on a molecular level, of myxobacteria to selected phytohormones and plant-related signals.

Moreover, the current evidence of plant recruitment of beneficial microbes is based on chemotaxis towards exudates passively lost from the roots such as organic acids, sugars, amino acids, and polysaccharides, as well as the formation of shared biosynthetic pathways to prove symbiosis for the purpose of promoting the nutrient acquisition and deterring pathogens;<sup>51,152</sup> nonetheless, it is also relevant to investigate the potential recruitment of beneficial bacteria via actively generated plant distress signals and signals that are leaked into the rhizosphere during phytopathogenesis. Assays in Chapter 3 demonstrated unique metabolomic and transcriptomic responses of *Archangium* sp. strain Cb G35 to certain phytohormones and how these responses correlated to increases in growth motility of the myxobacteria.

Lastly, current literature shows limited access to specialized metabolites from extracts of axenic myxobacterial cultures resulting in most research focus on genome-mining strategies and techniques.<sup>7,9,153–156</sup> Because myxobacteria naturally develop niches in microbial-rich habitats,<sup>3,4,10</sup> the expected environmental and chemical cues experienced by these bacteria are lost in axenic laboratory cultures. This study offers a method that has the potential to imitate rhizospheric chemical cues while maintaining axenic cultivations as well as provide access to myxobacterial contributions to the shared chemical space within the rhizosphere. We show in Chapter 3, the generation of unique specialized metabolites resulting from both activation of the biosynthetic gene clusters of *Archangium* sp. strain Cb G35 and biotransformation of supplemented phytohormones. These significantly impacted antimicrobial activities as illustrated in Chapter 4 and gives evidence for an influence of plant-related signals on the metabolism of *Archangium* sp. strain Cb G35.

## CHAPTER 2. PROFILING THE BIOSYNTHETIC CAPACITY OF *ARCHANGIUM* SP.

### STRAIN CB G35

#### 2.1 Aims

The search for understudied bacteria that produce unique specialized metabolites has increased interest in the exploration of myxobacteria. These groups of bacteria are usually found in diverse habitats raising the idea of the existence of undiscovered or elusive strains which could immensely contribute to natural product discovery efforts.<sup>1,9</sup>

Considering the lack of genomic data on the myxobacteria, *Archangium* sp. strain Cb G35 belonging to the *Archangiaceae* family and Cystobacterineae suborder, this research sought to highlight the biosynthetic potentials of this *Archangium* strain and fill the gap in knowledge through the following objectives:

1. Obtain, sequence, and make publicly available the genomic information of *Archangium* sp. strain Cb G35
2. Analyze the biosynthetic and metabolic capacities of *Archangium* sp. strain Cb G35 using bioinformatics tools

Obtained results will facilitate the use of genome-mining techniques in accessing novel specialized metabolites from myxobacteria.



This part of Chapter 2 is published and has been formatted to follow the University of Mississippi's guidelines for dissertation preparation.

## 2.2 Draft Genome Sequence of *Archangium* sp. strain Cb G35

Barbara I. Adaikpoh, Scot E. Dowd and D. Cole Stevens.

*Genome Announc.* 2017, 5:e01678-16

### 2.2.1 Abstract

In an effort to explore myxobacterial natural product biosynthetic pathways, the draft genome sequence of *Archangium* sp. strain Cb G35 has been obtained. Analysis of the genome using antiSMASH predicts 49 natural product biosynthetic pathways. This genome will contribute to the investigation of myxobacterial secondary metabolite biosynthetic pathways.

### 2.2.2 Introduction

Myxobacteria produce a plethora of structurally diverse bioactive natural products.<sup>25,153,157</sup> Isolated from tree bark in Bangalore, India, *Archangium* sp. strain Cb G35 (DSM 52696) was reported to produce the antibiotic roimatacene, as well as six novel *p*-hydroxyacetophenone amides.<sup>158,159</sup> Herein, we report a draft genome sequence for *Archangium* sp. strain Cb G35, which was collected in an effort to explore myxobacterial natural product biosynthesis.

### 2.2.3 Materials and Methods

*Archangium* sp. strain Cb G35 was acquired from the German Collection of Microorganisms DSMZ) in Braunschweig (DSM 52696). *Archangium* sp. strain Cb G35 has been referenced as *Cystobacter ferrugineus* strain Cb G35 and *Cystobacter gracilis* strain Cb G35 prior to a suggested reclassification.<sup>158–160</sup> Genomic DNA was isolated using a GeneJET genomic DNA purification kit (Thermo Fisher). Sequencing was performed at MR DNA (Shallowater, TX) using an Illumina HiSeq system. Nextera DNA sample preparation kit was

used for library construction (Illumina) according to the manufacturer's user guide. Following the library preparation, the final concentration of the library (7.32 ng/l) was measured using the Qubit double-stranded DNA (dsDNA) high-sensitivity (HS) assay kit (Life Technologies, Inc.), and the average library size (881 bp) was determined using the Agilent 2100 Bioanalyzer (Agilent Technologies). The libraries were pooled and diluted (to 10.0 pM) and paired-end sequenced for 500 cycles, with an average coverage of 50. An initial annotation was completed using the Rapid Annotations using Subsystems Technology (RAST) server,<sup>161</sup> with further annotation requested by the NCBI Prokaryotic Genome Annotation Pipeline.<sup>162,163</sup> The draft genome contains 12,927,638 bp with 89 identified RNAs, 10,395 coding sequences, and a 68.8% GC content across 41 contigs containing protein-coding genes.

#### 2.2.4 Results and Discussion

Ultimately, 49 unique secondary metabolite biosynthetic pathways were identified using antiSMASH (version 3.0.5), including pathways for 10 hybrid nonribosomal peptide polyketides, six nonribosomal peptides, six bacteriocins, five polyketides, five terpenes, four lantipeptides, and two microviridins.<sup>164</sup> The biosynthetic pathways for reported natural products roimatacene and *p*-hydroxyacetophenone amides were not obvious from antiSMASH analysis and require further investigation.

Accession number(s): This whole-genome shotgun project has been deposited in DDBJ/ENA/GenBank under the accession number MPOI00000000.

We believe the draft genome sequence will help facilitate the characterization of myxobacterial secondary metabolite biosynthetic pathways and the discovery of new myxobacterial natural products.

## 2.3 Analysis of the Metabolic Capacity of *Archangium* sp. strain Cb G35

### 2.3.1 Abstract

Genome mining techniques have benefitted from the increased accessibility of bacterial genome sequences and facilitated natural product discovery. As sources of diverse specialized metabolites, myxobacteria have gained attention with increased efforts to access new and rare strains. Using the antiSMASH and Antibiotic Resistance Target Seeker platforms, six resistance models were found to cluster with seven biosynthetic gene clusters that encoded for unique specialized metabolites. This analysis will facilitate genome-mining efforts from myxobacteria.

### 2.3.2 Introduction

Initially observed in 1809, over 600 compounds with unique scaffolds have been reported from the Myxococcales. This order of bacteria provides a prolific source of diverse specialized metabolites with a broad range of activities that has caught the attention of the agricultural, biotechnological and medical systems.<sup>21,25,26,157,158</sup> Studies on myxobacterial specialized metabolites have significantly benefitted from genomics analysis.<sup>153</sup> With the increased access to high-throughput genome sequencing methods, *in silico* analysis of biosynthetic gene capacities of microorganisms has led to the development of sophisticated genome-mining tools and techniques.<sup>9,165,166</sup> Sequence-based approaches to the discovery of microbial natural products bypasses the limitations of rediscovery, silent gene clusters and

uncultivable microbes often encountered in the laboratory.<sup>167,168</sup> Currently, only roimatacene and *p*-hydroxyacetophenone amides have been reported from *Archangium* sp. strain Cb G35 even though the genomic sequence of these bacteria comprise more biosynthetic machineries capable of encoding specialized metabolites.<sup>158,159,169</sup> Markers in the genome are useful for identifying and manipulating genes of interest. Often times, self-resistance determinants are found clustering with biosynthetic gene clusters (BGCs) capable of encoding antimicrobials and has resulted in approaches that target such indicators.<sup>155,170</sup> Herein, the analysis of the genomic sequence of *A.* sp. strain Cb G35 using bioinformatics tools to display the biosynthetic profile of the myxobacteria is presented. To find potential antibiotic targets, the antibiotic resistance markers were identified from the genome.

### 2.3.3 Materials and Methods

#### 2.3.3.1 Medias and Strains

*Archangium* sp. strain Cb G35 (DSM 52696) initially obtained from the German Collection of Microorganisms (DSMZ) in Braunschweig was grown on VY/2 agar (5 g/L baker's yeast, 1.36 g/L CaCl<sub>2</sub>, 0.5 mg/L vitamin B12, 15 g/L agar, pH 7.2) at 30°C for 7 days. Filter-sterilized kanamycin (40 µg/mL), tetracycline (10 µg/mL), ampicillin (100 µg/mL), hygromycin (150 µg/mL), gentamycin (50 µg/mL), chloramphenicol (30 µg/mL), polymyxin (50 µg/mL) and spectinomycin (50 µg/mL) were added to pre-cooled VY/2 agar when appropriate.<sup>171,172</sup>

### 2.3.3.2 Analysis with antiSMASH and Antibiotics Resistance Target seeker (ARTS)

Accession number was submitted to antiSMASH version 5.0 with the ClusterFinder algorithm to generate identified biosynthetic gene clusters. antiSMASH facilitates the identification and annotation of BGCs in bacterial and fungal genomes based on BGC-specific profile hidden Markov models of genes.<sup>166</sup> The ARTS webserver (version 2) was used to directly detect potential antibiotic targets in the genome and known resistance markers were identified. ARTS acquires information about antibiotic targets from published Pfam models of targeted essential genes and resistance factors from public databases including the Jacobi and Bush collection, the Comprehensive Antibiotic Resistance Database (CARD), the LACTamase Engineering Database (LACED) and ResFams.<sup>173</sup>

### 2.3.4 Results and Discussion

Traditional methods of screening microbial extracts for bioactivity can be laborious and often suffers from high rediscovery rates.<sup>167</sup> Genome-mining processes use bioinformatics tools to target specific biosynthetic gene clusters of interest. We report a high diversity of BGCs of *A. sp.* strain Cb G35, observable in both antiSMASH and ARTS analysis (Table 2.1). antiSMASH analysis detected 48 regions, which differ from our previous reports<sup>169</sup> and ARTS analysis. However, these changes are expected because large BGCs like polyketide synthases (PKS) and non-ribosomal peptide synthases (NRPS) can split across contigs and increase the number of predicted BGCs. The co-localized resistance markers and essential genes suggest that the corresponding BGCs will have antibacterial properties.

Table 2.1. Summary of identified biosynthetic gene clusters (BGCs) and other potential targets from the analysis of the genome of *A. sp. Cb G35*

Summary of BGC hits	<i>A. sp. strain Cb G35</i>
antiSMASH identification	48
Number of hits to MIBiG database	46
Predicated by ARTS	47
Number of co-localized essential genes	36
Number of duplicated essential genes	36
Number of co-localized known resistance models	7

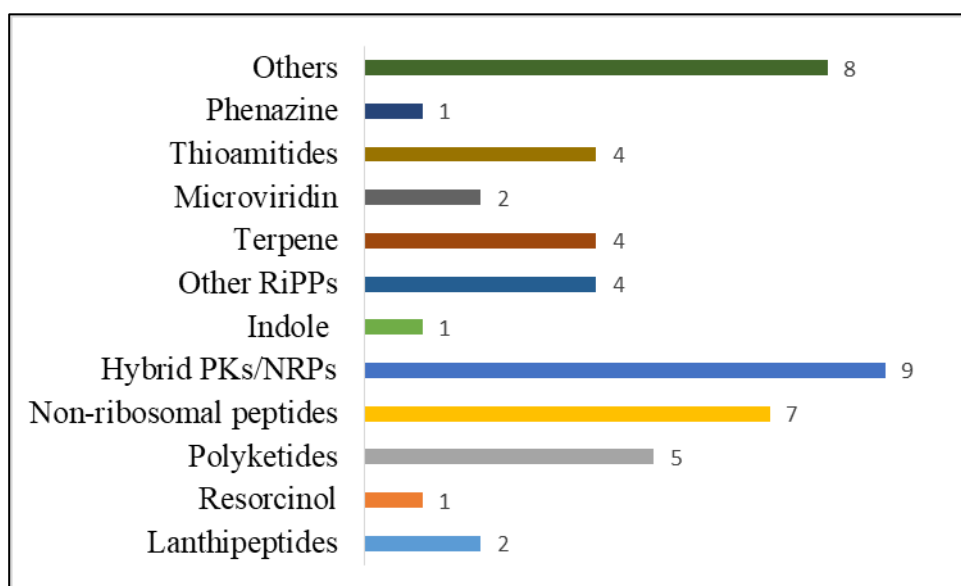


Figure 2.1. antiSMASH v6.0 predicted biosynthetic gene clusters from the genome of *Archangium sp. strain Cb G35*. The number of identified BGCs is indicated.

All but two BGCs are similar to known BGCs from the MIBiG database<sup>174</sup> suggesting the potential for encoding novel metabolites. The most abundant BGCs were predicted to encode for hybrid PKs/NRPs and NRPs (Figure 2.1) and on further inspection, some homologies to known BGCs that encode for gephyronic acid, nostopeptolide A2, rhizomide, melithiazol A and microsclerodermin metabolites were detected. Similar metabolites have been isolated from other myxobacterial strains.<sup>26</sup> Myxobacterial specialized metabolites that

have been isolated are mostly of the PKs, NRPs, hybrids of PK/NRP, and terpenoids classes;<sup>26,157</sup> *A. sp.* genomic information shows a similar pattern of potential specialized metabolites with the most abundant BGCs encoding for the hybrid PK/NRP compounds (Figure 2.1). We have provided exhaustive homology networks of BGCs shared by all myxobacteria with publicly available genome sequences.<sup>24</sup>

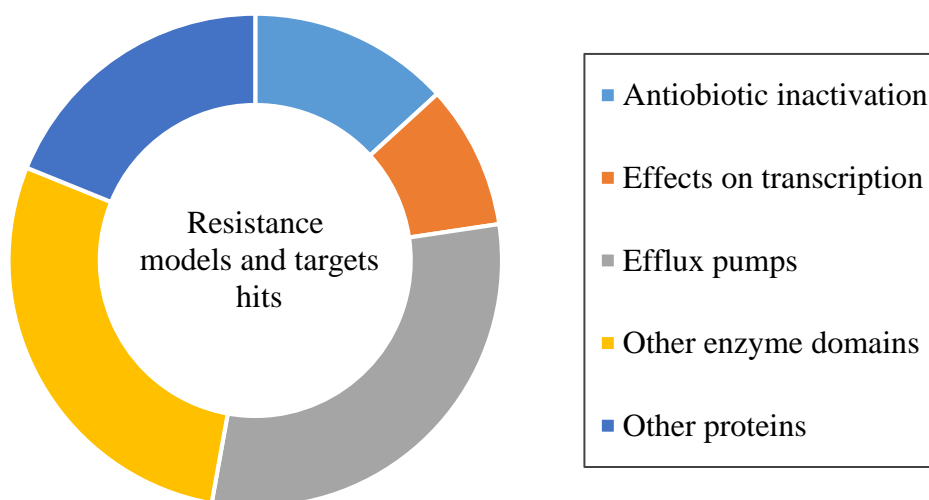


Figure 2.2. ARTS rendered hits to known resistance models and targets grouped according to the mechanism of resistance. Complete lists of models and targets are available in Table A.1, Appendix.

Strategies to target antibiotic resistance genes are based on the idea that microbes that generate antimicrobials have developed a way to protect themselves from the toxicity of the metabolites.<sup>155,170</sup> ARTS tool also associates essential genes with gene duplication or co-localization in the BGCs as important in this strategy.<sup>175</sup> 53 known antibiotic resistance gene models including resistance housekeeping genes were observed from ARTS analysis of the genome (Table A.1, Appendix). Although most identified resistance genes were efflux pumps (Figure 2.2), seven resistance markers were found to cluster close to six BGCs, with most BGCs belonging to the PK/NRP hybrid class (Table 2.2, Table A.2, Appendix).



Table 2.2. Proximity hits of resistance markers to biosynthetic gene clusters from ARTS analysis.

<b>Cluster number</b>	<b>Type</b>	<b>Source</b>	<b>Location</b>	<b>Resistance model hit</b>
cluster-13_1	NRPS, Type 1-PKS	scaffold_13	41163 - 93514	Pentapeptide repeats (9 copies) (2 models)
cluster-13_2	Type 3 PKS	scaffold_13	276511 - 331711	Pentapeptide repeats (4 copies)
cluster-13_3	NRPS, Type 1-PKS	scaffold_13	419025 - 486153	Class D $\beta$ -lactamases
cluster-3_2	Lanthipeptide	scaffold_3	254542 - 277791	Resistance-nodulation-cell division efflux pump
cluster-3_3	NRPS, Type 1-PKS	scaffold_3	387410 - 488811	ATP-binding cassette (ABC) efflux pump
cluster-17_1	NRPS, arylpolyene, Type 1 PKS	scaffold_17	154502 - 238295	ATP-binding cassette (ABC) efflux pump

Table 2.3. Sensitivity testing of *A. sp.* strain Cb G35 to antibiotics. - (negative) - sensitive, + (positive) - resistant, SG (slight growth)

<b>Antibiotics (ug/mL)</b>	<b>Growth</b>
Kanamycin (40)	-
Tetracycline (10)	SG
Spectinomycin (50)	SG
Gentamycin (50)	+
Chloramphenicol (30)	SG
Hygromycin (150)	-
Ampicillin (100)	+
Polymixin (50)	+

Information on these resistance markers were also found in the antiSMASH analysis. Furthermore, this study reports the sensitivity of *A. sp.* strain Cb G35 to kanamycin and hygromycin (Table 2.3). The analysis of the spectrum of resistance contributes to the physiological characterization of the myxobacteria.<sup>171,172,176</sup> Our results provide the genome-mining potential for *Archangium sp.* strain Cb G35 that will serve as a resource for natural product discovery.

## 2.4 Conclusions

We have established the biosynthetic capacity of *Archangium sp.* strain Cb G35. Profiling of the genome sequence of this myxobacterium reveals the potential for accessing a high diversity of specialized metabolites and selected BGCs can be prioritized for investigation.

## CHAPTER 3. ASSESSING RESPONSES OF *ARCHANGIUM* SP. STRAIN CB G35 TO PHYTOHORMONES AND PLANT-RELATED SIGNALS

### 3.1 Aims

To understand the ecological roles of organisms, distinct environments like the rhizosphere have been identified to possess unique chemical spaces. The rhizospheric environment benefits from chemical interactions resulting from plant-microbe and microbe-microbe interactions that shape the community structure.<sup>177-179</sup> Plants recruit beneficial bacteria, through the secretion of exudates, for aid in nutrient acquisition and protection from phytopathogens.<sup>41,42,180</sup> The study of the influence that phytohormones and plant-related signals have on the metabolism of *Archangium* sp. strain Cb G35 is essential because these myxobacteria have been associated with plants.<sup>169</sup> Exogenous supplementation of phytohormones and plant-related signals, at ecologically equivalent titers, in axenic culture conditions of these bacteria will be studied under the following goals:

1. Determine impacts on the rate of swarming to observe selective chemo-attraction of *A.* sp. strain Cb G35 to phytohormones and plant-related signals
2. Ascertain global changes in the transcriptome of *A.* sp. strain Cb G35 in response to the perception of phytohormones and plant-related signals
3. Identify induced changes in the metabolome induced by phytohormones and plant-related signals in the micro-environment of the bacteria

Observed changes in motility, global transcriptome, and metabolome will give a comprehensive story of the intricate relationship that potentially occurs between *A. sp.* strain Cb G35 and plants in the rhizosphere.

This part of Chapter 3 is published and has been formatted to follow the University of Mississippi's guidelines for dissertation preparation.

### 3.2 Myxobacterial Response to Methyljasmonate Exposure Indicates Contribution to Plant Recruitment of Micropredators

Barbara I. Adaikpoh, Shukria Akbar, Hanan Albataineh, Sandeep K. Misra, Joshua S. Sharp and D. Cole Stevens. *Front. Microbiol.* (2020) 11:34.

### 3.2.1 Abstract

Chemical exchanges between plants and microbes within rhizobiomes are critical to the development of community structure. Volatile root exudates such as the phytohormone methyljasmonate (MeJA) contribute to various plant stress responses and have been implicated to play a role in the maintenance of microbial communities. Myxobacteria are competent predators of plant pathogens and are generally considered beneficial to rhizobiomes. While plant recruitment of myxobacteria to stave off pathogens has been suggested, no involved chemical signaling processes are known. Herein we expose predatory myxobacteria to MeJA and employ untargeted mass spectrometry, motility assays, and RNA sequencing to monitor changes in features associated with predation such as specialized metabolism, swarm expansion, and production of lytic enzymes. From a panel of four myxobacteria, we observe the most robust metabolic response from plant-associated *Archangium* sp. strain Cb G35 with 10  $\mu$ M MeJA impacting the production of at least 300 metabolites and inducing a  $\geq$  four-fold change in transcription for 56 genes. We also observe that MeJA induces *A.* sp. motility supporting plant recruitment of a subset of the investigated micropredators. Provided the varying responses to MeJA exposure, our observations indicate that MeJA contributes to the recruitment of select predatory myxobacteria suggesting further efforts are required to explore the microbial impact of plant exudates associated with biotic stress.

Keywords: myxobacteria, methyljasmonate, rhizobiome, micropredator, phytohormones

### 3.2.2 Introduction

Complex communities of microbes within rhizobiosomes significantly benefit plant health.<sup>168,178–184</sup> The role that plants might play in curating these microbial populations remains mostly theoretical.<sup>178,179,183,185–190</sup> However, metagenomic studies have indicated numerous plant species maintain distinct rhizobiosomes.<sup>183,189,191–196</sup> While a variety of factors contribute to these organized communities, volatile exudates or volatile organic compounds such as the phytohormone methyljasmonate (MeJA) are associated with defense responses utilized by plants to combat pathogenic microorganisms and herbivorous insects.<sup>14,177,183,197–199</sup> Considering the requirement of these exudates to be produced at titers sufficient for communication throughout soils, exudates might also facilitate recruitment or maintenance of beneficial microbial populations of the root microbiome.<sup>183</sup> Microbes belonging to one such group of bacteria considered beneficial, the Myxococcales, more colloquially referred to as myxobacteria, are micropredators that are ubiquitous in soils and capably predate microbes from genera that include plant pathogens.<sup>5,8,10,200–205</sup> Predatory myxobacteria demonstrate complicated social features, contribute to carbon turnover, produce a variety of antimicrobial specialized metabolites, and significantly impact the microbial food web within soils.<sup>1,3,8,23,26,206–208</sup> Myxobacteria have also been observed to activate predatory features when exposed to exogenous, quorum signaling molecules typically produced by prey bacteria; this precedent for community signal perception and response makes myxobacteria excellent candidates for MeJA exposure experiments.<sup>144</sup> Given their potential as pathogen-suppressing bacteria beneficial to root microbiomes, we sought to investigate how myxobacteria respond when exposed to ecologically equivalent titers of the phytohormone MeJA.<sup>209–211</sup>

We suggest the following responses to MeJA exposure would support plant recruitment of myxobacteria: (1) global changes in metabolism, (2) increased motility to support recruitment, and (3) impacted production of predation-associated lytic enzymes. Myxobacteria are broadly referenced as beneficial to rhizobiomes without distinction between phylogenetically dissimilar members. For these experiments, the myxobacteria *Archangium* sp. strain Cb G35, *Corallocooccus coralloides* strain M2, *Cystobacter ferrugineus* strain Cbfe23, and *Nannocystis pusilla* strain Na p2 were exposed to MeJA and induced metabolic responses were determined using untargeted mass spectrometrybased profiling.<sup>158,169,212</sup> The MeJA-impacted motilities of *A. sp.*, *C. coralloides*, and *C. ferrugineus* and transcriptomic responses from the plant-associated myxobacterium *A. sp.* strain Cb G35, originally isolated from tree bark in India, were also determined using swarming assays and RNA sequencing.<sup>158,169</sup>

### 3.2.3 Materials and Methods

#### 3.2.3.1 Medias and Strains

For all assays, *A. sp.* strain Cb G35 (DSM 52696), *C. coralloides* strain M2 (DSM 2259), *C. ferrugineus* strain Cb fe23 (DSM 52764), and *N. pusilla* strain Na p20 (DSM 53165) initially obtained from the German Collection of Microorganisms (DSMZ) in Braunschweig were used. Myxobacteria were grown on VY/2 agar (5 g/L baker's yeast, 1.36 g/L CaCl<sub>2</sub>, 0.5 mg/L vitamin B12, 15 g/L agar, pH 7.2).



### 3.2.3.2 MeJA Exposure Experiments

For MeJA exposure conditions, required volumes of filter sterilized, ( $\pm$ )-MeJA (Cayman Chemical) from a 150 mM stock prepared in DMSO were added to autoclaved medium at 55°C. For RNA-seq and LC-MS/MS analysis, *A. sp.* was cultivated on VY/2 media supplemented with 10  $\mu$ M MeJA where appropriate and grown at 30°C for 7 days. While similar MeJA exposure experiments conducted with the plant pathogen *R. radiobacter* utilized MeJA concentrations as high as 250  $\mu$ M, a more conservative MeJA concentration of 10  $\mu$ M informed by literature investigating plant responses to exogenous MeJA exposure as well as stress induced production of jasmonates was utilized throughout.<sup>209,211,213</sup>

### 3.2.3.3 Metabolite Extraction and Analysis

After 5–7 days of cultivation, myxobacterial plates were manually diced and extracted with excess EtOAc. Pooled EtOAc was filtered and dried *in vacuo* to provide crude extracts for LC-MS/MS analysis. LC-MS/MS analysis of the extracted samples was performed on an Orbitrap Fusion instrument (Thermo Scientific, San Jose, CA, United States) controlled with Xcalibur version 2.0.7 and coupled to a Dionex Ultimate 3000 nanoUHPLC system. Samples were loaded onto a PepMap 100 C18 column (0.3 mm  $\times$  150 mm, 2  $\mu$ m, Thermo Fisher Scientific). Separation of the samples was performed using mobile phase A (0.1% formic acid in water) and mobile phase B (0.1% formic acid in acetonitrile) at a rate of 6  $\mu$ L/min. The samples were eluted with a gradient consisting of 5–60% solvent B over 15 min, ramped to 95% B over 2 min, held for 3 min, and then returned to 5% B over 3 min and held for 8 min. All data were acquired in positive ion mode. Collision-induced dissociation (CID) was used to fragment molecules, with an isolation width of 3 m/z units. The spray voltage was set to 3600 V, and the temperature of the heated capillary was set to 300°C. In CID mode, full

MS scans were acquired from m/z 150 to 1200 followed by eight subsequent MS2 scans on the top eight most abundant peaks. The orbitrap resolution for both the MS1 and MS2 scans was 120,000. The expected mass accuracy was < 3 ppm.

#### 3.2.3.4 GNPS, NAP, and XCMS-MRM Analysis

Generated data were converted to .mzXML files using MSConvert and mass spectrometry molecular networks were generated using the GNPS platform.<sup>168</sup> A figure of the corresponding Cytoscape-rendered molecular network is provided.<sup>214</sup> LC-MS/MS data for this analysis were also deposited in the MassIVE Public GNPS dataset . For subsequent NAP analysis, the cluster index (127) that included 225.148 m/z identified as MeJA and confirmed via standard was submitted to the NAP\_CCMS2 (version 1.2.5) workflow. Control experiments with MeJA supplemented media and no myxobacteria were run for 7 days, extracted, and analyzed to confirm the absence of any oxidized MeJA analogs; only saponification of MeJA to jasmonic acid was observed after 7 days. Pairwise analysis of converted .mzXML files was performed using XCMS-MRM and the default HPLC/Orbitrap (136) parameters. Within the XCMS-MRM result tables, determination of MeJA-impacted detected features was afforded by filtering results for those with a  $\geq$  five-fold change and  $p \leq 0.05$ .

#### 3.2.3.5 Motility Assays

To monitor swarm expansion rates, the bacteria were cultured on their respective media as described above. After 24 h of incubation, 5 mM stock solutions of MeJA and decanoic acid were spotted onto the solid media, to a concentration of 0.17% v/v, around cells and swarm diameters were recorded daily for 4 days. DMSO was used as vehicle control

for comparison. Minimum of six replicates were included in all motility assays. PRISM v7.0d was used to measure the statistical significance of changes in swarm expansion rates across the strains using two-way ANOVA and the Dunnett's multiple comparisons test to compare simple effects within rows.

#### 3.2.3.6 RNAseq Analysis

Total RNA was isolated from the samples using the RNeasy PowerSoil Total RNA Kit (Qiagen) following the manufacturer's instructions; 500 mg sample was used for extractions. The concentration of total RNA was determined using the Qubit R RNA Assay Kit (Life Technologies). For rRNA depletion, first, 1000 ng of total RNA was used to remove the DNA contamination using Baseline-ZERO™ DNase (Epicentre) following the manufacturer's instructions followed by purification using the RNA Clean and Concentrator5 columns (Zymo Research). DNA free RNA samples were used for rRNA removal by using RiboMinus™ rRNA Removal Kit (Bacteria; Thermo Fisher Scientific) and final purification was performed using the RNA Clean and Concentrator-5 columns (Zymo Research). rRNA depleted samples were used for library preparation using the KAPA mRNA HyperPrep Kits (Roche) by following the manufacturer's instructions. Following the library preparation, the final concentration of each library was measured using the Qubit R dsDNA HS Assay Kit (Life Technologies), and average library size for each was determined using the Agilent 2100 Bioanalyzer (Agilent Technologies). The libraries were then pooled in equimolar ratios of 0.75 nM, and sequenced paired end for 300 cycles using the NovaSeq 6000 system (Illumina). RNAseq analysis was performed using ArrayStar V15. All sequencing services were provided by MR DNA, Molecular Research LP (Shallowater, TX, United States). Raw data fastq files from these experiments are deposited in the Sequence Read Archive at the

National Center for Biotechnology Information and are publicly available (PRJNA555342). All *A. sp.* genes with MeJA-impacted transcription  $\geq$  four-fold change at 99% confidence are provided as Supplementary material that also provides linear total RPKM values, DNA sequences, and protein IDs for all replicates.

### 3.2.4 Results

#### 3.2.4.1 MeJA Exposure Impacts Myxobacterial Metabolism

Myxobacteria utilize a combination of antimicrobial specialized metabolites and lytic enzymes to facilitate consumption of prey<sup>3,26</sup> If the plant phytohormone MeJA is involved in recruitment of myxobacteria to stave off pathogens, a shift in metabolism to produce predation-associated metabolites during exposure experiments might be observable. Utilizing XCMS-MRM to compare untargeted mass spectrometry datasets from MeJA exposed extracts against unexposed extracts, each investigated myxobacteria demonstrated a significant, albeit varied, metabolic shift (Figure 2.1).<sup>215,216</sup> From these datasets, we observe various changes in detected intensities ranging from 54–349 total metabolites with *C. coralloides* extracts being the least impacted and *A. sp.* being the most (Figure 2.1). Extracts from *A. sp.* had the most features with a  $\geq$  five-fold increase in detection with a total of 245, and *N. pusilla* had the most features with a  $\geq$  five-fold decrease in detection with a total of 224. Subsequent molecular networking of the datasets using the Global Natural Products Social Molecular Networking (GNPS) platform, suggested each myxobacteria capably metabolized MeJA to afford observable oxidized analogs.<sup>168</sup> LCMS/MS data from *A. sp.* extracts are available in a MassIVE Public GNPS dataset (MSV000083921). Considering the plant pathogen *Magnaporthe oryzae* oxidizes jasmonic acid to 12-hydroxyjasmonic acid (colloquially referred to as tuberonic acid) to subvert jasmonate-associated immune response,

we utilized the GNPS-affiliated, theoretical/in silico tool, Network Annotation Propagation (NAP) to explore the identity of the putative MeJA-associated metabolites.<sup>168,217,218</sup> Structural predictions provided by NAP suggested all four investigated myxobacteria might produce any one of the following known jasmonic acid analogs 12-hydroxyjasmonic acid, 11-hydroxyjasmonic acid, or 8-hydroxyjasmonic acid (227.127 m/z) as well as the known metabolite 4,5-didehydrojasmonate (223.133 m/z) previously isolated from *Jasminum grandiflorum*.<sup>219,220</sup> (Figure 2.2A) However, dissimilar retention times and fragmentation patterns of the oxidized MeJA metabolites when compared to a purchased standard confirmed that none of the investigated myxobacteria produce the pathogen-associated analog 12-hydroxyjasmonic acid.

Of the features within *A. sp.* extracts identified by GNPS with high fragmentation similarities (cosine > 0.8) to databases entries, a total of two demonstrated a significant change in detected quantities when exposed to MeJA. The identified metabolites included  $\alpha$ -bisabolol (205.195 m/z; [M + HH<sub>2</sub>O]) and 4-(3-hydroxybutyl)-3,5,5-trimethylcyclohex-3-en-1-ol (213.185 m/z; [M + H]). Detected quantities of both metabolites were decreased in *A. sp.* extracts exposed to MeJA (Figure 2.2B). While *A. sp.* demonstrated the most robust metabolic response to MeJA exposure, the previously reported antimicrobial metabolite roimatacene was conspicuously absent from all generated extracts.<sup>158</sup> However, this absence can reasonably be attributed to the difference in *A. sp.* cultivation conditions and medias combined with the reported instability of roimatacene.<sup>158</sup>

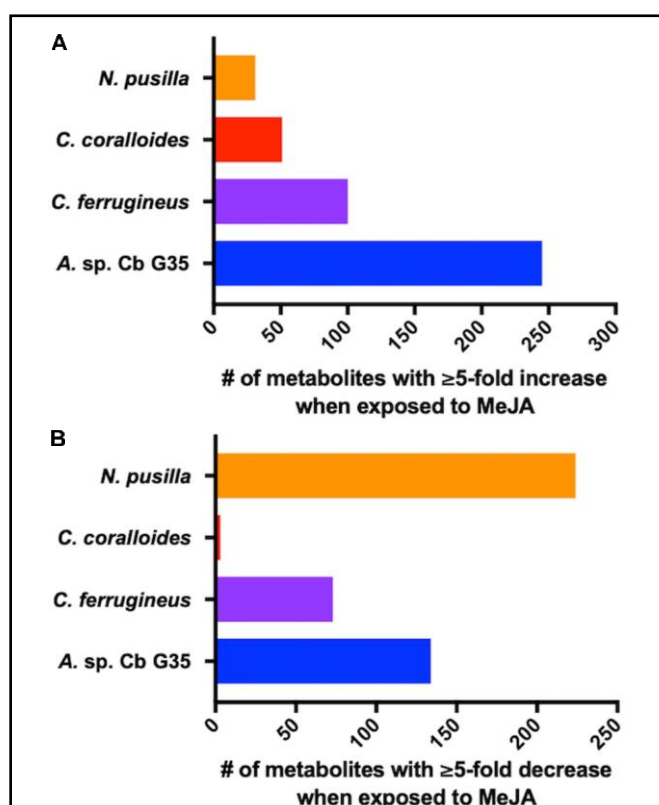


Figure 3.1. MeJA-impacted features provided by XCMS analysis of LC-MS/MS data after filtering feature tables for those with a  $\geq$  fivefold change and  $p \leq 0.05$  with (A) depicting increased metabolites and (B) depicting decreased metabolites

### 3.2.4.2 MeJA Exposure Influences *A. sp.* Motility

Any increased motility induced by MeJA exposure would also support plant recruitment of myxobacteria. Growth of myxobacteria in cooperative swarms affords the ability to observe growth as a function of swarm expansion rate.<sup>221,222</sup> The impact of MeJA exposure on swarm expansion rates was observed by measuring swarm diameters daily for MeJA exposed and unexposed myxobacteria. *N. pusilla* was excluded from motility assays due to the agarolytic growth and atypical swarming patterns. Each myxobacterium was also exposed to 10  $\mu$ M decanoic acid due its previously reported impact on myxobacterial motility.<sup>221</sup> A significant increase in *A. sp.* swarm diameters was observed in MeJA-exposed

samples when compared to unexposed samples after 4 days of growth with the most significant increase in swarm diameter occurring after the first day of exposure (Figure 2.3). Interestingly, both decanoic acid and MeJA induced significant changes in *A. sp.* swarming. Of the three myxobacteria subjected to motility assays, only *A. sp.* demonstrated a response (Figure 2.3).

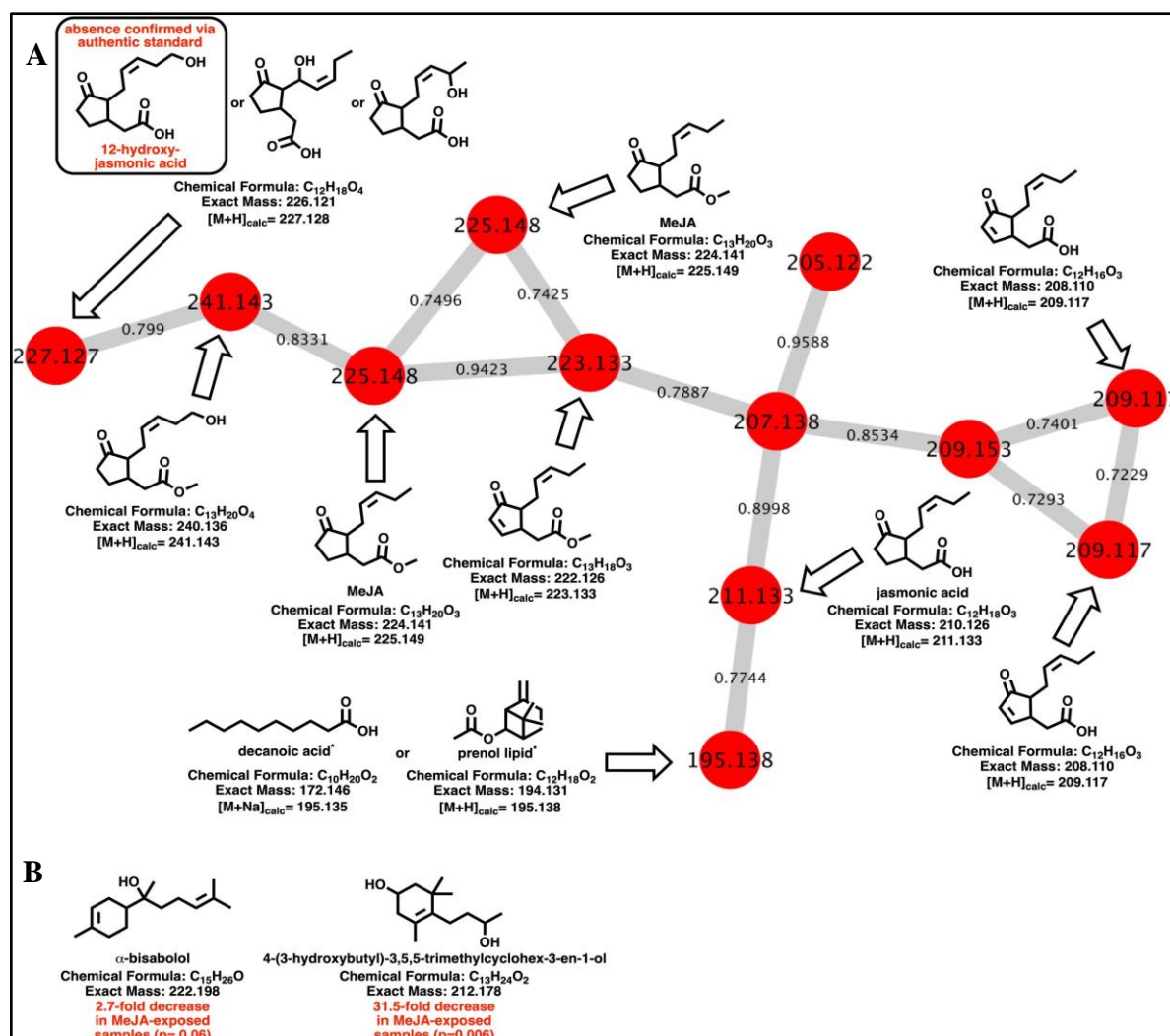


Figure 3.2. (A) Molecular network of MeJA and associated metabolites including nodes labeled with detected parent ions and edges labeled with cosine values. Predicted metabolites provided by NAP analysis of the GNPS-rendered cluster. \*Multiple fatty acids and prenol lipids with identical exact masses predicted by NAP analysis. (B) Metabolites identified by GNPS analysis (cosine > 0.8) impacted by MeJA exposure.

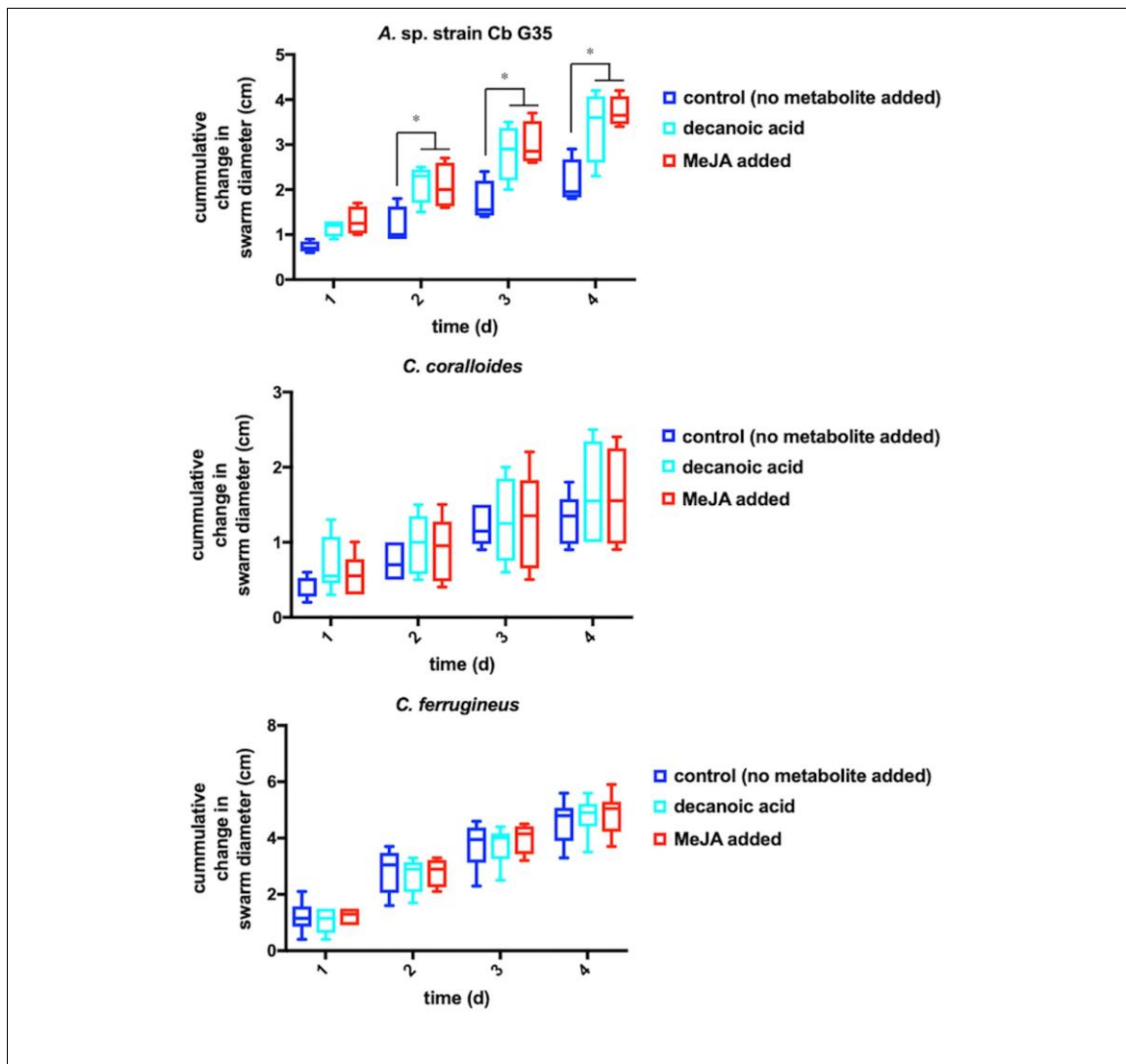


Figure 3.3. Motility assays depicting cumulative change in swarm diameter post MeJA exposure. The symbol “\*” indicates  $p < 0.05$ .

Decanoic acid induced activation of the frizzy (*frz*) signal transduction pathway associated with chemotaxis has been reported from in the model myxobacterium *Myxococcus xanthus*.<sup>221</sup> The similar responses between decanoic acid and MeJA exposures combined with the observed MeJA-induced metabolite from *A. sp.* predicted to be decanoic acid (Figure 2.2) suggests overlap between metabolic and motility responses.



### 3.2.4.3 MeJA Exposure Induces Changes in *A. sp.* Transcriptome and Activates

#### Transcription of Lytic Enzymes

Increased transcription of lytic enzymes induced by MeJA exposure would support exudate-associated predation and correlate with previously observed MeJA-induced metabolic shifts. Provided the robust metabolic response and MeJA impacting motility from *A. sp.*, RNA sequencing was employed to provide transcriptomes for MeJA exposed and unexposed cultures of *A. sp.* Using the sequenced genome for *A. sp.* strain Cb G35 (NZ\_MPOI00000000.1) as a reference, a total of 56 genes were determined to experience a statistically significant, > four-fold difference in expression (Tables 2.1, 2.2 and Figure 2.4).<sup>169</sup> A total of 15 overexpressed genes during MeJA exposure increased four to 147-fold including a 73-fold change for a predicted lytic amidase with an identified CHAP domain.<sup>223,224</sup>

Table 3.1. Associated gene products and fold change for genes with increased transcription during MeJA exposure conditions<sup>a</sup>.

<b>Gene product</b>	<b>Description</b>	<b>Fold change</b>
WP_073560412.1	FAD-dependent oxidoreductase	111
WP_073565080.1	DUF2085 containing membrane protein	79
WP_143195895.1	CHAP domain amidase	73
WP_073564464.1	Bifunctional hydroxymethyl pyrimidine kinase	63
WP_073560372.1	ABC transporter	25
WP_073559495.1	$\alpha/\beta$ hydrolase	23
WP_073566151.1	Radical SAM pyruvate-formate lyase activating enzyme	14
WP_143195831.1	Xylan/chitin deacetylase	12
WP_073563387.1	Histidine kinase	5
<i><sup>a</sup>Gene products annotated as hypothetical proteins omitted.</i>		

Other genes demonstrating increased transcription are associated with proteins that include a histidine kinase, a bifunctional hydroxymethyl pyrimidine kinase homologous to ThiD from thiamine biosynthesis, an ATP-binding ABC exporter with homology to CcmA, a radical S-

adenosylmethionine (SAM) pyruvate-formate lyase activating enzyme, an  $\alpha/\beta$ -hydrolase with homology to MhpC, and a NodB-like xylan/chitin deacetylase (Table 2.1).<sup>225–230</sup> A total of 41 genes were observed to be downregulated between four and 182-fold under MeJA exposure conditions (Table 2.2 and Figure 2.4). Interestingly, none of the upregulated genes induced by MeJA exposure obviously correspond to the observed shifts in metabolism, and genes impacted by MeJA with predicted roles in specialized metabolism were downregulated upon exposure.

Table 3.2. Associated gene products and fold change for genes with decreased transcription during MeJA exposure conditions<sup>a</sup>.

<b>Gene product</b>	<b>Description</b>	<b>Fold change</b>
WP_083681520.1	TOMM kinase cyclase	5
WP_073566534.1	Serine protease	10
WP_143195956.1	PAP2 family protein	14
WP_143195341.1	DUF 2254 domain-containing protein	14
WP_083680826.1	Membrane chloride channel	15
WP_073560908.1	Histidine kinase	15
WP_143195863.1	Sulfate transporter	16
WP_073567587.1	FAD-dependent oxidoreductase	16
WP_073562695.1	Chain-length determining protein	16
WP_083681843.1	IS21 family transposase	16
WP_073565888.1	Galactose oxidase	18
WP_073565697.1	Tyrosinase	20
WP_073560909.1	Protocatechuate 3,4-dioxygenase	23
WP_073558654.1	Glutathione-dependent formaldehyde dehydrogenase	25
WP_073559864.1	SAM-dependent methyltransferase	26
WP_073559966.1	Cholesterol acyltransferase	27
WP_073559409.1	DUF3616 domain-containing protein	28
WP_083680758.1	Cyclopropane fatty-acyl-phospholipid synthase	30
WP_073562546.1	ATP-dependent endonuclease	33
WP_073558548.1	Cytochrome P450	34
WP_073566525.1	Osmotic shock protein	43
WP_073567786.1	Uma2 family endonuclease	55
WP_083680900.1	Histidine kinase-like ATPase	61
WP_073565950.1	Acyl-CoA thioesterase	69
WP_083680891.1	GntR family transcriptional regulator	67

*Gene products annotated as hypothetical proteins omitted.*

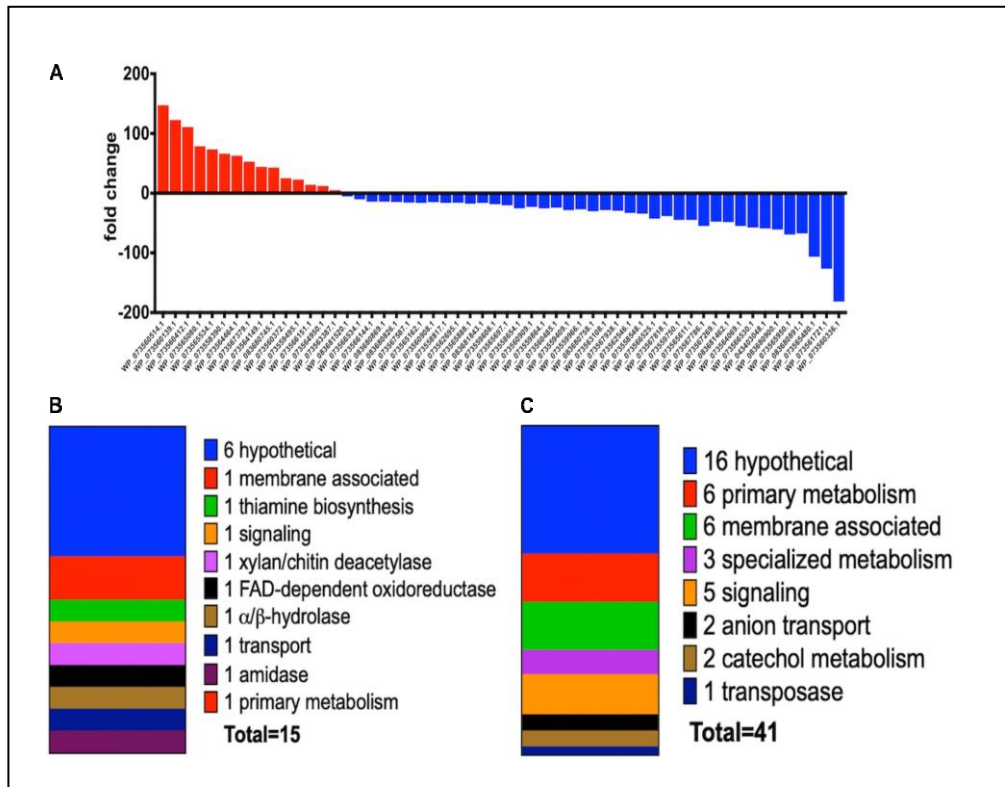


Figure 3.4. (A) Fold change data observed from *A. sp.* MeJA exposure experiments with increased transcription indicated with red and positive fold change values and decreased transcription indicated with blue and negative fold change values. Data represented for all genes with  $\geq$  fourfold change ( $p < 0.05$ ;  $n = 3$  per condition). (B) General categories and classes associated with *A. sp.* genes with observed  $\geq$  fourfold increases in transcription during MeJA exposure. (C) General categories associated with *A. sp.* genes with observed  $\geq$  fourfold decreases in transcription during MeJA exposure.

### 3.2.5 Discussion

Analysis of extracts from four soil-associated myxobacteria using untargeted mass spectrometry demonstrated the varying metabolic shifts experienced by each myxobacterium upon exposure to MeJA. Our original assertion that this metabolic shift might be attributed to increased production of predation-associated specialized metabolites is not necessarily supported by our subsequent transcriptomic analysis of MeJA exposed *A. sp.* samples. This is perhaps best explained by the observation that myxobacteria constitutively produce predation-associated features and instead regulate subsequent feeding when exposed to lysed

prey.<sup>28</sup> We suspect that continued exploration of this MeJA-impacted metabolic space utilizing the nutrient rich medias and increased cultivation volumes previously attributed to *A. sp.* antimicrobial production will facilitate natural product discovery and provide insight into this discrepancy.<sup>158</sup> Interestingly, all of the library hits provided by GNPS analysis were mono- or sesquiterpene metabolites that have previously been considered plant metabolites.<sup>231–233</sup> Although production of  $\alpha$ -bisabolol and characterization of the corresponding synthase (AB621339.1) from *Streptomyces citricolor* have been reported, no homology to this synthase was observed when comparing the six putative terpene synthases from *A. sp.* identified by antiSMASH.<sup>166,234</sup> While the previously referenced constitutive toxicity observed from myxobacteria and our observation of MeJA-impacted production of biologically active terpene metabolites is certainly intriguing, subsequent efforts are required for confirmation and characterization of the associated biosynthetic gene clusters.

This analysis also provided insight into myxobacterial metabolism of MeJA, and a variety of known jasmonate associated metabolites were predicted using the GNPS-affiliated NAP platform.<sup>168,218</sup> The 111-fold increase in transcription of a predicted FAD-dependent oxidoreductase during MeJA exposure provides a likely candidate involved in the oxidation of MeJA to provide either of the oxidized MeJA analogs predicted to be either 8-hydroxyjasmonic acid or 10-hydroxyjasmonic acid and determined not to be the pathogen-associated metabolite 12-hydroxyjasmonic acid.<sup>217</sup>

The MeJA-dependent presence of a metabolite predicted to be either a saturated fatty acid, including decanoic acid, or a prenol lipid (Figure 2.2A) is also intriguing as a variety of saturated fatty acids activate the frizzy (frz) signal transduction pathway associated with chemotaxis in the myxobacterium *M. xanthus*.<sup>221</sup> This result also provides insight into the increased motility observed when exposing *A. sp.* to MeJA. While the transcription of the

FrzCD homolog from *A. sp.*, WP\_073562522.1, was not impacted by MeJA exposure, FrzCD is a methylaccepting chemotaxis protein (MCP) with elicitor-induced activation attributed to covalent modification via demethylation and not transcriptional activation.<sup>221</sup> While FrzCD homologs from myxobacteria possess highly conserved MCP signaling domains, modest sequence variability about the N-termini seem to correlate with taxonomic structure of myxobacterial genera.<sup>221,235</sup> Interestingly, deletion of the N-terminal region of FrzCD *M. xanthus* was found to only minimally impact swarming.<sup>235</sup>

From these preliminary observations, we suggest that further investigation on the effect of MeJA on the frz signaling pathway of *A. sp.* will provide insight into this unique response and any contributions of the frz signaling pathway in the potential plant recruitment of micropredators.

We were also excited to see increased transcription of a putative lytic CHAP amidase during MeJA exposure conditions. Combined with previous induced changes in metabolism and motility, we consider increased production of a lytic enzyme to round out the support for the predatory response of *A. sp.* when exposed to MeJA. Of the other genes upregulated when exposed to MeJA, both the xylan/chitin deacetylase (12-fold increase) and the bifunctional hydroxymethyl pyrimidine kinase (63-fold increase) also stand out due to their previously known association with phytohormone responses<sup>236–239</sup> The plant pathogen *Rhizobium radiobacter* demonstrated a 4.6-fold increase in functional xylanase production when exposed to 250  $\mu$ M MeJA.<sup>213</sup> To date, cellulose degradation has been exclusively demonstrated by myxobacteria from the suborder Sorangiineae, and not observed from myxobacterium within the suborder Cystobacterineae, which includes *A. sp.*<sup>7,169,240,241</sup> While increased expression of a xylan degrading enzyme might simply be an opportunistic switch to consume plant cellulose when exposed to MeJA, high homology to chitin deacetylase, NodB,

and its role in the biosynthesis of lipo-chitinoligosaccharides (LCOs), or synonymously Nod-factors, suggests a more nuanced impact on symbiosis, as LCOs are chemical entities known to facilitate plant–microbe symbiosis.<sup>239</sup> Fungal pathogen-induced enrichment of carbohydrate active enzymes within root microbiomes by members of the genera *Chitinophaga* and *Flavobacterium* has also been associated with disease suppression.<sup>29</sup> The only prior association between myxobacteria and LCO biosynthesis, the identification of a homolog for the LCO biosynthetic enzyme NodC from the myxobacterium *Stigmatella aurantiaca*, does not provide additional insight as *A. sp.* does not possess a NodC homolog.<sup>242</sup> Chitin deacetylation has also been associated with accumulation of N-glucosamines and a stimulated increase in plant systemic resistance.<sup>243</sup>

Also associated with nodule growth and root nodule symbiosis, thiamine biosynthesis is critical to both plant and prokaryote growth.<sup>237,238</sup> Interestingly, MeJA exposure significantly increased expression of a bifunctional hydroxymethyl pyrimidine kinase ThiD homolog involved in two, sequential phosphorylations of 4-amino-5-hydroxymethyl-2-methylpyrimidine (HMP) to generate 4-amino-5-hydroxymethyl-2-methylpyrimidine pyrophosphate (HMP-PP) and decreased transcription of an identified ThiE homolog responsible for coupling HMP-PP with 4-methyl-5-( $\beta$ -hydroxyethyl) thiazole (HET-P) to afford thiamine monophosphate (THP).<sup>226,228</sup> This change in thiamine-associated features suggests that *A. sp.* accumulates HMP-PP when exposed to MeJA. Interestingly, root nodule symbiosis induces expression of the HET-P biosynthetic gene *THI1* and slightly downregulates expression of *thiD* and *thiE* homologs in the plant *Lotus japonicas*.<sup>189</sup> Combined these results provide further evidence implying thiamine biosynthesis as a component of plant–microbe symbiosis and suggest accumulation of HMP-PP by beneficial bacteria and HET-P by plants might benefit precursor pools required for thiamine biosynthesis within the rhizobiome.<sup>237,238</sup> Also of note, a bacterial riboswitch that employs an

HMP-PP-binding aptamer has been recently identified and implicated in bacterial regulation of thiamine biosynthesis.<sup>244</sup> The regulatory impact of HMP-PP accumulation and its potential to modulate bacterial riboswitches could also contribute to the broad transcriptional impact of MeJA exposure. Provided these results, we are enthusiastic to investigate the symbiotic potential of predatory myxobacteria within the rhizobiome and the roles of LCO and thiamine metabolites.

While the majority of genes downregulated during MeJA exposure were hypothetical, significant repression of genes associated with membrane features and signaling such as a chain length determining protein responsible for exopolysaccharide biosynthesis, a cyclopropane fatty-acyl-phospholipid synthase, a GntR family transcriptional regulator, and a histidine kinase like ATPase suggest the broad scope of phytohormone-impacted features (Table 2.2 and Figure 2.4). Downregulated specialized metabolite features that might be associated with observed MeJA induced metabolic shifts included a thiazole/oxazole modified microcin (TOMM) kinase/cyclase fusion protein potentially involved in the biosynthesis of bacteriocin-like metabolites, a SAM-dependent methyltransferase, and a cytochrome p450.<sup>245</sup>

Our data demonstrate that myxobacteria demonstrate varying metabolic responses to MeJA exposure and are capable of metabolic modification of MeJA. Interestingly, only one of the four investigated myxobacteria satisfied all three of our suggested criteria supporting plant recruitment of micropredators via the phytohormone MeJA. We suspect subsequent investigations that also include better studied myxobacteria such as the model myxobacterium *M. xanthus* as well as additional signaling metabolites associated with biotic stress responses from plants will provide more insight into associated myxobacterial responses as well as the physiological systems involved. Detection of a potential fatty acid

metabolite known to induce myxobacterial motility exclusively within our MeJA exposed samples and MeJA-impacted motility of *A. sp.* provides the first metabolic insight into plant recruitment and maintenance of beneficial micropredators within the rhizobiome. Overall, the combination of impacted motility, metabolism, and lytic enzyme production from our MeJA exposure experiments demonstrate a significant response from the predatory myxobacterium *A. sp.* strain Cb G35. Considering the  $\geq$  four-fold change in transcription for 56 genes and significant impact on metabolism, we conclude that the plant phytohormone MeJA might contribute to recruitment and maintenance of other myxobacteria within rhizobiomes and suggest that the impact of plant exudates on microbial community structure and maintenance requires further investigation.

The Supplementary materials for this article can be found online

at: <https://www.frontiersin.org/articles/10.3389/fmicb.2020.00034/full#supplementary-material>.

### 3.3 Selective Responses of *Archangium sp.* Cb G35 to Phytohormones and Plant-Related Signals

#### 3.3.1 Abstract

Plant-microbe interactions highlight the unique chemical space that exists within the rhizosphere. Through root exudations, plants establish their rhizobiome and utilize hormonal signaling pathways to activate systemic resistance during abiotic or biotic stress. Beneficial microorganisms in addition to providing nutritional benefits assist plants in staving off pathogens. However, soil myxobacteria possessing predatory habits and known for generating antimicrobials have not received much attention for their potential in benefiting



plant health. *Archangium* sp. strain Cb G35 was initially isolated from tree bark and showed strong attraction to methyljasmonate in addition to transcriptomic and metabolic changes. Here, the investigation of the changes in motility on exposure to phytohormones and plant-related signals and utilized untargeted mass spectrometry to observe changes in metabolism is reported. Salicylic acid (SA) and abscisic acid (ABA) induced motility with SA impacting the production of at least 800 metabolites. Investigations showed that *A. sp.* selectively responds to phytohormones and plant-related signals suggesting the potential for this myxobacteria to be recruited by plants.

### 3.3.2 Introduction

Root colonization in the rhizosphere by beneficial microorganisms is essential to plant health, and sequencing in addition to metagenomic and transcriptomic techniques have studied the conglomeration of plant-beneficial microorganisms to report the activation of genes involved in chemo-attraction and activation of disease-suppressive states in the rhizosphere.<sup>29,119,190</sup> Plant hosts activate hormonal signaling pathways either to establish symbiosis with beneficial microorganisms or to protect against phytopathogens.<sup>36,37,40,103</sup> However the perception of plant hormones by plant-beneficial bacteria and the ensuing responses have yet to be thoroughly investigated. We recently reported the potential plant recruitment of *A. sp.* strain Cb G35 via methyljasmonate (MeJA) phytohormone with an observed increase in motility, shifts in metabolism, and activation of lytic enzyme production.<sup>246</sup> With these unique responses of *A. sp.* to MeJA, there were speculations that other defense-related phytohormones could elicit similar responses, as these signals are also present in the rhizosphere. Each defense-related phytohormone plays specific roles in the crosstalk of the hormonal regulatory network of plant defense systems,<sup>37,103,247</sup> therefore there

is the expectation of *A. sp.* to selectively respond to phytohormones. Herein, the influence of phytohormones and plant-related signals on motility and metabolism was explored.

Because the chemical space within the rhizosphere comprises contributions from both plant-microbe and microbe-microbe interactions, the choice to investigate the perception of our myxobacteria to (1) abscisic acid (ABA), salicylic acid (SA), gibberellic acid (GA), and auxin, as these phytohormones play important roles in the activation of systemic resistance in plants and have been manipulated by phytopathogens (Table 1.1); (2) jasmonic acid-isoleucine (JA-Ile) and the diffusible signal factor (DSF), 11-methyl-2*E*-dodecenoic acid to represent the metabolic contributions by phytopathogenic microorganisms because the DSF functions to regulate cell-cell communications in the rhizosphere while JA-Ile has been generated as jasmonate mimic to hijack the jasmonate pathway;<sup>59,87,248–250</sup> and (3) the plant stress signal, methylglyoxal (MG).<sup>251–253</sup> Linolenic acid, the jasmonate precursor, and linoleic acid were also investigated and compared with the above-listed signals.

### 3.3.3 Materials and Methods

#### 3.3.3.1 Medias and Strains

*Archangium sp.* strain Cb G35 (DSM 52696) initially obtained from the German Collection of Microorganisms (DSMZ) in Braunschweig was grown on VY/2 agar (5 g/L baker's yeast, 1.36 g/L CaCl<sub>2</sub>, 0.5 mg/L vitamin B12, 15 g/L agar, pH 7.2).

#### 3.3.3.2 Phytohormones and plant-related signals

Stock solutions (150 mM) of Gibberellic Acid (Cayman Chemical), Indole-3-propionic Acid (Cayman Chemicals), (+)-Abscisic Acid (Cayman Chemicals), 11-methyl-2*E*-

dodecenoic acid (Cayman Chemical), ( $\pm$ )-Jasmonic Acid-Isoleucine (Cayman Chemicals), Salicylic Acid (Sigma-Aldrich), Methylglyoxal solution (Sigma-Aldrich), Linolenic Acid (Sigma-Aldrich) and Linoleic Acid (Sigma-Aldrich) were prepared in DMSO. Experiments on the exogenous applications of these signals to plants and micro-organisms have been conducted in literature which informed our choice of 10  $\mu$ M concentration for supplementation of each signal in our investigations.<sup>252–260</sup>

### 3.3.3.3 Motility Assays

To monitor swarm expansion rates, the bacterium was cultured on VY/2 media as described above. After 24 h of incubation, 5 mM stock solutions of phytohormones and plant-related signals were spotted onto the solid media, to a concentration of 0.17% v/v, around cells and swarm diameters were recorded daily for 6 days. DMSO was used as vehicle control for comparison. Minimum of six replicates were included in all motility assays. Statistical significance of changes in swarm expansion rates across the strains was calculated using Student's t.test and the Holm's method to compare effects of individual signal with control in R studio.

### 3.3.3.4 Exposure to Signals, Metabolite Extraction and Analysis

For LC-MS/MS analysis, required volumes of filter sterilized phytohormones and plant-related signals from a 150 mM stock were added to autoclaved medium at 55°C to give ten conditions (including the no-signal control). Minimum of four replicates were included in all exposure assays for metabolomic analysis. *Archangium* sp. was cultivated on VY/2 media supplemented with 10  $\mu$ M of signals at 30°C. After 7 days of cultivation, myxobacterial plates chopped, extracted with EtOAc and dried *in vacuo* to provide crude extracts. LC-

MS/MS analysis of the extracted samples was performed on an Orbitrap Fusion instrument (Thermo Scientific, San Jose, CA, United States) controlled with Xcalibur version 2.0.7 and coupled to a Dionex Ultimate 3000 nanoUHPLC system. Samples were loaded onto a PepMap 100 C18 column (0.3 mm × 150 mm, 2 μm, Thermo Fisher Scientific). Separation of the samples was performed using mobile phase A (0.1% formic acid in water) and mobile phase B (0.1% formic acid in acetonitrile) at a rate of 6 μL/min. The samples were eluted with a gradient consisting of 5–60% solvent B over 15 min, ramped to 95% B over 2 min, held for 3 min, and then returned to 5% B over 3 min and held for 8 min. All data were acquired in positive ion mode. Collision-induced dissociation (CID) was used to fragment molecules, with an isolation width of 3 m/z units. The spray voltage was set to 3600 V, and the temperature of the heated capillary was set to 300°C. In CID mode, full MS scans were acquired from m/z 150 to 1200 followed by eight subsequent MS<sub>2</sub> scans on the top eight most abundant peaks. The orbitrap resolution for both the MS<sub>1</sub> and MS<sub>2</sub> scans was 120,000. The expected mass accuracy was < 3 ppm.

#### 3.3.3.5 GNPS, Cytoscape and XCMS-MRM Analysis

Generated data were converted to .mzXML files using MSConvert and mass spectrometry molecular networks were generated using the GNPS platform.<sup>168</sup> All MS/MS fragment ions within +/- 17 Da of the precursor m/z were removed to filter the data. MS/MS spectra were window filtered by choosing only the top 6 fragment ions in the +/- 50Da window throughout the spectrum. Precursor ion mass tolerance of 0.02 Da and a MS/MS fragment ion tolerance of 0.02 Da were set. Molecular networks were then created where edges were filtered to have a cosine score above 0.7 and more than 6 matched peaks. Further, edges between two nodes were kept in the network if and only if each of the nodes appeared

in each other's respective top 10 most similar nodes. Finally, the maximum size of a molecular family was set to 100, and the lowest scoring edges were removed from molecular families until the molecular family size was below this threshold. The spectra in the network were then searched against GNPS' spectral libraries. The library spectra were filtered in the same manner as the input data and was allowed to search for analogs. All matches kept between network spectra and library spectra were required to have a score above 0.7 and at least 6 matched peaks.<sup>168</sup> Molecular networks were rendered and annotated on Cytoscape 3.8.2<sup>214</sup> Using the default HPLC/Orbitrap (136) parameters, pairwise analysis of converted .mzXML files was performed on XCMS-MRM webserver. Within the XCMS-MRM result tables, determination of signal-impacted detected features was afforded by filtering results for those with a  $\geq$  five-fold change and  $p \leq 0.05$ .

### 3.3.4 Results

#### 3.3.4.1 Exposures to SA, ABA and DSF Differentially Influences *A. sp.* Motility

The impacts of exposure to phytohormones and plant-related signals were recorded by the daily measurement of swarm diameters. Because myxobacteria exhibit social cooperative behaviors in motility and predation, the change in swarm expansion rate can be used to observe growth and motility.<sup>221,222</sup> Similar to our previous work with methyljasmonate, an increase in motility induced by a signal would infer the use of that signal for the recruitment of myxobacteria by plants.<sup>246</sup> Significant increases in swarm rates in response to SA exposure, when compared to the no exposure control, were observed after 6 days of growth with the most significant increase occurring 24 h after exposure (Figure 3.5A). ABA exposure induced significant increases in swarm rates for the first 3 days of growth while the DSF showed significantly increased swarm rates on the fourth and fifth day (Figure 3.5A).

Interestingly, exposure to the jasmonate mimic, JA-Ile,<sup>87</sup> and the jasmonate precursor, linolenic acid,<sup>210</sup> showed no significant increases in swarm rates (Figure 3.5) confirming our previous reports of the specificity in *A. sp.* responses to methyljasmonate.<sup>246</sup>

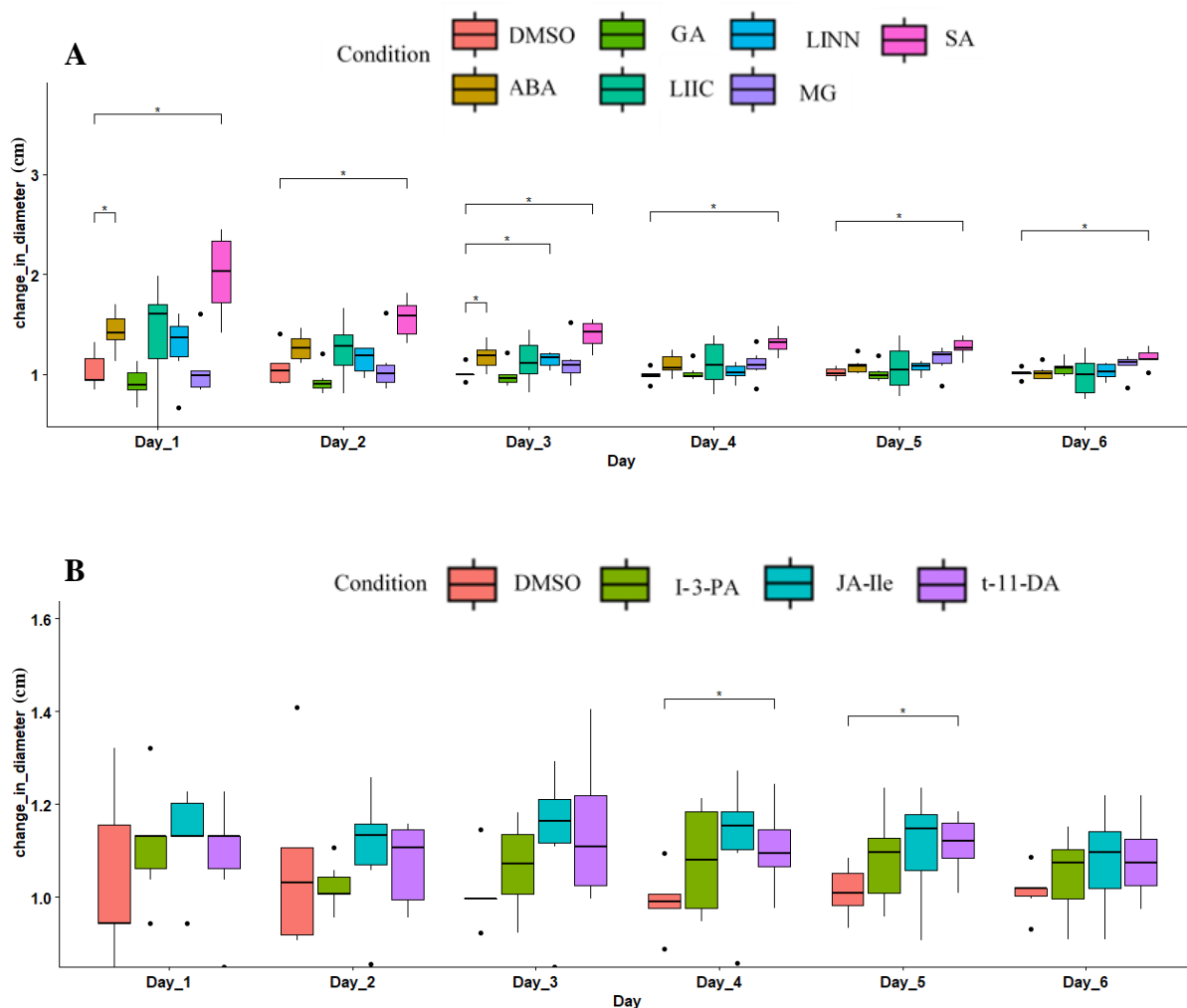


Figure 3.5. Motility assays showing cumulative change in swarm diameters after exposure to (A) phytohormones and (B) plant-related signals. “\*” indicates  $p < 0.05$ . DMSO = no signal control, ABA = abscisic acid, GA = gibberellic acid, LIIC = linoleic acid, LINN = linolenic acid, MG = methylglyoxal, SA = salicylic acid, I-3-PA = indole-3-propionic acid, JA-Ile = jasmonic acid-isoleucine and t-11-DA = 11-methyl-2*E*-dodecenoic acid

### 3.3.4.2 Unique Signal-Induced Changes in *A. sp.* Metabolism

Myxobacterial metabolism has produced a plethora of structurally diverse chemical entities with unusual mechanisms of biological activities, different from structural classes

identified from other well-studied bacteria.<sup>26,157</sup> In investigating the plant recruitment of myxobacteria in the rhizosphere, the pattern of metabolic shifts observed on exposure to phytohormones and plant-related signals should indicate how myxobacteria would respond. Comparing untargeted mass spectrometry datasets from exposure conditions against the unexposed control using XCMS-MRM, significant shifts in metabolism were observed (Figure 3.6).<sup>215,216</sup>

Extracts from ABA exposure conditions had the least features with a  $\geq$  five-fold increase with a total of seven while MG had the most features with a  $\geq$  five-fold decrease with a total of 459. SA had the most features with a  $\geq$  five-fold increase with a total of 614 and displayed the highest signal-induced impact on *A. sp.* strain Cb G35 metabolism.

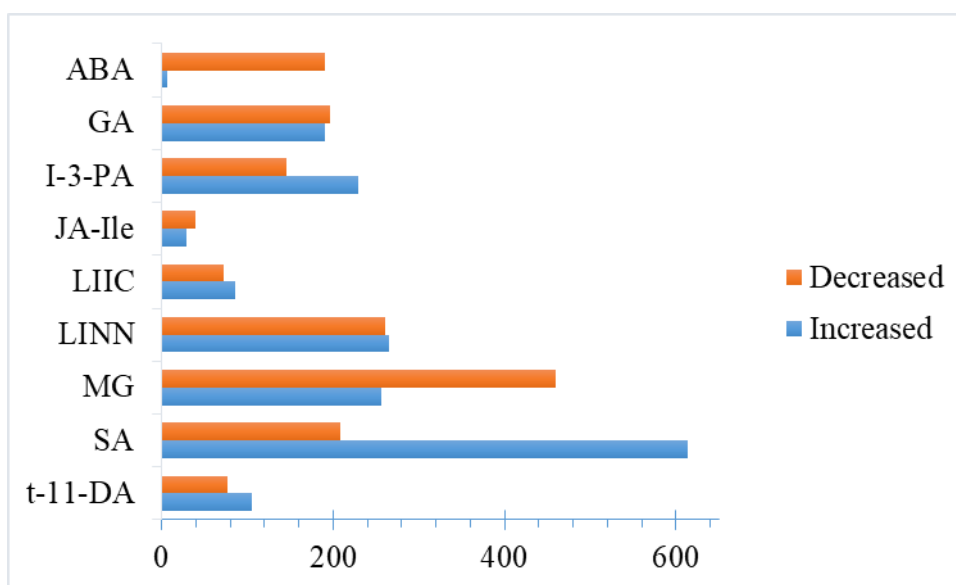


Figure 3.6. Signal-impacted features reported from XCMS analysis of LC-MS/MS datasets showing decreased and increased features compared to the no-exposure control. Feature tables were filtered to provide those with a  $\geq$  fivefold change and  $p \leq 0.05$ . ABA = abscisic acid, GA = gibberellic acid, LIIC = linoleic acid, LINN = linolenic acid, MG = methylglyoxal, SA = salicylic acid, I-3-PA = indole-3-propionic acid, JA-Ile = jasmonic acid-isoleucine and t-11-DA = 11-methyl-2*E*-dodecenoic acid

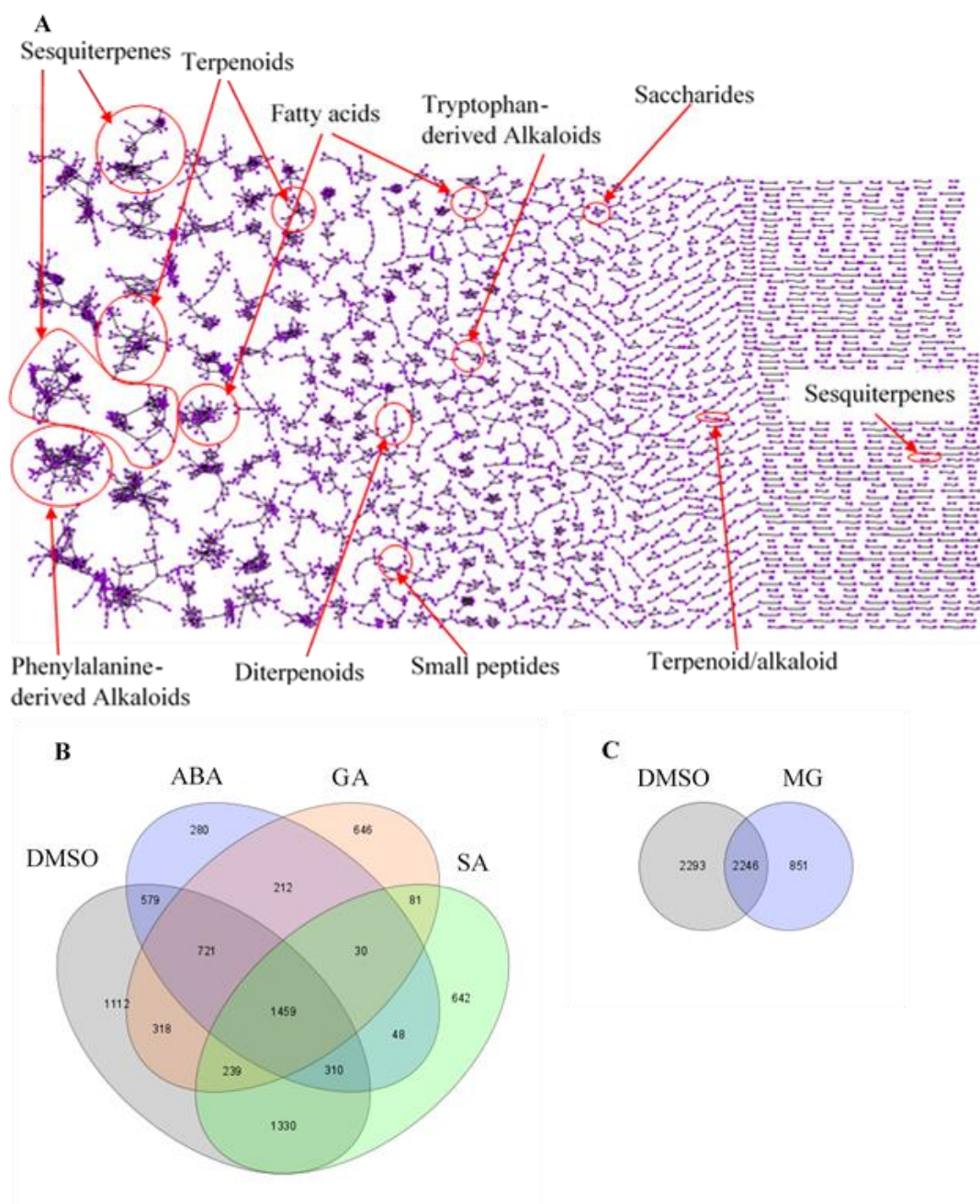


Figure 3.7. Metabolomics analysis of extracts from SA, ABA, GA, LINN, MG, and no-signal control culture conditions. (A) Molecular network annotated with compound classes based on library hits. Singletons are excluded from the network. (B) Venn diagram of features contributed by SA, ABA, GA, and control culture conditions. (C) Venn diagram of features contributed by MG compared to control. Node counts based on ion distribution are shown. Link to network file is available in Appendix B.1. DMSO = no signal control, ABA = abscisic acid, GA = gibberellic acid, SA = salicylic acid and MG = methylglyoxal



Next, molecular networking of MS<sup>2</sup> data was generated on the GNPS platform. To observe different classes of compounds, LC-MS/MS datasets were grouped into the “phytohormone exposure” group and “other signal exposure” group for clarity, and GNPS analysis was performed. Analysis with GNPS creates molecular networks by combining identical MS<sup>2</sup> spectra into single nodes and based on similarities in chemical scaffolds, lines, called edges, connect the nodes according to a pre-set cosine score cut-off to create clusters.<sup>168</sup> Sometimes, clustered nodes could represent bio- or chemical transformations of a molecule. Molecular networking with the “phytohormone exposure” group including SA, ABA, GA, MG, and linolenic acid with the control culture conditions generated 11, 947 nodes with 2106 nodes (3532 including linolenic acid exposure) generated solely from phytohormone exposure (Figure 3.7) while networking with the “other exposure” group including JA-Ile, t-11-DA and I-3-PA culture conditions with the control generated 6,311 nodes with 2,133 exclusive to culture conditions (Figure 3.8). Additionally, annotations were achieved when experimental MS<sup>2</sup> spectra matched MS<sup>2</sup> spectra of known compounds/classes available in public libraries (Figure 3.7A and Figure 3.8A).<sup>168</sup> However, the databases are limited in the collection of mass spectra of myxobacterial compounds and some nodes had no library hits to determine their structural classes. Using the library hits from GNPS analysis, annotations of terpenoids including sesquiterpenes and diterpenes, peptides, alkaloids, fatty acids, and carbohydrate compounds were annotated. Based on node counts, the most unique features were seen in MG, SA, and GA with 28%, 16%, and 17% of nodes unshared (Figure 3.7B). 11%, 12%, and 8% of nodes from I-3-PA, JA-Ile, and t-11-DA exposure experiments respectively were also condition-specific (Figure 3.8B). These results illustrate the high amount of unique impacts on *A. sp.* metabolism by the different exposure conditions.

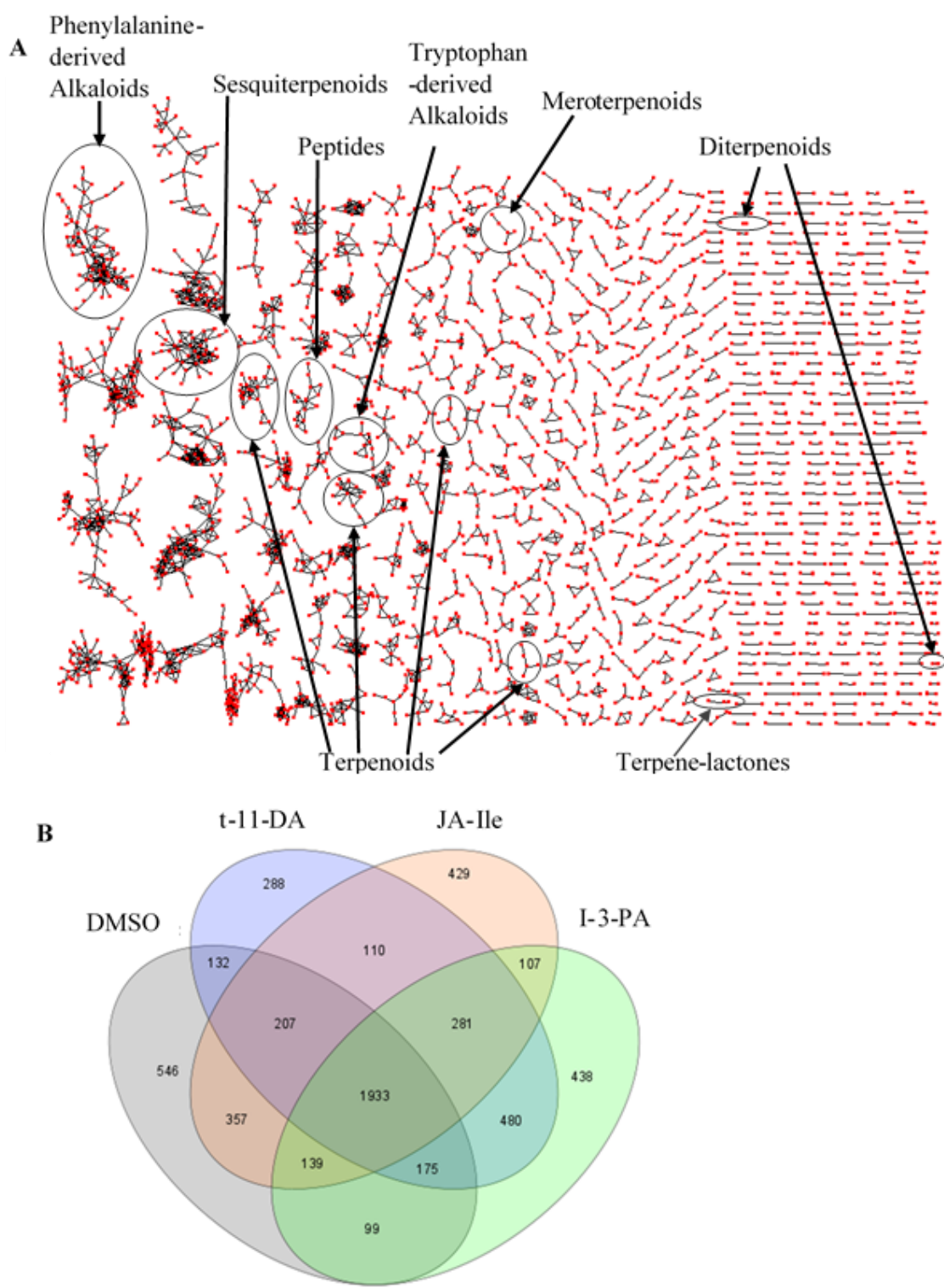


Figure 3.8. Metabolomics analysis of extracts from JA-Ile, I-3-PA, t-11-DA, and no-signal control culture conditions. (A) Molecular network annotated with compound classes based on library hits. Singletons are excluded from the network. (B) Venn diagram of features contributed by SA, ABA, GA, and control culture conditions. Node counts based on ion distribution are shown. Link to network file is available in Appendix B.2. I-3-PA = indole-3-propionic acid, JA-Ile = jasmonic acid-isoleucine, t-11-DA = 11-methyl-2*E*-dodecenoic acid and DMSO = no signal control.

### 3.3.5 Discussion

Phytohormones are important in regulating signaling networks when plants respond to abiotic and biotic stress and are present in micro-titer concentrations in the rhizosphere.<sup>38–40</sup> Playing roles as a secondary defense to plants, beneficial bacteria are recruited to colonize the rhizobiome via root exudates and rhizodeposit.<sup>41,42,180</sup> Motility assays revealed that SA and ABA could potentially act as chemoattractants to recruit the plant-associated *A. sp.* strain Cb G35 to the rhizosphere. Although ABA is sometimes reported to negatively regulate the activation of plant systemic resistance, it plays a role in encouraging microbial colonization because high concentrations in roots are common during the establishment of mycorrhizal and endophytic symbiosis.<sup>261,262</sup> Interestingly, both GNPS and XCMS analysis revealed low percentages of generated features with ABA exposure suggesting that this phytohormone may only act as an attractant to the myxobacteria, however, because chemotaxis is usually coupled with cellular processes like activation of adhesion and secretory systems in beneficial bacterial,<sup>35,55</sup> further transcriptomic investigations of impacted genes are suggested.

On the other hand, *Archangium sp.* strain Cb G35 exposed to SA uniquely displayed a continuous increase in swarm rates throughout the experimental period and metabolomic analysis showed several features generated. SA, having the most features shared with the control (Figure 3.7B), together with the significant increase in generated features observed from XCMS analysis (Figure 3.6) inevitably suggests that the biosynthesis of some specialized metabolites was increased. However, it is not obvious if these increases resulted from upregulation of gene expressions or SA acting as a precursor for the biochemical pathways. JA-Ile and linolenic acid did not change the swarm rates of *A. sp.* confirming our previous reports of the unique impacts of MeJA exposure.<sup>246</sup> Besides, XCMS analysis

revealed low changes in the metabolism induced by JA-Ile exposure unlike with linolenic acid, suggestive of the possible use of linolenic acid as a carbon source.

Several terpenoids, especially sesquiterpenes were annotated in the molecular networks consistent with the observed high numbers of biosynthetic gene clusters that encode for terpene synthases in the *A. sp.* genome (Figure 2.1). Due to limited publicly available mass spectra of myxobacterial specialized metabolites, condition-specific nodes could not be dereplicated and currently remain unknown. Perhaps the difficulty in growing and handling myxobacteria contributes to the rarity of these data. Thus, in-house libraries of known myxobacterial metabolites are necessary to be developed. Noteworthy is the high density of predatory *A. sp.* BGCs that encode specialized metabolites, compared to those with saprophytic nutritional habits, in addition to the bio-transformed products of supplemented signals that contribute to the observation of large networks.<sup>25,246</sup>

The phytopathogenic *Xanthomonas campestris* pv. *campestris* performs cell-cell communication signaling via DSF to regulate the activation of virulence factors during pathogenesis.<sup>59,249,250</sup> *Myxococcus xanthus*, a predatory myxobacterium, showed increased motility and predation on perceiving selected exogenous acylhomoserine lactones revealing the ability to sense prey communication.<sup>144</sup> Our motility assays revealed an increase in swarm rates of *A. sp.* at days 4 and 5 of t-11-DA exposure experiments. This might be indicative of an extended log phase in the bacterial growth due to exposure to the DSF but more investigations are required.

Our analysis of changes in both motility and metabolism demonstrate that *A. sp.* exhibit unique responses to different phytohormones involved in the biotic stress response of plants and plant-related signals. We suggest subsequent transcriptomic analysis will give more insight into the potential roles the bacteria could play in influencing plant health.

### 3.4 Conclusion

Studies of the response of the plant-associated *A. sp.* strain Cb G35 to phytohormones and plant signals are relevant to research that focuses on plant-microbial interactions, especially in the search for stable and competent biological alternatives in controlling plant diseases. Overall, these investigations show that *A. sp.* is chemically attracted to methyljasmonate, salicylic acid, and abscisic acid. The metabolic analysis also reveals condition-specific potential for discovering novel specialized metabolites that would contribute to natural product discovery.

CHAPTER 4. EVALUATING THE IMPACTS OF PHYTOHORMONES AND PLANT-RELATED SIGNALS EXPOSURE ON ANTIBACTERIAL PRODUCTION BY *ARCHANGIUM* SP. STRAIN CB G35 CULTURES

#### 4.1 Aims

Although various antimicrobial specialized metabolites have been identified from myxobacteria, only two compounds are associated with *Archangium* sp. strain Cb G35 metabolism.<sup>169</sup> The rhizosphere provides a unique environment to explore chemical interactions that occur between species and across kingdoms.<sup>30,43,178,262</sup> A beneficial role that *Archangium* sp. strain Cb G35 is suggested to have is the maintenance of plant health through the suppression of pathogens in the rhizosphere. Hence, we proposed to observe the impacts that phytohormones and plant-related signals will have on the antimicrobial production of this myxobacterium. Aims for this study include:

1. Determine phytohormones and plant signal that induce an increase in the antibacterial activities of *Archangium* sp. strain Cb G35 compared to a no-signal control
2. Identify structural classes of specialized metabolites from active fraction using bioinformatic tools

From a functional and metabolomics perspective, an observation of how *A. sp.* generates specialized metabolites that may benefit plant health is possible. Focusing on antibacterial activity will help streamline the annotation of structural classes of specialized metabolites involved in the chemical interactions that occur between these bacteria and plants.

## 4.2 Abstract

Plants are involved in structuring their rhizobiome via the recruitment of beneficial microorganisms with a secondary function of staving off pathogens. The potential of predatory myxobacteria to benefit plant health is suggested to involve the production of antimicrobials. Metabolomic tools have the potential to reveal the shifts in metabolism activated by biotic stress responses of plants; however, the application of this tool in studying plant-microbial interactions is not common. This study utilizes metabolomic tools with antibacterial testing to monitor condition-specific activation of metabolites. Active fractions from salicylic acid (SA) and methylglyoxal (MG) exposure conditions consisted of specialized metabolites from terpenoids, alkaloids, fatty acids, polyketides, and peptides molecular families. Results suggest the potential of SA and MG to activate *A.sp.* strain Cb G35 production of antibacterials and further efforts to explore condition-specific impacts on other myxobacteria is required to explore the roles of these bacteria in the rhizosphere.

## 4.3 Introduction

Root exudates have been proven to alter gene expressions in microorganisms resulting in either the recruitment of beneficial microbes to the rhizosphere or the activation of pathogenesis in phytopathogens.<sup>41,49,84,183,197,263</sup> Investigations of the functional potential of endophytes in the rhizosphere of sugar beets observed the enrichment of biosynthetic gene clusters that encoded polyketides, non-ribosomal peptides, terpenes, aryl polyenes, lasso peptides, lanthipeptides, and bacteriocins in fungal pathogen-suppressive soils.<sup>29</sup> Compared to disease-conducive soils in the study, these specialized metabolites were thought to contribute to the protection of the plant.

Studies of endophytic establishments with plant hosts revealed that rice root exudates downregulated the differential expression of non-ribosomal peptide synthases that encoded pyoverdine-like metabolites in *Burkholderia kururiensis* M130, while upregulating genes that regulated chemotaxis, adhesion, and secretion systems.<sup>35</sup> Additionally, components of plant root exudates were associated with activating the expression of biosynthetic pathways that encode phenazine antifungals in *Pseudomonas aureofaciens* PGS12, and tomato root exudates were shown to influence the antifungal activities of *Pseudomonas chlororaphis* SPB1217 and *Pseudomonas fluorescens* SPB2137.<sup>264,265</sup>

Myxobacteria, the gliding Gram-negative  $\delta$ -proteobacteria exhibiting predatory and social behaviors, are found in microbial-rich habitats. Consequently, these bacteria often engage in the complex chemical interactions of the rhizosphere necessitating the study of their interactions with the plant hosts.<sup>3,10</sup> While transcriptomics has facilitated the study of microbial responses to plant hosts, metabolomics analyses can potentially observe the functional alterations that occur during plant-microbe interactions. Without the requirement of genomic information, the targeted or untargeted metabolomic analyses give access to novel bioactive metabolites in natural product discovery.<sup>266</sup> Herein, antimicrobial analysis with extracts of *Archangium* sp. strain Cb G35, from culture conditions exposed to a panel of environmentally equivalent concentrations of phytohormones and plant-related signals was performed.<sup>252-260</sup> Active extracts were selected for fractionation, antimicrobial testing and comparative mass spectral analysis to identify the changes in antimicrobial production influenced by phytohormones and plant-related signals.



## 4.4 Materials and Methods

### 4.4.1 Medias and Strains

*Archangium* sp. strain Cb G35 (DSM 52696) initially obtained from the German Collection of Microorganisms (DSMZ) in Braunschweig, *Escherichia coli* (DH5a), *Bacillus subtilis* (ATCC 6051) and the phytopathogen, *Rhizobium radiobacter* (previously *Agrobacterium tumefaciens* ATCC 51350) obtained from American Type Culture Collection (ATCC) were used. Depending on the nutritional requirements of the bacteria, VY/2 agar (5 g/L baker's yeast, 1.36 g/L CaCl<sub>2</sub>, 0.5 mg/L vitamin B<sub>12</sub>, 15 g/L agar, pH 7.2) and Luria-Bertani (LB) broth (10 g/L peptone, 5 g/L yeast extract, 5 g/L sodium chloride) were used.

### 4.4.2 Phytohormones and plant-related signals

Stock solutions (150 mM) of Gibberellic Acid (Cayman Chemical), Indole-3-propionic Acid (Cayman Chemicals), (+)-Abscisic Acid (Cayman Chemicals), 11-methyl-2E-dodecenoic acid (Cayman Chemical), (±)-Jasmonic Acid-Isoleucine (Cayman Chemicals), Salicylic Acid (Sigma-Aldrich), Methylglyoxal solution (Sigma-Aldrich), Linolenic Acid (Sigma-Aldrich) and Linoleic Acid (Sigma-Aldrich) were prepared in DMSO.

### 4.4.3 Exposure to Phytohormones and Plant-Related Signals Experiments

To observe the impacts of signals on antimicrobial production, filter sterilized signals were added to autoclaved medium at 55°C to make a final concentration of 10 µM, a concentration informed by literature.<sup>252–260</sup> *Archangium* sp. was cultivated on supplemented VY/2 media and grown at 30°C for 7 days. Dimethylsulfoxide was used as control.

#### 4.4.4 Metabolite Extraction, Antibacterial testing and Fractionation

After 7 days of cultivation, *A. sp.* strain Cb G35 plates were chopped, extracted with EtOAc and dried *in vacuo* to provide crude extracts.

Antibacterial analysis: Following methods from Clinical Laboratory Standards Institute (CLSI),<sup>267</sup> 12.8 mg/mL (in DMSO) stock solutions of extracts (and when necessary fractions) was diluted serially across the 96-well assay plate (Costar). The 11th well served as culture media control (no microbe added) and the 12th well served as negative control (no sample added). Overnight seed cultures of the test microbes were diluted to a final OD<sub>600</sub> of 0.05, added to wells 1-10 and 12 and plates were incubated at appropriate optimal temperature depending on the microbe. Optical densities of the plates were recorded at the start of incubation and after 18 hrs. Statistical significance were measured with PRISM v7.0d using two-way ANOVA and the Dunnett's multiple comparisons test methods. The supplemented phytohormones and plant-related signals were also confirmed to have no antibacterial effects on the test microbes (Figure C.1, Appendix).

Fractionation: Flash silica gel column was set up with silica gel 60 (230-450 mesh, Alfa Aesar). Approximately 240 plates of *A. sp.* cultures with no supplementation (5.5 L of media) yielded 283.1 mg of extract which was fractionated on a flash silica gel column using a polarity gradient from EtOAc to MeOH to give 12 fractions [AspFr-1 (EtOAc); AspFr-2 (EtOAc); AspFr-3 (EtOAc); AspFr-4 (EtOAc); AspFr-5 (EtOAc); AspFr-6 (EtOAc); AspFr-7 (EtOAc); AspFr-8 (1:1 EtOAc-MeOH); AspFr-9 (1:1 EtOAc-MeOH); AspFr-10 (1:1 EtOAc-MeOH); AspFr-11 (MeOH); AspFr-12 (Acetone wash)]. Fractions were monitored with thin layer chromatography (TLC Silica gel 60 F<sub>254</sub>, Merck) Antibacterial assay of crude extracts revealed significant increases in activities of salicylic acid and methylglyoxal culture conditions informing the selection of these extracts for fractionation (Figure 4.1). Eighty

plates (2 L of media) of *A. sp.* cultures with salicylic acid exposure yielded 106.5 mg of extract, which was fractionated on a flash silica gel column. Using a polarity gradient from EtOAc to MeOH, Eight fractions were eluted [SAFr-1 (EtOAc); SAFr-2 (EtOAc); SAFr-3 (EtOAc); SAFr-4 (EtOAc); SAFr-5 (1:1 EtOAc-MeOH); SAFr-6 (1:1 EtOAc-MeOH); SAFr-7 (1:1 EtOAc-MeOH); SAFr-8 (MeOH)]. Eighty plates (2 L of media) of *A. sp.* cultures with methylglyoxal exposure yielded 161.3 mg of extract and was fractionated on a flash silica gel column. Eight fractions were obtained using a polarity gradient from EtOAc to MeOH, [MGFr-1 (EtOAc); MGFr-2 (EtOAc); MGFr-3 (EtOAc); MGFr-4 (EtOAc); MGFr-5 (1:1 EtOAc-MeOH); MGFr-6 (1:1 EtOAc-MeOH); MGFr-7 (1:1 EtOAc-MeOH); MGFr-8 (MeOH)]. These fractions were tested for antibacterial activity.

#### 4.4.5 GNPS, Cytoscape and Analysis

Mass Spectrometric Analysis: Performance of LC-MS/MS analysis on the fractions was accomplished on an Orbitrap Fusion instrument (Thermo Scientific, San Jose, CA, United States) controlled with Xcalibur version 2.0.7 and coupled to a Dionex Ultimate 3000 nanoUHPLC system. Samples were loaded onto a PepMap 100 C18 column (0.3 mm × 150 mm, 2 μm, Thermo Fisher Scientific). Separation of the samples was performed using mobile phase A (0.1% formic acid in water) and mobile phase B (0.1% formic acid in acetonitrile) at a rate of 6 μL/min. The samples were eluted with a gradient consisting of 5–60% solvent B over 15 min, ramped to 95% B over 2 min, held for 3 min, and then returned to 5% B over 3 min and held for 8 min. All data were acquired in positive ion mode. Collision-induced dissociation (CID) was used to fragment molecules, with an isolation width of 3 m/z units. The spray voltage was set to 3600 V, and the temperature of the heated capillary was set to 300°C. In CID mode, full MS scans were acquired from m/z 150 to 1200 followed by eight

subsequent MS2 scans on the top eight most abundant peaks. The orbitrap resolution for both the MS1 and MS2 scans was 120,000. The expected mass accuracy was < 3 ppm.

Mass spectral data were converted to .mzXML files using MSConvert and molecular networks of fragmentation patterns were generated using the GNPS platform.<sup>168</sup> All MS/MS fragment ions within +/- 17 Da of the precursor m/z were removed to filter the data. MS/MS spectra were window filtered by choosing only the top 6 fragment ions in the +/- 50Da window throughout the spectrum. Precursor ion mass tolerance of 0.02 Da and a MS/MS fragment ion tolerance of 0.02 Da were set. Molecular networks were then created where edges were filtered to have a cosine score above 0.7 and more than 6 matched peaks. Further, edges between two nodes were kept in the network if and only if each of the nodes appeared in each other's respective top 10 most similar nodes. Finally, the maximum size of a molecular family was set to 100, and the lowest scoring edges were removed from molecular families until the molecular family size was below this threshold. The spectra in the network were then searched against GNPS' spectral libraries. The library spectra were filtered in the same manner as the input data and was allowed to search for analogs. All matches kept between network spectra and library spectra were required to have a score above 0.7 and at least 6 matched peaks.<sup>168</sup> Cytoscape 3.8.2 was used to visualize and annotate the generated network.<sup>214</sup>

#### 4.5. Results

Shifts in metabolism are often indicators of chemical influences on an organism because the generation of antimicrobial metabolites is essential in surviving the chemical warfare that occurs among the rhizobiome and for myxobacterial predation.<sup>3,26,138</sup> If phytohormones and other plant-related signals are involved in the recruitment of

myxobacteria to stave off pathogens, activation of the production of antimicrobials might be observable in culture conditions exposed to signals. When compared to control, crude extracts from methylglyoxal and salicylic acid exposed extracts demonstrated significant changes ( $p \leq 0.005$ ) in antibacterial activities against *R. radiobacter* and *E.coli* at concentrations as low as 6.4 and 12.8 mg/mL respectively (Figure 4.1). No significant changes in antibacterial activities were observed with *B. subtilis*.

Subsequently, these extracts were selected for fractionation and antibacterial testing to afford the active fractions. Because myxobacteria capably produce antibacterial metabolites, the no-condition extracts were also fractionated for comparison. Focusing on bioactivity at 6.4 mg/mL of fractions obtained from salicylic acid exposure experiments, SAfr-3 and SAfr-6 showed decreases in optical densities compared to the bacterial control. Similarly, MGfr-2 and MGfr-3 from methylglyoxal exposure experiments and ASPfr-4 and ASPfr-10 fractions from extracts of *A. sp.* cultures with no supplementation control showed lowered optical densities (Figure 4.2). These results prioritized these fractions for comparative metabolomics analysis with GNPS.

To observe shifts in metabolism that influenced antibacterial activity, MS<sup>2</sup> spectra were analyzed with GNPS to create molecular networks of 6567 nodes. Up to 2692 nodes were clustered into molecular families and 3875 nodes were singletons. Shared and unique metabolites can be observed across fractions. Euler plots summarizing the ion distribution of generated molecular network showed that some features were shared between the active fractions from SA and no-signal exposure assays, suggesting that the active specialized metabolites from MG extracts might be unique (Figure 4.3).

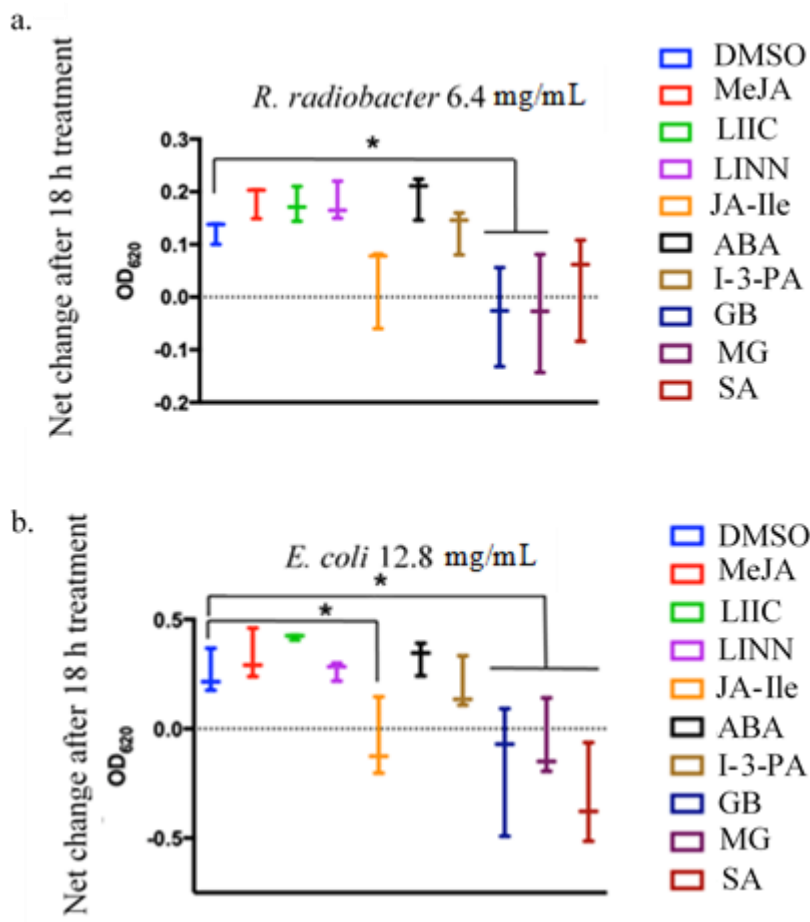


Figure 4.1 Minimum concentration of crude extracts that impacted antibacterial activities at  $p \leq 0.005$  against *R. radiobacter* and  $p \leq 0.0001$  against *E. coli*. ABA= Abscisic acid, GA= Gibberellic acid, I-3-PA= Indole-3-propionic acid, JA-Ile= Jasmonic acid-isoleucine, LIIC= Linoleic acid, LINN= Linolenic acid, MG= Methylglyoxal, SA = Salicylic acid exposure.

Using information from public datasets on GNPS, 5.2% of nodes (344 of 6567) were dereplicated to belong to the alkaloid, fatty acid, peptide, polyketide, and terpenoid classes of compounds (Figure 4.4). Nodes identified as alkaloids derived from ornithine and the polyketide/terpene hybrids (meroterpenes) were observed to be generated in exposure cultures.

## 4.6 Discussion

During predation, myxobacteria generate antimicrobials with varied modes-of-actions and high chemical diversity.<sup>25,26,157</sup> Most times, these metabolites are absent in axenic culture conditions even though the genomic information of the bacteria shows biosynthetic gene clusters (BGCs) that encode such metabolites. Myxobacterial predation was reportedly increased by prey quorum signals and the methyljasmonate phytohormone.<sup>144,246</sup> Results from these antibacterial assays of crude extracts show that the phytohormones SA and GB, as well as the plant stress signal MG, may induce the production of antibacterials against *E.coli* (Figure 4.1B). Because plants generate these signals as biotic stress responses to activate systemic resistance, investigations to observe for similar effects with other known plant beneficial bacteria will benefit studies of plant-microbial interactions.

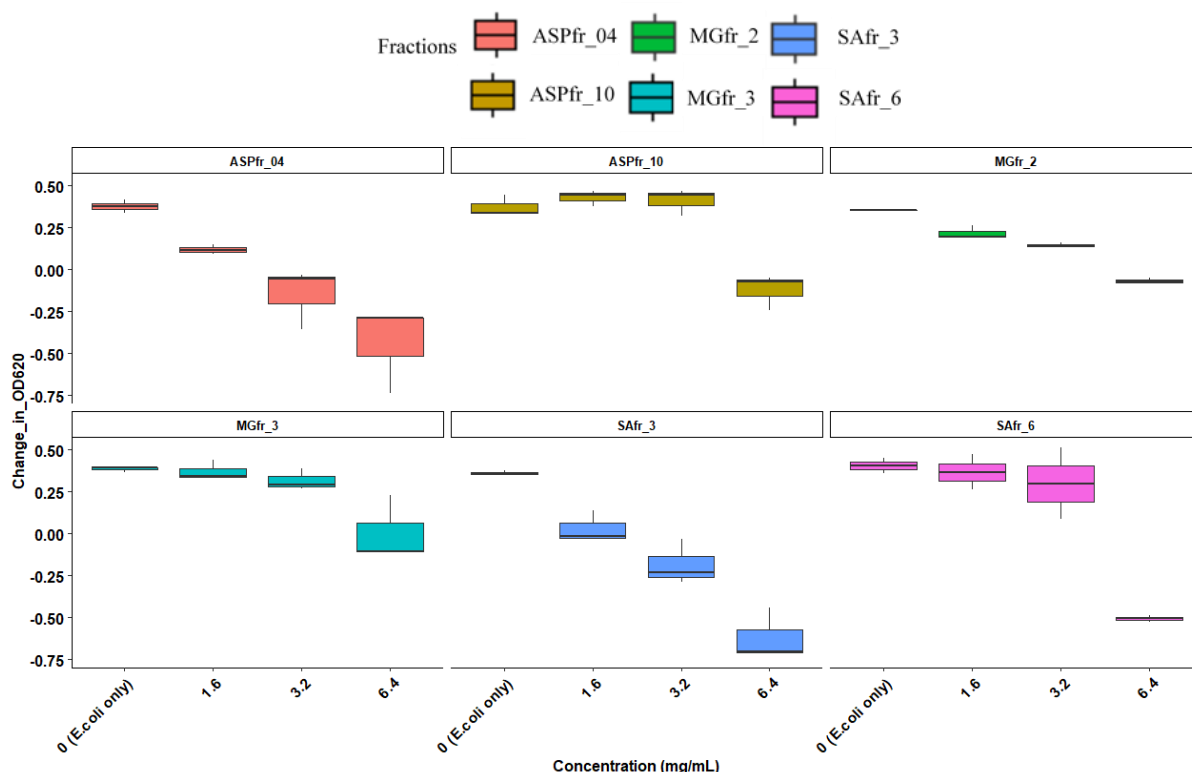


Figure 4.2. Results from antibacterial activity testing showing the effects of active fractions against *E. coli*.

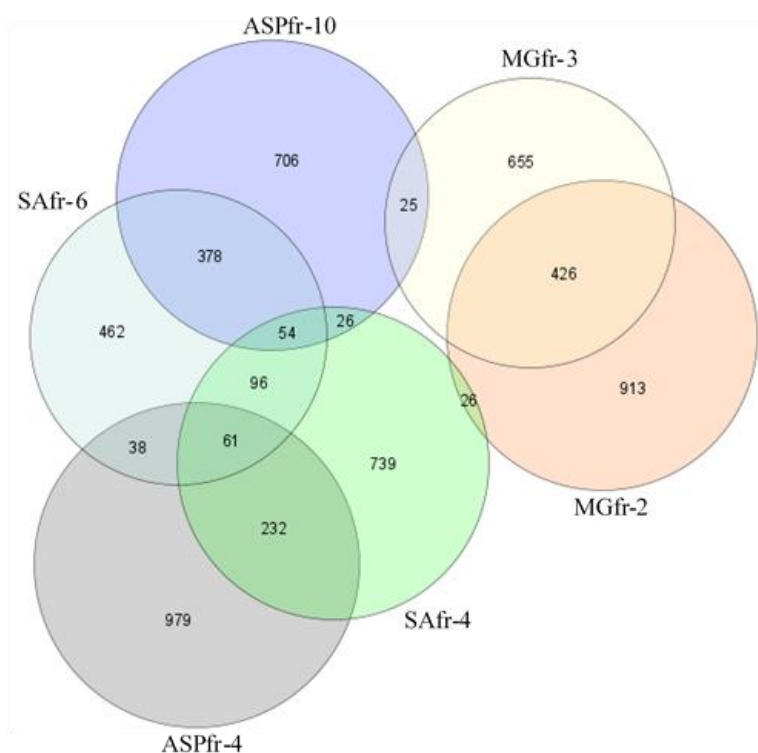


Figure 4.3. Euler plot of features contributed by ASPfr-4, ASPfr-10, SAfr-3, SAfr-6, MGfr-2, and MGfr-3. Node counts based on ion distribution are shown. Link to network file is available in Appendix B.3.

The application of metabolomics tools to study the outcomes of interactions between plants and microorganisms has provided an insight in linking modifications in the metabolism of pathogens and activation of plant systemic resistance.<sup>266</sup> Conversely, these tools can also be applied in studying the roles of plant-beneficial bacteria. Molecular networking analysis indicated the high potential for identifying new bioactive metabolites from *A. sp.* because the dereplication of observed features only led to the identification of molecular families.

The diversity of structural classes of antimicrobial metabolites from myxobacteria has been recorded<sup>26</sup> and similar varieties were observed in the annotated network (Figure 4.4).

Prior to this investigation, only the roimantacene polyene and *p*-hydroxyacetophenone amides reportedly active against Gram-negative bacteria and algae respectively have been identified from *A. sp.* metabolism. Observations of terpenes, fatty acids, polyketides, and



peptides metabolites in active fractions are consistent with the presence of encoding BGCs found in the *A. sp.* genome.<sup>169</sup>

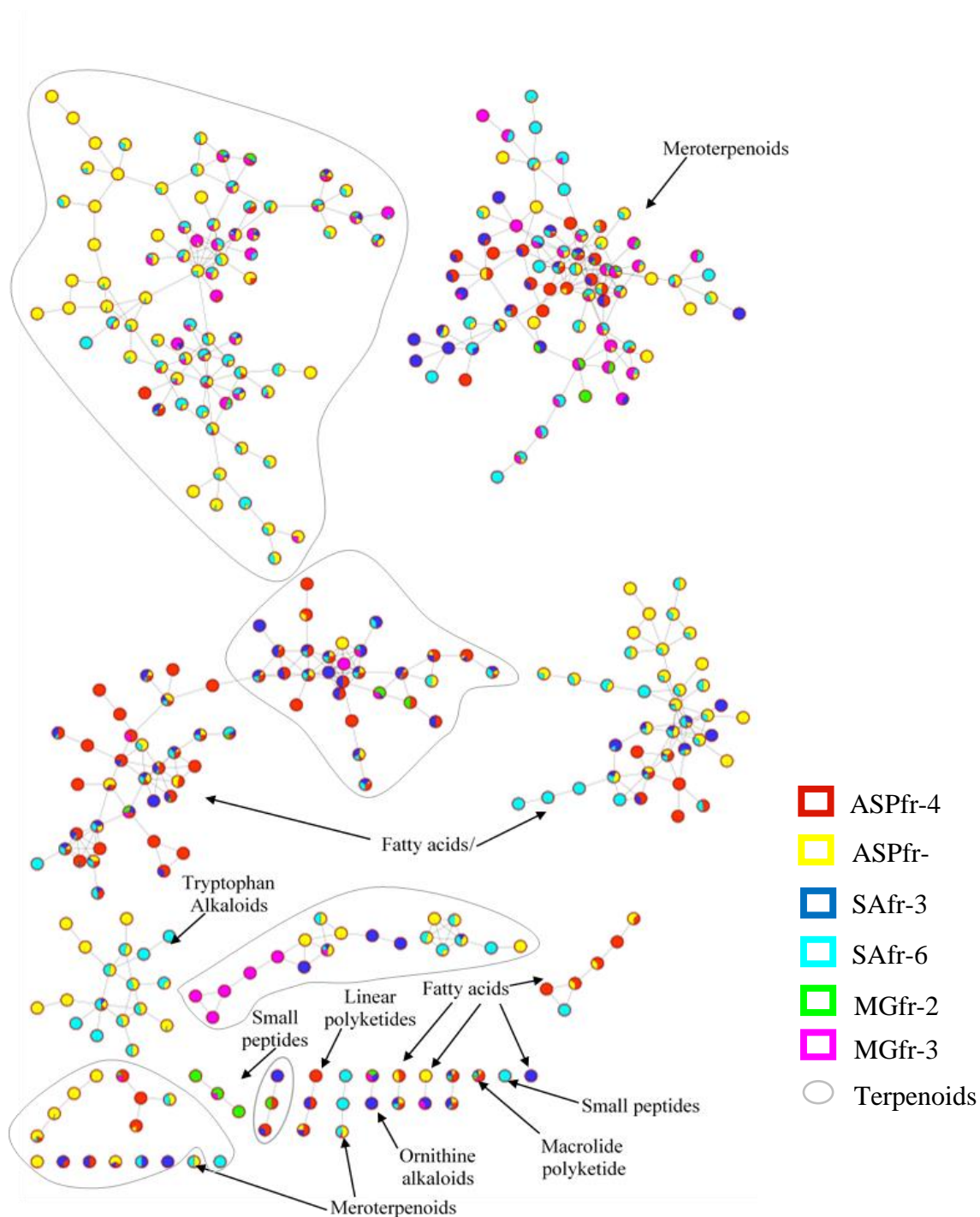


Figure 4.4. Dereplicated and mined molecular network of features from ASPfr-4, ASPfr-10, SAfr-3, SAfr-6, MGfr-2, and MGfr-3 based on GNPS library hits. The pie chart represents the number of spectra observed for each feature. Link to complete network file is available in Appendix B.3.

Meroterpenoids, hybrids of polyketide and terpene scaffolds, appeared to be predominantly influenced by signal exposure, as most nodes observed in the cluster were culture-specific. The annotated terpenoids consisted of sesquiterpenes, diterpenes, and sterols suggesting the potential types of terpene synthases from this strain. Carotenoids and geosmin are common terpenes that have been isolated from the model myxobacterium *Myxococcus xanthus* DK1622 with the former responsible for pigmentation and the latter involved in protecting the bacteria from bacteriophagous grazers.<sup>25,268</sup> Abundance of terpenoids annotated from molecular networks of *A.sp.* suggests that terpenes might play important roles in myxobacterial interactions with the environment. Terpenoids have been suggested to be utilized in myxobacterial communications.<sup>269</sup> Another large group of nodes was annotated as fatty acids in the network. Through metabolomic analysis, the homospermidine lipids, generated during fruiting bodies formation, were isolated from the *M. xanthus* and exhibited high activities against Gram-positive bacteria.<sup>22</sup> It is speculated that this metabolite class could also contribute to the antibacterial activities of active fractions but further investigations are required. Data from this study demonstrate the potential of observing phytohormone- and signal-activated production of functional metabolites in the rhizosphere. Interestingly, only a few signals displayed the potential to activate more bioactive compounds in extracts compared to the control. Perhaps similar investigations on the well-studied *M. xanthus* will provide more publicly accessible spectra libraries to observe the shifts in metabolome induced by plant signals.

#### 4.7 Conclusion

Utilizing functional and metabolomic analysis reveals the potential for plants to activate antimicrobial production in myxobacteria during biotic stress. Results from our

analysis will guide the development of methodologies to access and characterize specialized metabolites from this myxobacterial strain.

## CHAPTER 5. FUTURE DIRECTIONS

MeJA exposure established the unique responses of *Archangium* sp. strain Cb G35 observed through changes in motility, transcriptomic and metabolomic profiles. Similar responses were observed with SA, ABS, and MG exposure assays. However, the impacts of biotic stress signals generated by plants are yet to be observed with other families of the myxococcales. We plan to investigate the species-specific responses that are induced by phytohormones and plant biotic stress-signals, to further explore and establish myxobacterial roles in the rhizobiome.

Given our analysis of the biosynthetic capacity of *A.* sp. and the metabolic profiles from untargeted mass spectra analysis of culture extracts, the terpenoid and polyketide scaffolds were abundant and appeared to be influenced by phytohormones. We will utilize bioinformatics-guided bottom-up strategies in identifying these metabolites from *A.* sp. by the heterologous expression of selected biosynthetic gene clusters in competent expression hosts. These strategies will afford higher concentrations of specialized metabolites for structural elucidation techniques and antimicrobial assays, increasing the known metabolites from *A.* sp.

## LIST OF REFERENCES

1. Mohr K. Diversity of Myxobacteria—We Only See the Tip of the Iceberg. *Microorganisms*. 2018;6(3):84. doi:10.3390/microorganisms6030084
2. Thiery S, Kaimer C. The Predation Strategy of *Myxococcus xanthus*. *Front Microbiol*. 2020; 11:2. doi:10.3389/fmicb.2020.00002
3. Findlay BL. The Chemical Ecology of Predatory Soil Bacteria. *ACS Chem Biol*. 2016;11(6):1502-1510. doi:10.1021/acscchembio.6b00176
4. Zhang L, Lueders T. Micropredator niche differentiation between bulk soil and rhizosphere of an agricultural soil depends on bacterial prey. *FEMS Microbiol Ecol*. 2017;93(9):1-11. doi:10.1093/femsec/fix103
5. Livingstone PG, Morpew RM, Whitworth DE. Myxobacteria are able to prey broadly upon clinically-relevant pathogens, exhibiting a prey range which cannot be explained by phylogeny. *Front Microbiol*. 2017;8:1593. doi:10.3389/fmicb.2017.01593
6. Reichenbach H. The ecology of the myxobacteria. *Environ Microbiol*. 1999;1(1):15-21. doi:10.1046/j.1462-2920.1999.00016.x
7. Mohr KI, Wolf C, Nübel U, Szafrńska AK, Steglich M, Hennesen F, Gemperlein K, Kämpfer P, Martin K, Müller R, Wink J. A polyphasic approach leads to seven new species of the cellulose-decomposing genus *Sorangium*, *Sorangium ambruticinum* sp. nov., *Sorangium arenae* sp. nov., *Sorangium bulgaricum* sp. nov., *Sorangium dawidii* sp. nov., *Sorangium kenyense* sp. nov., *Sorangium orientale* sp. nov. and *Sorangium reichenbachii* sp. nov.. *Int J Syst Evol Microbiol*. 2018;68(11):3576-3586. doi:10.1099/ijsem.0.003034
8. Petters S, Söllinger A, Bengtsson MM, Urich T. The soil microbial food web revisited with metatranscriptomics - Predatory Myxobacteria as keystone taxon? *bioRxiv*. July 2018:373365. doi:10.1101/373365
9. Hoffmann T, Krug D, Bozkurt N, Duddela S, Jansen R, Garcia R, Gerth K, Steinmetz H, Müller R. Correlating chemical diversity with taxonomic distance for discovery of natural products in myxobacteria. *Nat Commun*. 2018;9(1):1-10. doi:10.1038/s41467-018-03184-1
10. Dawid W. Biology and global distribution of myxobacteria in soils. *FEMS Microbiol Rev*. 2000;24(4):403-427. doi:10.1111/j.1574-6976.2000.tb00548.x
11. Jurkevitch E, Minz D, Ramati B, Barel G. Prey range characterization, ribotyping, and diversity of soil and rhizosphere *Bdellovibrio* spp. isolated on phytopathogenic bacteria. *Appl Environ Microbiol*. 2000;66(6):2365-2371. doi:10.1128/AEM.66.6.2365-2371.2000
12. Massart S, Margarita MM, Jijakli MH. Biological control in the microbiome era: Challenges and opportunities. *Biol Control*. 2015;89(2015):98-108. doi:10.1016/j.biocontrol.2015.06.003
13. Youdkes D, Helman Y, Burdman S, Matan O, Jurkevitch E. Potential Control of Potato Soft Rot Disease by the Obligate Predators *Bdellovibrio* and Like Organisms.

- Alexandre G, ed. *Appl Environ Microbiol*. 2020;86(6):e02543-19. doi:10.1128/AEM.02543-19
14. Lugtenberg B, Rozen DE, Kamilova F. Wars between microbes on roots and fruits. *F1000Research*. 2017;6. doi:10.12688/f1000research.10696.1
  15. Fira D, Dimkić I, Berić T, Lozo J, Stanković S. Biological control of plant pathogens by *Bacillus* species. *J Biotechnol*. 2018;285:44-55. doi:10.1016/j.jbiotec.2018.07.044
  16. Alenezi FN, Rekik I, Bełka M, Ibrahim AF, Luptakova L, Jaspars M, Woodward S, Belbahri L. Strain-level diversity of secondary metabolism in the biocontrol species *Aneurinibacillus migulanus*. *Microbiol Res*. 2016;182:116-124. doi:10.1016/j.micres.2015.10.007
  17. Diallo S, Crépin A, Barbey C, Orange N, Burini JF, Latour X. Mechanisms and recent advances in biological control mediated through the potato rhizosphere. *FEMS Microbiol Ecol*. 2011;75(3):351-364. doi:10.1111/j.1574-6941.2010.01023.x
  18. Bratanis E, Andersson T, Lood R, Bukowska-Faniband E. Biotechnological Potential of *Bdellovibrio* and Like Organisms and Their Secreted Enzymes. *Front Microbiol*. 2020;11. doi:10.3389/fmicb.2020.00662
  19. Besset-Manzoni Y, Rieusset L, Joly P, Comte G, Prigent-Combaret C. Exploiting rhizosphere microbial cooperation for developing sustainable agriculture strategies. *Environ Sci Pollut Res*. 2018;25(30):29953-29970. doi:10.1007/s11356-017-1152-2
  20. Ye X, Li Z, Luo X, Wang W, Li Y, Li R, Zhang B, Qiao Y, Zhou J, Fan J, Wang H, Huang Y, Cao H, Cui Z, Zhang R. A predatory myxobacterium controls cucumber Fusarium wilt by regulating the soil microbial community. *Microbiome*. 2020;8(1):1-17. doi:10.1186/s40168-020-00824-x
  21. Bull CT, Shetty KG, Subbarao K V. Interactions between myxobacteria, plant pathogenic fungi, and biocontrol agents. *Plant Dis*. 2002;86(8):889-896. doi:10.1094/PDIS.2002.86.8.889
  22. Hoffmann M, Auerbach D, Panter F, Hoffmann T, Dorrestein PC, Müller R. Homospermidine Lipids: A Compound Class Specifically Formed during Fruiting Body Formation of *Myxococcus xanthus* DK1622. *ACS Chem Biol*. 2018;13(1):273-280. doi:10.1021/acscchembio.7b00816
  23. Muñoz-Dorado J, Marcos-Torres FJ, García-Bravo E, Moraleda-Muñoz A, Pérez J. Myxobacteria: Moving, killing, feeding, and surviving together. *Front Microbiol*. 2016;7:781. doi:10.3389/fmicb.2016.00781
  24. Gregory K, Salvador LA, Akbar S, Adaikpoh BI, Cole Stevens D. Survey of biosynthetic gene clusters from sequenced myxobacteria reveals unexplored biosynthetic potential. *Microorganisms*. 2019;7(6). doi:10.3390/microorganisms7060181
  25. Korp J, Vela Gurovic MS, Nett M. Antibiotics from predatory bacteria. *Beilstein J Org Chem*. 2016;12:594-607. doi:10.3762/bjoc.12.58

26. Herrmann J, Fayad AA, Müller R. Natural products from myxobacteria: Novel metabolites and bioactivities. *Nat Prod Rep*. 2017;34(2):135-160. doi:10.1039/c6np00106h
27. Berleman JE, Allen S, Danielewicz MA, Remis JP, Gorur A, Cunha J, Hadi MZ, Zusman DR, Northen TR, Witkowska HE, Auer M. The lethal cargo of *Myxococcus xanthus* outer membrane vesicles. *Front Microbiol*. 2014;5(474):1-11. doi:10.3389/fmicb.2014.00474
28. Livingstone PG, Millard AD, Swain MT, Whitworth DE. Transcriptional changes when *Myxococcus xanthus* preys on *Escherichia coli* suggest myxobacterial predators are constitutively toxic but regulate their feeding. *Microb genomics*. 2018;4(2). doi:10.1099/mgen.0.000152
29. Carrión VJ, Perez-Jaramillo J, Cordovez V, Tracanna V, De Hollander M, Ruiz-Buck D, Mendes LW, van Ijcken WFJ, Gomez-Exposito R, Elsayed SS, Mohanraju P, Arifah A, van der Oost J, Paulson JN, Mendes R, van Wezel GP, Medema MH, Raaijmakers JM. Pathogen-induced activation of disease-suppressive functions in the endophytic root microbiome. *Science* (80- ). 2019;366(6465):606-612. doi:10.1126/science.aaw9285
30. Venturi V, Fuqua C. Chemical Signaling Between Plants and Plant-Pathogenic Bacteria. *Annu Rev Phytopathol*. 2013;51(1):17-37. doi:10.1146/annurev-phyto-082712-102239
31. Pfeilmeier S, Caly DL, Malone JG. Bacterial pathogenesis of plants: future challenges from a microbial perspective: Challenges in Bacterial Molecular Plant Pathology. *Mol Plant Pathol*. 2016;17(8):1298-1313. doi:10.1111/mpp.12427
32. Hossain MJ, Ran C, Liu K, Ryu CM, Rasmussen-Ivey CR, Williams MA, Hassan MK, Choi SK, Jeong H, Newman M, Kloepper JW, Liles MR. Deciphering the conserved genetic loci implicated in plant disease control through comparative genomics of *Bacillus amyloliquefaciens* subsp. *plantarum*. *Front Plant Sci*. 2015;6:631. doi:10.3389/fpls.2015.00631
33. Naidoo S, Visser EA, Zwart L, Toit Y, Bhadauria V, Shuey LS. Dual RNA-seq to Elucidate the Plant – Pathogen Duel. *Curr Issues Mol Biol*. 2014;27:127-141.
34. Liu Z, Beskrovnaya P, Melnyk RA, Hossain SS, Khorasani S, O'Sullivan LR, Wiesmann CL, Bush J, Richard JD, Haney CH. A Genome-Wide Screen Identifies Genes in Rhizosphere-Associated *Pseudomonas* Required to Evade Plant Defenses. *MBio*. 2018;9(6). doi:10.1128/mBio.00433-18
35. Coutinho BG, Licastro D, Mendonça-Previato L, Cámara M, Venturi V. Plant-Influenced gene expression in the rice endophyte *Burkholderia kururiensis* M130. *Mol Plant-Microbe Interact*. 2015;28(1):10-21. doi:10.1094/MPMI-07-14-0225-R
36. Bari R, Jones JDG. Role of plant hormones in plant defence responses. *Plant Mol Biol*. 2009;69(4):473-488. doi:10.1007/s11103-008-9435-0
37. Verma V, Ravindran P, Kumar PP. Plant hormone-mediated regulation of stress responses. *BMC Plant Biol*. 2016;16(1):1-10. doi:10.1186/s12870-016-0771-y
38. Mhlongo MI, Piater LA, Madala NE, Labuschagne N, Dubery IA. The chemistry of plant–microbe interactions in the rhizosphere and the potential for metabolomics to reveal



signaling related to defense priming and induced systemic resistance. *Front Plant Sci.* 2018; 9:112. doi:10.3389/fpls.2018.00112

39. Bedini A, Mercy L, Schneider C, Franken P, Lucic-Mercy E. Unraveling the initial plant hormone signaling, metabolic mechanisms and plant defense triggering the endomycorrhizal symbiosis behavior. *Front Plant Sci.* 2018;9:1800.

doi:10.3389/fpls.2018.01800

40. Backer R, Rokem JS, Ilangumaran G, Lamont J, Praslickova D, Ricci E, Subramanian S, Smith DL. Plant growth-promoting rhizobacteria: Context, mechanisms of action, and roadmap to commercialization of biostimulants for sustainable agriculture. *Front Plant Sci.* 2018; 9:1473. doi:10.3389/fpls.2018.01473

41. Bais HP, Weir TL, Perry LG, Gilroy S, Vivanco JM. The Role of Root Exudates in Rhizosphere Interactions With Plants and Other Organisms. *Annu Rev Plant Biol.* 2006;57(1):233-266. doi:10.1146/annurev.arplant.57.032905.105159

42. Canarini A, Kaiser C, Merchant A, Richter A, Wanek W. Root exudation of primary metabolites: Mechanisms and their roles in plant responses to environmental stimuli. *Front Plant Sci.* 2019; 10:157. doi:10.3389/fpls.2019.00157

43. Haldar S, Sengupta S. Plant-microbe Cross-talk in the Rhizosphere: Insight and Biotechnological Potential. *Open Microbiol J.* 2015;(9):1-7.

44. Dijkstra FA, Carrillo Y, Pendall E, Morgan JA. Rhizosphere priming: A nutrient perspective. *Front Microbiol.* 2013;4(216):1-8. doi:10.3389/fmicb.2013.00216

45. Cowan MM. Plant Products as Antimicrobial Agents. *Clin Microbiol Rev.* 1999;12(4):564-582.

46. Abreu AC, McBain AJ, Simões M. Plants as sources of new antimicrobials and resistance-modifying agents. *Nat Prod Rep.* 2012;29(9):1007-1021. doi:10.1039/c2np20035j

47. Mattio LM, Catinella G, Dallavalle S, Pinto A. Stilbenoids: A natural arsenal against bacterial pathogens. *Antibiotics.* 2020;9(6):1-40. doi:10.3390/antibiotics9060336

48. Cappiello F, Loffredo MR, Plato C Del, Cammarone S, Casciaro B, Quaglio D, Mangoni ML, Botta B, Ghirga F. The revaluation of plant-derived terpenes to fight antibiotic-resistant infections. *Antibiotics.* 2020;9(6):1-33. doi:10.3390/antibiotics9060325

49. Matilla MA, Espinosa-Urgel M, Rodríguez-Herva JJ, Ramos JL, Ramos-González MI. Genomic analysis reveals the major driving forces of bacterial life in the rhizosphere. *Genome Biol.* 2007;8(9):1-13. doi:10.1186/gb-2007-8-9-r179

50. Li J, Mavrodi O V., Hou J, Blackmon C, Babiker EM, Mavrodi D V. Comparative Analysis of Rhizosphere Microbiomes of Southern Highbush Blueberry (*Vaccinium corymbosum* L.), Darrow's Blueberry (*V. darrowii* Camp), and Rabbit-eye Blueberry (*V. virgatum* Aiton). *Front Microbiol.* 2020; 11:370. doi:10.3389/fmicb.2020.00370

51. Scharf BE, Hynes MF, Alexandre GM. Chemotaxis signaling systems in model beneficial plant-bacteria associations. *Plant Mol Biol.* 2016;90(6):549-559. doi:10.1007/s11103-016-0432-4

52. Zhou H, Wang Y-H, Hai-Zhen Zhu, Ekaterina P. Andrianova, Cheng-Ying Jiang, Jie Feng Z-PL, Xiang H, Igor B. Zhulin S-JL. Cross Talk between Chemosensory Pathways That Modulate. *MBio*. 2019;10(1):1-15.
53. Parkinson JS, Hazelbauer GL, Falke JJ. Signaling and sensory adaptation in *Escherichia coli* chemoreceptors: 2015 update. *Trends Microbiol*. 2015;23(5):257-266. doi:10.1016/j.tim.2015.03.003
54. Welch M, Oosawa K, Aizawa S, Eisenbach M. Phosphorylation-dependent binding of a signal molecule to the flagellar switch of bacteria. *Proc Natl Acad Sci U S A*. 1993;90(19):8787-8791. doi:10.1073/pnas.90.19.8787
55. Liu X, Liu W, Sun Y, Xia C, Elmerich C, Xie Z. A cheZ-like gene in *Azorhizobium caulinodans* is a key gene in the control of chemotaxis and colonization of the host plant. *Appl Environ Microbiol*. 2018;84(3):1-15. doi:10.1128/AEM.01827-17
56. Guo M, Huang Z, Yang J. Is there any crosstalk between the chemotaxis and virulence induction signaling in *Agrobacterium tumefaciens*? *Biotechnol Adv*. 2017;35(4):505-511. doi:10.1016/j.biotechadv.2017.03.008
57. Bertrand JJ, West JT, Engel JN. Genetic analysis of the regulation of type IV pilus function by the Chp chemosensory system of *Pseudomonas aeruginosa*. *J Bacteriol*. 2010;192(4):994-1010. doi:10.1128/JB.01390-09
58. Corral-Lugo A, De la Torre J, Matilla MA, Fernández M, Morel B, Espinosa-Urgel M, Krell T. Assessment of the contribution of chemoreceptor-based signalling to biofilm formation. *Environ Microbiol*. 2016;18(10):3355-3372. doi:10.1111/1462-2920.13170
59. He Y-W, Zhang L-H. Quorum sensing and virulence regulation in *Xanthomonas campestris*. *FEMS Microbiol Rev*. 2008;32(5):842-857. doi:10.1111/j.1574-6976.2008.00120.x
60. Anja Brenic and Stephen C Winans. Detection of and Response to Signals Involved in Host-Microbe Interactions by Plant-Associated Bacteria. *Microbiol Mol Biol Rev*. 2005;69(1):155-194. doi:10.1128/MMBR.69.1.155-194.2005
61. Hacquard S, Spaepen S, Garrido-Oter R, Schulze-Lefert P. Interplay Between Innate Immunity and the Plant Microbiota. *Annu Rev Phytopathol*. 2017;55(1):565-589. doi:10.1146/annurev-phyto-080516-035623
62. Bringhurst RM, Gage DJ. Control of inducer accumulation plays a key role in succinate-mediated catabolite repression in *Sinorhizobium meliloti*. *J Bacteriol*. 2002;184(19):5385-5392. doi:10.1128/jb.184.19.5385-5392.2002
63. Poole PS, Blyth A, Reid CJ, Walters K. Myo-inositol catabolism and catabolite regulation in *Rhizobium leguminosarum* bv. viciae. *Microbiology*. 1994;140(10):2787-2795. doi:10.1099/00221287-140-10-2787
64. Mukherjee A, Ghosh S. Regulation of fructose uptake and catabolism by succinate in *Azospirillum brasilense*. *J Bacteriol*. 1987;169(9):4361-4367. doi:10.1128/jb.169.9.4361-4367.1987

65. Moebius N, Üzüüm Z, Dijksterhuis J, Lackner G, Hertweck C. Active invasion of bacteria into living fungal cells. *Elife*. 2014;3:e03007. doi:10.7554/eLife.03007
66. Kumar P, Dubey RC, Maheshwari DK. Bacillus strains isolated from rhizosphere showed plant growth promoting and antagonistic activity against phytopathogens. *Microbiol Res*. 2012;167(8):493-499. doi:10.1016/j.micres.2012.05.002
67. Ali S, Hameed S, Shahid M, Iqbal M, Lazarovits G, Imran A. Functional characterization of potential PGPR exhibiting broad-spectrum antifungal activity. *Microbiol Res*. 2020;232:126389. doi:10.1016/j.micres.2019.126389
68. Korotkov K V., Sandkvist M, Hol WGJJ. The type II secretion system: Biogenesis, molecular architecture and mechanism. *Nat Rev Microbiol*. 2012;10(5):336-351. doi:10.1038/nrmicro2762
69. Cortes-Tolalpa L, Wang Y, Salles JF, van Elsas JD. Comparative Genome Analysis of the Lignocellulose Degrading Bacteria *Citrobacter freundii* so4 and *Sphingobacterium multivorum* w15. *Front Microbiol*. 2020; 11:248. doi:10.3389/fmicb.2020.00248
70. Helmann TC, Deutschbauer AM, Lindow SE. Genome-wide identification of *Pseudomonas syringae* genes required for fitness during colonization of the leaf surface and apoplast. *Proc Natl Acad Sci U S A*. 2019;116(38):18900-18910. doi:10.1073/pnas.1908858116
71. Lerouge I, Vanderleyden J. O-antigen structural variation: Mechanisms and possible roles in animal/plant-microbe interactions. *FEMS Microbiol Rev*. 2002;26(1):17-47. doi:10.1016/S0168-6445(01)00070-5
72. Deangelis KM, Lindow SE, Firestone MK. Bacterial quorum sensing and nitrogen cycling in rhizosphere soil. *FEMS Microbiol Ecol*. 2008;66(2):197-207. doi:10.1111/j.1574-6941.2008.00550.x
73. Siddiqui IA, Haas D, Heeb S. Extracellular protease of *Pseudomonas fluorescens* CHA0, a biocontrol factor with activity against the root-knot nematode *Meloidogyne incognita*. *Appl Environ Microbiol*. 2005;71(9):5646-5649. doi:10.1128/AEM.71.9.5646-5649.2005
74. Lian LH, Tian BY, Xiong R, Zhu MZ, Xu J, Zhang KQ. Proteases from *Bacillus*: A new insight into the mechanism of action for rhizobacterial suppression of nematode populations. *Lett Appl Microbiol*. 2007;45(3):262-269. doi:10.1111/j.1472-765X.2007.02184.x
75. Timm CM, Campbell AG, Utturkar SM, Jun SR, Parales RE, Tan WA, Robeson MS, Lu TYS, Jawdy S, Brown SD, Ussery DW, Schadt CW, Tuskan GA, Doktycz MJ, Weston DJ, Pelletier DA. Metabolic functions of *Pseudomonas fluorescens* strains from *Populus deltoides* depend on rhizosphere or endosphere isolation compartment. *Front Microbiol*. 2015;6:1118. doi:10.3389/fmicb.2015.01118
76. Kumar G, Kanaujia N, Bafana A. Functional and phylogenetic diversity of root-associated bacteria of *Ajuga bracteosa* in Kangra valley. *Microbiol Res*. 2012;167(4):220-225. doi:10.1016/j.micres.2011.09.001

77. Yilin Gu, Jing Wang ZX and H-LW. Characterization of a Versatile Plant Growth-Promoting Rhizobacterium *Pseudomonas mediterranea* Strain S58. *Microorganisms*. 2020;8:334. doi:10.3390/microorganisms8030334
78. Ramírez-Flandes S, González B, Ulloa O. Redox traits characterize the organization of global microbial communities. *Proc Natl Acad Sci U S A*. 2019;116(9):3630-3635. doi:10.1073/pnas.1817554116
79. Zou Q, Luo S, Wu H, He D, Li X, Cheng G. A GMC Oxidoreductase GmcA Is Required for Symbiotic Nitrogen Fixation in *Rhizobium leguminosarum* bv. *viciae*. *Front Microbiol*. 2020;11:394. doi:10.3389/fmicb.2020.00394
80. Peng A, Liu J, Ling W, Chen Z, Gao Y. Diversity and distribution of 16S rRNA and phenol monooxygenase genes in the rhizosphere and endophytic bacteria isolated from PAH-contaminated sites. *Sci Rep*. 2015;5:12173. doi:10.1038/srep12173
81. Nagarajkumar M, Jayaraj J, Muthukrishnan S, Bhaskaran R, Velazhahan R. Detoxification of oxalic acid by *Pseudomonas fluorescens* strain PfMDU2: Implications for the biological control of rice sheath blight caused by *Rhizoctonia solani*. *Microbiol Res*. 2005;160(3):291-298. doi:10.1016/j.micres.2005.02.002
82. Liu Y, Jiang X, Guan D, Zhou W, Ma M, Zhao B, Cao F, Li L, Li J. Transcriptional analysis of genes involved in competitive nodulation in *Bradyrhizobium diazoefficiens* at the presence of soybean root exudates. *Sci Rep*. 2017;7(1):1-11. doi:10.1038/s41598-017-11372-0
83. Ankati S, Rani TS, Podile AR. Partner-triggered proteome changes in the cell wall of *Bacillus sonorensis* and roots of groundnut benefit each other. *Microbiol Res*. 2018;217:91-100. doi:10.1016/j.micres.2018.10.003
84. Pliego C, Vicente A De, Cazorla FM, Ramos C. Response of the Biocontrol Agent *Pseudomonas*. 2019;85(3):1-17.
85. Subramoni S, Gonzalez JF, Johnson A, Péchy-Tarr M, Rochat L, Paulsen I, Loper JE, Keel C, Venturi V. Bacterial subfamily of LuxR regulators that respond to plant compounds. *Appl Environ Microbiol*. 2011;77(13):4579-4588. doi:10.1128/AEM.00183-11
86. Uppalapati SR, Ayoubi P, Weng H, Palmer DA, Mitchell RE, Jones W, Bender CL. The phytotoxin coronatine and methyl jasmonate impact multiple phytohormone pathways in tomato. *Plant J*. 2005;42(2):201-217. doi:10.1111/j.1365-313X.2005.02366.x
87. Chini A, Cimmino A, Masi M, Reveglia P, Nocera P, Solano R, Evidente A. The fungal phytotoxin lasiojasmonate A activates the plant jasmonic acid pathway. *J Exp Bot*. 2018;69(12):3095-3102. doi:10.1093/jxb/ery114
88. Doornbos RF, Geraats BPJ, Kuramae EE, Van Loon LC, Bakker PAHM. Effects of jasmonic acid, ethylene, and salicylic acid signaling on the rhizosphere bacterial community of *Arabidopsis thaliana*. *Mol Plant-Microbe Interact*. 2011;24(4):395-407. doi:10.1094/MPMI-05-10-0115

89. Nahar K, Kyndt T, Nzogela YB, Gheysen G. Abscisic acid interacts antagonistically with classical defense pathways in rice-migratory nematode interaction. *New Phytol.* 2012;196(3):901-913. doi:10.1111/j.1469-8137.2012.04310.x
90. Mine A, Berens ML, Nobori T, Anver S, Fukumoto K, Winkelmüller TM, Takeda A, Becker D, Tsuda K. Pathogen exploitation of an abscisic acid- and jasmonate-inducible MAPK phosphatase and its interception by *Arabidopsis* immunity. *Proc Natl Acad Sci U S A.* 2017;114(28):7456-7461. doi:10.1073/pnas.1702613114
91. Ding X, Cao Y, Huang L, Zhao J, Xu C, Li X, Wang S. Activation of the indole-3-acetic acid-amido synthetase GH3-8 suppresses expansin expression and promotes salicylate- and jasmonate-independent basal immunity in rice. *Plant Cell.* 2008;20(1):228-240. doi:10.1105/tpc.107.055657
92. Sørensen JL, Benfield AH, Wollenberg RD, Westphal K, Wimmer R, Nielsen MR, Nielsen KF, Carere J, Covarelli L, Beccari G, Powell J, Yamashino T, Kogler H, Sondergaard TE, Gardiner DM. The cereal pathogen *Fusarium pseudograminearum* produces a new class of active cytokinins during infection. *Mol Plant Pathol.* 2018;19(5):1140-1154. doi:10.1111/mpp.12593
93. Van Bockhaven J, Spíchal L, Novák O, Strnad M, Asano T, Kikuchi S, Höfte M, De Vleeschauwer D. Silicon induces resistance to the brown spot fungus *Cochliobolus miyabeanus* by preventing the pathogen from hijacking the rice ethylene pathway. *New Phytol.* 2015;206(2):761-773. doi:10.1111/nph.13270
94. Berrocal-Lobo M, Molina A, Solano R. Constitutive expression of Ethylene-Response-Factor1 in arabidopsis confers resistance to several necrotrophic fungi. *Plant J.* 2002;29(1):23-32. doi:10.1046/j.1365-313x.2002.01191.x
95. Qin X, Liu JH, Zhao WS, Chen XJ, Guo ZJ, Peng YL. Gibberellin 20-Oxidase Gene OsGA20ox3 regulates plant stature and disease development in rice. *Mol Plant-Microbe Interact.* 2013;26(2):227-239. doi:10.1094/MPMI-05-12-0138-R
96. Yang DL, Li Q, Deng YW, Lou YG, Wang MY, Zhou GX, Zhang YY, He ZH. Altered disease development in the eui mutants and Eui overexpressors indicates that gibberellins negatively regulate rice basal disease resistance. *Mol Plant.* 2008;1(3):528-537. doi:10.1093/mp/ssn021
97. Djamei A, Schipper K, Rabe F, Ghosh A, Vincon V, Kahnt J, Osorio S, Tohge T, Fernie AR, Feussner I, Feussner K, Meinicke P, Stierhof YD, Schwarz H, MacEk B, Mann M, Kahmann R. Metabolic priming by a secreted fungal effector. *Nature.* 2011;478(7369):395-398. doi:10.1038/nature10454
98. Turnbull D, Yang L, Naqvi S, Breen S, Welsh L, Stephens J, Morris J, Boevink PC, Hedley PE, Zhan J, Birch PRJ, Gilroy EM. RXLR effector AVR2 up-regulates a brassinosteroid-responsive bHLH transcription factor to suppress immunity. *Plant Physiol.* 2017;174(1):356-369. doi:10.1104/pp.16.01804
99. de Vleeschauwer D, van Buyten E, Satoh K, Balidion J, Mauleon R, Choi IR, Vera-Cruz C, Kikuchi S, Höfte M. Brassinosteroids antagonize gibberellin- and salicylate-

- mediated root immunity in rice. *Plant Physiol.* 2012;158(4):1833-1846.  
doi:10.1104/pp.112.193672
100. Umehara M, Hanada A, Yoshida S, Akiyama K, Arite T, Takeda-Kamiya N, Magome H, Kamiya Y, Shirasu K, Yoneyama K, Kyoizuka J, Yamaguchi S. Inhibition of shoot branching by new terpenoid plant hormones. *Nature.* 2008;455(7210):195-200.  
doi:10.1038/nature07272
101. Gomez-Roldan V, Fermas S, Brewer PB, Puech-Pagès V, Dun EA, Pillot JP, Letisse F, Matusova R, Danoun S, Portais JC, Bouwmeester H, Bécard G, Beveridge CA, Rameau C, Rochange, SF. Strigolactone inhibition of shoot branching. *Nature.* 2008;455(7210):189-194.  
doi:10.1038/nature07271
102. Antunez-Lamas M, Cabrera E, Lopez-Solanilla E, Solano R, González-Melendi P, Chico JM, Toth I, Birch P, Pritchard L, Liu H, Rodriguez-Palenzuela P. Bacterial chemoattraction towards jasmonate plays a role in the entry of *Dickeya dadantii* through wounded tissues. *Mol Microbiol.* 2009;74(3):662-671. doi:10.1111/j.1365-2958.2009.06888.x
103. Derksen H, Rampitsch C, Daayf F. Signaling cross-talk in plant disease resistance. *Plant Sci.* 2013;207:79-87. doi:10.1016/j.plantsci.2013.03.004
104. Bignell DRD, Cheng Z, Bown L. The coronafacoyl phytotoxins: structure, biosynthesis, regulation and biological activities. *Antonie van Leeuwenhoek, Int J Gen Mol Microbiol.* 2018;111(5):649-666. doi:10.1007/s10482-017-1009-1
105. Bignell DRD, Selpke RF, Huguet-Tapla JC, Chambers AH, Parry RJ, Lorla R. *Streptomyces scabies* 87-22 contains a coronafacic acid-like biosynthetic cluster that contributes to plant-microbe interactions. *Mol Plant-Microbe Interact.* 2010;23(2):161-175.  
doi:10.1094/MPMI-23-2-0161
106. Plett JM, Daguerre Y, Wittulsky S, Vayssières A, Deveau A, Melton SJ, Kohler A, Morrell-Falvey JL, Brun A, Veneault-Fourrey C, Martin F. Effector MiSSP7 of the mutualistic fungus *Laccaria bicolor* stabilizes the Populus JAZ6 protein and represses jasmonic acid (JA) responsive genes. *Proc Natl Acad Sci U S A.* 2014;111(22):8299-8304.  
doi:10.1073/pnas.1322671111
107. Li Y, Liu J, Díaz-Cruz G, Cheng Z, Bignell DRD. Virulence mechanisms of plant-pathogenic *Streptomyces* species: An updated review. *Microbiol (United Kingdom).* 2019;165(10):1025-1040. doi:10.1099/mic.0.000818
108. Duke SO, Dayan FE. Modes of action of microbially-produced phytotoxins. *Toxins (Basel).* 2011;3(8):1038-1064. doi:10.3390/toxins3081038
109. Scholz-Schroeder BK, Hutchison ML, Grgurina I, Gross DC. The contribution of syringopeptin and syringomycin to virulence of *Pseudomonas syringae* pv. *syringae* strain B301D on the basis of sypA and syrB1 biosynthesis mutant analysis. *Mol Plant-Microbe Interact.* 2001;14(3):336-348. doi:10.1094/MPMI.2001.14.3.336
110. Dudnik A, Bigler L, Dudler R. Production of proteasome inhibitor syringolin a by the endophyte *Rhizobium* sp. Strain AP16. *Appl Environ Microbiol.* 2014;80(12):3741-3748.  
doi:10.1128/AEM.00395-14

111. Krahn D, Ottmann C, Kaiser M. The chemistry and biology of syringolins, glidobactins and cepafungins (syrbactins). *Nat Prod Rep*. 2011;28(11):1854-1867. doi:10.1039/c1np00048a
112. Murai Y, Mori S, Konno H, Hikichi Y, Kai K. Ralstonins A and B, Lipopeptides with Chlamydospore-Inducing and Phytotoxic Activities from the Plant Pathogen *Ralstonia solanacearum*. *Org Lett*. 2017;19(16):4175-4178. doi:10.1021/acs.orglett.7b01685
113. Spraker JE, Wiemann P, Baccile JA, Venkatesh N, Schumacher J, Schroeder FC, Sanchez LM, Keller NP. Conserved responses in a war of small molecules between a plant-pathogenic bacterium and fungi. *MBio*. 2018;9(3):1-14. doi:10.1128/mBio.00820-18
114. Ishikawa Y, Murai Y, Sakata M, Mori S, Matsuo S, Senuma W, Ohnishi K, Hikichi Y, Kai K. Activation of Ralfuranone/Ralstonin Production by Plant Sugars Functions in the Virulence of *Ralstonia solanacearum*. *ACS Chem Biol*. 2019;14(7):1546-1555. doi:10.1021/acscchembio.9b00301
115. Li X, Li Y, Wang R, Wang Q, Lu L. Toxoflavin Produced by *Burkholderia gladioli* from Lycoris. *Appl Environ Microbiol*. 2019; 85(9): e00106-19.
116. Lee J, Park J, Kim S, Park I, Seo YS. Differential regulation of toxoflavin production and its role in the enhanced virulence of *Burkholderia gladioli*. *Mol Plant Pathol*. 2016;17(1):65-76. doi:10.1111/mpp.12262
117. Azegami K, Nishiyama K, Watanabe Y, Suzuki T, Yoshida M, Nose K, Toda S. Tropolone as a root growth-inhibitor produced by a plant pathogenic *Pseudomonas* sp. causing seedling blight of rice. *Japanese J Phytopathol*. 1985;51(3):315-317. doi:10.3186/jjphytopath.51.315
118. Gerwick BC, Fields SS, Graupner PR, Gray JA, Chapin EL, Cleveland JA, Heim DR. Pyridazocidin, A New Microbial Phytotoxin with Activity in the Mehler. *Weed Science* 1997;45(5):654-657.
119. Mendes R, Kruijt M, De Bruijn I, Dekkers E, Van Der Voort M, Schneider JHM, Piceno YM, DeSantis TZ, Andersen GL, Bakker PAHM, Raaijmakers JM. Deciphering the rhizosphere microbiome for disease-suppressive bacteria. *Science* 6033(332)1097-1100. 2011;332(6033):1097-1100. doi:10.1126/science.1203980
120. Kai K. Bioorganic chemistry of signaling molecules in microbial communication. *J Pestic Sci*. 2019;44(3):200-207. doi:10.1584/jpestics.J19-02
121. Grandclément C, Tannières M, Moréra S, Dessaux Y, Faure D. Quorum quenching: Role in nature and applied developments. *FEMS Microbiol Rev*. 2015;40(1):86-116. doi:10.1093/femsre/fuv038
122. Cirou A, Mondy S, An S, Charrier A, Sarrazin A, Thoison O, Bow MD, Faure D. Efficient biostimulation of native and introduced quorum-quenching *Rhodococcus erythropolis* populations is revealed by a combination of analytical chemistry, microbiology, and pyrosequencing. *Appl Environ Microbiol*. 2012;78(2):481-492. doi:10.1128/AEM.06159-11

123. Dong YH, Gusti AR, Zhang Q, Xu J-L, Zhang L-H. Identification of quorum-quenching N-acyl homoserine lactonases from *Bacillus* species. *Appl Environ Microbiol.* 2002;68(4):1754-1759. doi:10.1128/aem.68.4.1754-1759.2002
124. Dong YH, Zhang XF, Xu JL, Zhang LH. Insecticidal *Bacillus thuringiensis* Silences *Erwinia carotovora* Virulence by a New Form of Microbial Antagonism, Signal Interference. *Appl Environ Microbiol.* 2004;70(2):954-960. doi:10.1128/AEM.70.2.954-960.2004
125. Dong YH, Xu JL, Li XZ, Zhang LH. AiiA, an enzyme that inactivates the acylhomoserine lactone quorum-sensing signal and attenuates the virulence of *Erwinia carotovora*. *Proc Natl Acad Sci U S A.* 2000;97(7):3526-3531. doi:10.1073/pnas.97.7.3526
126. Shepherd RW, Lindow SE. Two dissimilar N-acyl-homoserine lactone acylases of *Pseudomonas syringae* influence colony and biofilm Morphology. *Appl Environ Microbiol.* 2009;75(1):45-53. doi:10.1128/AEM.01723-08
127. Crits-Christoph A, Diamond S, Butterfield CN, Thomas BC, Banfield JF. Novel soil bacteria possess diverse genes for secondary metabolite biosynthesis. *Nature.* 2018;558(7710):440-444. doi:10.1038/s41586-018-0207-y
128. Rabbee MF, Sarafat Ali M, Choi J, Hwang BS, Jeong SC, Baek K hyun. *Bacillus velezensis*: A valuable member of bioactive molecules within plant microbiomes. *Molecules.* 2019;24(6):1-13. doi:10.3390/molecules24061046
129. Kaspar F, Neubauer P, Gimpel M. Bioactive Secondary Metabolites from *Bacillus subtilis*: A Comprehensive Review. *J Nat Prod.* 2019;82(7):2038-2053. doi:10.1021/acs.jnatprod.9b00110
130. Chowdhury SP, Hartmann A, Gao XW, Borriss R. Biocontrol mechanism by root-associated *Bacillus amyloliquefaciens* FZB42 - A review. *Front Microbiol.* 2015;6:780. doi:10.3389/fmicb.2015.00780
131. Wu L, Wu H, Chen L, Yu X, Borriss R, Gao X. Difficidin and bacilysin from *Bacillus amyloliquefaciens* FZB42 have antibacterial activity against *Xanthomonas oryzae* rice pathogens. *Sci Rep.* 2015;5:12975. doi:10.1038/srep12975
132. Liu Z, Budiharjo A, Wang P, Shi H, Fang J, Borriss R, Zhang K, Huang X. The highly modified microcin peptide plantazolicin is associated with nematicidal activity of *Bacillus amyloliquefaciens* FZB42. *Appl Microbiol Biotechnol.* 2013;97(23):10081-10090. doi:10.1007/s00253-013-5247-5
133. Raaijmakers JM, De Bruijn I, De Kock MJD. Cyclic lipopeptide production by plant-associated *Pseudomonas* spp.: Diversity, activity, biosynthesis, and regulation. *Mol Plant-Microbe Interact.* 2006;19(7):699-710. doi:10.1094/MPMI-19-0699
134. De Bruijn I, De Kock MJD, De Waard P, Van Beek TA, Raaijmakers JM. Massetolide A biosynthesis in *Pseudomonas fluorescens*. *J Bacteriol.* 2008;190(8):2777-2789. doi:10.1128/JB.01563-07
135. Thrane C, Harder Nielsen T, Neiendam Nielsen M, Sørensen J, Olsson S. Viscosinamide-producing *Pseudomonas fluorescens* DR54 exerts a biocontrol effect on



- Pythium ultimum in sugar beet rhizosphere. *FEMS Microbiol Ecol.* 2000;33(2):139-146. doi:10.1016/S0168-6496(00)00054-4
136. Simionato AS, Navarro MOP, de Jesus MLA, Barazetti AR, da Silva CS, Simões GC, Balbi-Peña MI, de Mello JCP, Panagio LA, de Almeida RSC, Andrade G, de Oliveira AG. The effect of phenazine-1-carboxylic acid on mycelial growth of *Botrytis cinerea* produced by *Pseudomonas aeruginosa* LV strain. *Front Microbiol.* 2017;8:1102. doi:10.3389/fmicb.2017.01102
137. Burkhead KD, Schisler DA, Slininger PJ. Pyrrolnitrin production by biological control agent *Pseudomonas cepacia* B37w in culture and in colonized wounds of potatoes. *Appl Environ Microbiol.* 1994;60(6):2031-2039. doi:10.1128/aem.60.6.2031-2039.1994
138. Jousset A, Rochat L, Scheu S, Bonkowski M, Keel C. Predator-prey chemical warfare determines the expression of biocontrol genes by rhizosphere-associated *Pseudomonas fluorescens*. *Appl Environ Microbiol.* 2010;76(15):5263-5268. doi:10.1128/AEM.02941-09
139. Calderón CE, de Vicente A, Cazorla FM. Role of 2-hexyl, 5-propyl resorcinol production by *Pseudomonas chlororaphis* PCL1606 in the multitrophic interactions in the avocado rhizosphere during the biocontrol process. *FEMS Microbiol Ecol.* 2014;89(1):20-31. doi:10.1111/1574-6941.12319
140. Mela F, Fritsche K, De Boer W, Van Veen JA, De Graaff LH, Van Den Berg M, Leveau JHJ. Dual transcriptional profiling of a bacterial/fungal confrontation: *Collimonas fungivorans* versus *Aspergillus niger*. *ISME J.* 2011;5(9):1494-1504. doi:10.1038/ismej.2011.29
141. Kai K, Sogame M, Sakurai F, Nasu N, Fujita M. Collimonins A-D, Unstable Polyynes with Antifungal or Pigmentation Activities from the Fungus-Feeding Bacterium *Collimonas fungivorans* Ter331. *Org Lett.* 2018;20(12):3536-3540. doi:10.1021/acs.orglett.8b01311
142. Yun SC. Selection and a 3-year field trial of *Sorangium cellulosum* KYC 3262 against anthracnose in hot pepper. *Plant Pathol J.* 2014;30(3):279-287. doi:10.5423/PPJ.OA.01.2014.0002
143. Cintas NA, Koike ST, Bunch RA, Bull CT. Holdover inoculum of *Pseudomonas syringae* pv. *alisalensis* from broccoli raab causes disease in subsequent plantings. *Plant Dis.* 2006;90(8):1077-1084. doi:10.1094/PD-90-1077
144. Lloyd DG, Whitworth DE. The myxobacterium *Myxococcus xanthus* can sense and respond to the quorum signals secreted by potential prey organisms. *Front Microbiol.* 2017; 8:439. doi:10.3389/fmicb.2017.00439
145. Mashburn-Warren L, Mclean RJC, Whiteley M. Gram-negative outer membrane vesicles: Beyond the cell surface. *Geobiology.* 2008;6(3):214-219. doi:10.1111/j.1472-4669.2008.00157.x
146. Li Z, Ye X, Liu M, Xia C, Zhang L, Luo X, Wang T, Chen Y, Zhao Y, Qiao Y, Huang Y, Cao H, Gu X, Fan J, Cui Z, Zhang Z, Li Z, Ye X, Liu M, Xia C, Zhang L, Luo X, Wang T, Chen Y, Zhao Y, Qiao Y, Huang Y, Cao H, Gu X, Fan J, Cui Z, Zhang Z, Li Z, Ye X, Liu M, Xia C, Zhang L, Luo X, Wang T, Chen Y, Zhao Y, Qiao Y, Huang Y, Cao H, Gu X, Fan J, Cui Z, Zhang Z. A novel outer membrane  $\beta$ -1,6-glucanase is deployed in the

predation of fungi by myxobacteria. *ISME J.* 2019;13(9):2223-2235. doi:10.1038/s41396-019-0424-x

147. Homma Y. Perforation and Lysis of Hyphae of *Rhizoctonia solani* and Conidia of *Cochliobolus miyabeanus* by Soil Myxobacteria. *Phytopathology.* 1984; 74(10):1234. doi:10.1094/phyto-74-1234

148. Fesel PH, Zuccaro A.  $\beta$ -glucan: Crucial component of the fungal cell wall and elusive MAMP in plants. *Fungal Genet Biol.* 2016; 90:53-60. doi:10.1016/j.fgb.2015.12.004

149. Lipke PN, Ovalle R. Cell wall architecture in yeast: New structure and new challenges. *J Bacteriol.* 1998;180(15):3735-3740. doi:10.1128/jb.180.15.3735-3740.1998

150. Farag MA, Zhang H, Ryu CM. Dynamic Chemical Communication between Plants and Bacteria through Airborne Signals: Induced Resistance by Bacterial Volatiles. *J Chem Ecol.* 2013;39(7):1007-1018. doi:10.1007/s10886-013-0317-9

151. Garbeva P, Weiskopf L. Airborne medicine: bacterial volatiles and their influence on plant health. *New Phytol.* 2020;226(1):32-43. doi:10.1111/nph.16282

152. Feng H, Zhang N, Du W, Zhang H, Liu Y, Fu R, Shao J, Zhang G, Shen Q, Zhang R. Identification of chemotaxis compounds in root exudates and their sensing chemoreceptors in plant-growth-promoting rhizobacteria *Bacillus amyloliquefaciens* SQR9. *Mol Plant-Microbe Interact.* 2018; 31(10):995-1005. doi:10.1094/MPMI-01-18-0003-R

153. Wenzel SC, Müller R. The impact of genomics on the exploitation of the myxobacterial secondary metabolome. *Nat Prod Rep.* 2009;26(11):1385-1407. doi:10.1039/b817073h

154. Bode HB, Zeggel B, Silakowski B, Wenzel SC, Reichenbach H, Müller R. Steroid biosynthesis in prokaryotes: Identification of myxobacterial steroids and cloning of the first bacterial 2,3(S)-oxidosqualene cyclase from the myxobacterium *Stigmatella aurantiaca*. *Mol Microbiol.* 2003;47(2):471-481. doi:10.1046/j.1365-2958.2003.03309.x

155. Panter F, Krug D, Baumann S, Müller R. Self-resistance guided genome mining uncovers new topoisomerase inhibitors from myxobacteria. *Chem Sci.* 2018;9(21):4898-4908. doi:10.1039/c8sc01325j

156. Sutton D, Livingstone PG, Furness E, Swain MT, Whitworth DE. Genome-Wide Identification of Myxobacterial Predation Genes and Demonstration of Formaldehyde Secretion as a Potentially Predation-Resistant Trait of *Pseudomonas aeruginosa*. *Front Microbiol.* 2019;10. doi:10.3389/fmicb.2019.02650

157. Schäberle TF, Lohr F, Schmitz A, König GM. Antibiotics from myxobacteria. *Nat Prod Rep.* 2014;31(7):953-972. doi:10.1039/c4np00011k

158. Zander W, Gerth K, Mohr KI, Kessler W, Jansen R, Müller R. Roimatacene: An antibiotic against gram-negative bacteria isolated from *Cystobacter ferrugineus* Cb G35 (Myxobacteria). *Chem - A Eur J.* 2011;17(28):7875-7881. doi:10.1002/chem.201003677

159. Zander W, Mohr KI, Gerth K, Jansen R, Müller R. *p*-hydroxyacetophenone amides from *Cystobacter ferrugineus* strain Cb G35. *J Nat Prod.* 2011;74(6):1358-1363. doi:10.1021/np1006789
160. Lang E, Schumann P, Tindall BJ, Mohr KI, Spröer C. Reclassification of *Angiococcus disciformis*, *Cystobacter minus* and *Cystobacter violaceus* as *Archangium disciforme* comb. nov., *Archangium minus* comb. nov. and *Archangium violaceum* comb. nov., Unification of the families *Archangiaceae* and *Cystobacteraceae*, *Int J Syst Evol Microbiol.* 2015;65(11):4032-4042. doi:10.1099/ijsem.0.000533
161. Overbeek R, Olson R, Pusch GD, Olsen GJ, Davis JJ, Disz T, Edwards RA, Gerdes S, Parrello B, Shukla M, Vonstein V, Wattam AR, Xia F, Stevens R. The SEED and the Rapid Annotation of microbial genomes using Subsystems Technology (RAST). *Nucleic Acids Res.* 2014;42(Database issue):D206-14. doi:10.1093/nar/gkt1226
162. Angiuoli S V., Gussman A, Klimke W, Cochrane G, Field D, Garrity G, Kodira CD, Kyrpides N, Madupu R, Markowitz V, Tatusova T, Thomson N, White O. Toward an online repository of standard operating procedures (SOPs) for (meta)genomic annotation. *Omi A J Integr Biol.* 2008;12(2):137-141. doi:10.1089/omi.2008.0017
163. Tatusova T, DiCuccio M, Badretdin A, Chetvermin V, Ciufu S, Li W. Prokaryotic Genome Annotation Pipeline, in *The NCBI Handbook*, 2nd ed. National Center for Biotechnology Information, Bethesda, MD.
164. Weber T, Blin K, Duddela S, Krug D, Kim HU, Bruccoleri R, Lee SY, Fischbach MA, Müller R, Wohlleben W, Breitling R, Takano E, Medema MH. AntiSMASH 3.0-A comprehensive resource for the genome mining of biosynthetic gene clusters. *Nucleic Acids Res.* 2015;43(W1):W237-W243. doi:10.1093/nar/gkv437
165. Navarro-Muñoz JC, Selem-Mojica N, Mullowney MW, Kautsar S, Tryon JH, Parkinson EI, De Los Santos ELC, Yeong M, Cruz-Morales P, Abubucker S, Roeters A, Lokhorst W, Fernandez-Guerra A, Dias Cappelini LT, Thomson RJ, Metcalf WW, Kelleher NL, Barona-Gomez F, Medema MH. A computational framework for systematic exploration of biosynthetic diversity from large-scale genomic data. *bioRxiv.* January 2018:445270. doi:10.1101/445270
166. Blin K, Shaw S, Steinke K, Villebro R, Ziemert N, Lee SY, Medema MH, Weber T. antiSMASH 5.0: updates to the secondary metabolite genome mining pipeline. *Nucleic Acids Res.* 2019;47(W1):W81-W87. doi:10.1093/nar/gkz310
167. Crüsemann M, O'Neill EC, Larson CB, Melnik AV, Floros DJ, Da Silva RR, Jensen PR, Dorrestein PC, Moore BS. Prioritizing Natural Product Diversity in a Collection of 146 Bacterial Strains Based on Growth and Extraction Protocols. *J Nat Prod.* 2017;80(3):588-597. doi:10.1021/acs.jnatprod.6b00722
168. Wang M, Carver JJ, Phelan VV, Sanchez LM, Garg N, Peng Y, Nguyen DD, Watrous J, Kapon CA, Luzzatto-Knaan T, Porto C, Bouslimani A, Melnik AV, Meehan MJ, Liu WT, Crüsemann M, Boudreau PD, Esquenazi E, Sandoval-Calderón M, Kersten RD, Pace LA, Quinn RA, Duncan KR, Hsu CC, Floros DJ, Gavilan RG, Kleigrew K, Northen T, Dutton RJ, Parrot D, Carlson EE, Aigle B, Michelsen CF, Jelsbak L, Sohlenkamp C, Pevzner P, Edlund A, McLean J, Piel J, Murphy BT, Gerwick L, Liaw CC, Yang YL, Humpf HU,

- Maansson M, Keyzers RA, Sims AC, Johnson AR, Sidebottom AM, Sedio BE, Klitgaard A, Larson CB, P CAB, Torres-Mendoza D, Gonzalez DJ, Silva DB, Marques LM, Demarque DP, Pociute E, O'Neill EC, Briand E, Helfrich EJN, Granatosky EA, Glukhov E, Ryffel F, Houson H, Mohimani H, Kharbush JJ, Zeng Y, Vorholt JA, Kurita KL, Charusanti P, McPhail KL, Nielsen KF, Vuong L, Elfeki M, Traxler MF, Engene N, Koyama N, Vining OB, Baric R, Silva RR, Mascuch SJ, Tomasi S, Jenkins S, Macherla V, Hoffman T, Agarwal V, Williams PG, Dai J, Neupane R, Gurr J, Rodríguez AMC, Lamsa A, Zhang C, Dorrestein K, Duggan BM, Almaliti J, Allard PM, Phapale P, Nothias LF, Alexandrov T, Litaudon M, Wolfender JL, Kyle JE, Metz TO, Peryea T, Nguyen DT, VanLeer D, Shinn P, Jadhav A, Müller R, Waters KM, Shi W, Liu X, Zhang L, Knight R, Jensen PR, Palsson BO, Pogliano K, Lington RG, Gutiérrez M, Lopes NP, Gerwick WH, Moore BS, Dorrestein PC, Bandeira N. Sharing and community curation of mass spectrometry data with Global Natural Products Social Molecular Networking. *Nat Biotechnol.* 2016;34(8):828-837. doi:10.1038/nbt.3597
169. Adaikpoh BI, Dowd SE, Cole Stevens D, Stevens DC. Draft Genome Sequence of *Archangium* sp. Strain Cb G35. *Genome Announc.* 2017;5(8):e01678-16. doi:10.1128/genomeA.01678-16
170. Kjærboelling I, Vesth T, Andersen MR. Resistance Gene-Directed Genome Mining of 50 *Aspergillus* Species. *mSystems.* 2019;4(4):1-13.
171. Mohr KI, Garcia RO, Gerth K, Irschik H, Müller R. *Sandaracinus amylolyticus* gen. nov., sp. nov., a starch-degrading soil myxobacterium, and description of *Sandaracinaceae* fam. nov. *Int J Syst Evol Microbiol.* 2012;62(5):1191-1198. doi:10.1099/ijms.0.033696-0
172. Charousová I, Medo J, Javoreková S. Isolation, antimicrobial activity of myxobacterial crude extracts and identification of the most potent strains. *Arch Biol Sci.* 2017;69(3):561-568. doi:10.2298/ABS161011132C
173. Mungan MD, Alanjary M, Blin K, Weber T, Medema MH, Ziemert N. ARTS 2.0: feature updates and expansion of the Antibiotic Resistant Target Seeker for comparative genome mining. *Nucleic Acids Res.* 2020;48(W1):W546-W552. doi:10.1093/nar/gkaa374
174. MIBiG: Minimum Information about a Biosynthetic Gene cluster. <https://mibig.secondarymetabolites.org/>. Accessed March 16, 2021.
175. Alanjary M, Kronmiller B, Adamek M, Blin K, Weber T, Huson D, Philmus B, Ziemert N. The Antibiotic Resistant Target Seeker (ARTS), an exploration engine for antibiotic cluster prioritization and novel drug target discovery. *Nucleic Acids Res.* 2017;45(W1):W42-W48. doi:10.1093/nar/gkx360
176. Sood S, Awal RP, Wink J, Mohr KI, Rohde M, Stadler M, Kämpfer P, Glaeser SP, Schumann P, Garcia R, Müller R. *Aggregicoccus edonensis* gen. nov., sp. nov., an unusually aggregating myxobacterium isolated from a soil sample. *Int J Syst Evol Microbiol.* 2015;65(3):745-753. doi:10.1099/ijms.0.061176-0
177. Massalha H, Korenblum E, Tholl D, Aharoni A. Small molecules below-ground: the role of specialized metabolites in the rhizosphere. *Plant J.* 2017;90(4):788-807. doi:10.1111/tbj.13543

178. Bulgarelli D, Schlaeppi K, Spaepen S, Van Themaat EVL, Schulze-Lefert P. Structure and functions of the bacterial microbiota of plants. *Annu Rev Plant Biol.* 2013;64:807-838. doi:10.1146/annurev-arplant-050312-120106
179. Müller DB, Vogel C, Bai Y, Vorholt JA. The Plant Microbiota: Systems-Level Insights and Perspectives. *Annu Rev Genet.* 2016;50:211-234. doi:10.1146/annurev-genet-120215-034952
180. Olanrewaju OS, Ayangbenro AS, Glick BR, Babalola OO. Plant health: feedback effect of root exudates-rhizobiome interactions. *Appl Microbiol Biotechnol.* 2019;103(3):1155-1166. doi:10.1007/s00253-018-9556-6
181. Berendsen RL, Pieterse CMJ, Bakker PAHM. The rhizosphere microbiome and plant health. *Trends Plant Sci.* 2012;17(8):478-486. doi:10.1016/j.tplants.2012.04.001
182. Richter-Heitmann T, Eickhorst T, Knauth S, Friedrich MW, Schmidt H. Evaluation of strategies to separate root-associated microbial communities: A crucial choice in rhizobiome research. *Front Microbiol.* 2016;7:773. doi:10.3389/fmicb.2016.00773
183. Sasse J, Martinoia E, Northen T. Feed Your Friends: Do Plant Exudates Shape the Root Microbiome? *Trends Plant Sci.* 2018;23(1):25-41. doi:10.1016/j.tplants.2017.09.003
184. Poudel R, Jumpponen A, Kennelly MM, Rivard CL, Gomez-Montano L, Garrett KA. Rootstocks shape the rhizobiome: Rhizosphere and endosphere bacterial communities in the grafted tomato system. *Appl Environ Microbiol.* 2019;85(2). doi:10.1128/AEM.01765-18
185. Lundberg DS, Lebeis SL, Paredes SH, Yourstone S, Gehring J, Malfatti S, Tremblay J, Engelbrekton A, Kunin V, Rio TGD, Edgar RC, Eickhorst T, Ley RE, Hugenholtz P, Tringe SG, Dangl JL. Defining the core *Arabidopsis thaliana* root microbiome. *Nature.* 2012;488(7409):86-90. doi:10.1038/nature11237
186. Chaparro JM, Badri D V., Vivanco JM. Rhizosphere microbiome assemblage is affected by plant development. *ISME J.* 2014;8(4):790-803. doi:10.1038/ismej.2013.196
187. Schreiter S, Ding GC, Heuer H, Neumann G, Sandmann M, Grosch R, Kropf S, Smalla K. Effect of the soil type on the microbiome in the rhizosphere of field-grown lettuce. *Front Microbiol.* 2014;5:144(1-13). doi:10.3389/fmicb.2014.00144
188. Reinhold-Hurek B, Bünge W, Burbano CS, Sabale M, Hurek T. Roots Shaping Their Microbiome: Global Hotspots for Microbial Activity. *Annu Rev Phytopathol.* 2015;53:403-424. doi:10.1146/annurev-phyto-082712-102342
189. Zgadzaj R, Garrido-Oter R, Jensen DB, Koprivova A, Schulze-Lefert P, Radutoiu S. Root nodule symbiosis in *Lotus japonicus* drives the establishment of distinctive rhizosphere, root, and nodule bacterial communities. *Proc Natl Acad Sci U S A.* 2016;113(49):E7996-E8005. doi:10.1073/pnas.1616564113
190. Berendsen RL, Vismans G, Yu K, Song Y, De Jonge R, Burgman WP, Burmølle M, Herschend J, Bakker PAHM, Pieterse CMJ. Disease-induced assemblage of a plant-beneficial bacterial consortium. *ISME J.* 2018;12(6):1496-1507. doi:10.1038/s41396-018-0093-1

191. Bulgarelli D, Rott M, Schlaeppi K, Ver Loren van Themaat E, Ahmadinejad N, Assenza F, Rauf P, Huettel B, Reinhardt R, Schmelzer E, Peplies J, Gloeckner FO, Amann R, Eickhorst T, Schulze-Lefert P. Revealing structure and assembly cues for Arabidopsis root-inhabiting bacterial microbiota. *Nature*. 2012;488(7409):91-95. doi:10.1038/nature11336
192. Peiffer JA, Spor A, Koren O, Jin Z, Tringe SG, Dangl JL, Buckler ES, Ley RE. Diversity and heritability of the maize rhizosphere microbiome under field conditions. *Proc Natl Acad Sci U S A*. 2013;110(16):6548-6553. doi:10.1073/pnas.1302837110
193. Schlaeppi K, Dombrowski N, Oter RG, Ver Loren Van Themaat E, Schulze-Lefert P. Quantitative divergence of the bacterial root microbiota in Arabidopsis thaliana relatives. *Proc Natl Acad Sci U S A*. 2014;111(2):585-592. doi:10.1073/pnas.1321597111
194. Coleman-Derr D, Desgarennes D, Fonseca-Garcia C, Gross S, Clingenpeel S, Woyke T, North G, Visel A, Partida-Martinez LP, Tringe SG. Plant compartment and biogeography affect microbiome composition in cultivated and native Agave species. *New Phytol*. 2016;209(2):798-811. doi:10.1111/nph.13697
195. Kawasaki A, Donn S, Ryan PR, Mathesius U, Devilla R, Jones A, Watt M. Microbiome and exudates of the root and rhizosphere of *Brachypodium distachyon*, a model for wheat. *PLoS One*. 2016;11(10). doi:10.1371/journal.pone.0164533
196. Shi S, Nuccio E, Herman DJ, Rijkers R, Estera K, Li J, Da Rocha UN, He Z, Pett-Ridge J, Brodie EL, Zhou J, Firestone M. Successional trajectories of rhizosphere bacterial communities over consecutive seasons. *MBio*. 2015;6(4). doi:10.1128/mBio.00746-15
197. Carvalhais LC, Dennis PG, Badri D V., Kidd BN, Vivanco JM, Schenk PM. Linking Jasmonic acid signaling, root exudates, and rhizosphere microbiomes. *Mol Plant-Microbe Interact*. 2015;28(9):1049-1058. doi:10.1094/MPMI-01-15-0016-R
198. Liu H, Brettell LE. Plant Defense by VOC-Induced Microbial Priming. *Trends Plant Sci*. 2019;24(3):187-189. doi:10.1016/j.tplants.2019.01.008
199. Junker RR, Tholl D. Volatile Organic Compound Mediated Interactions at the Plant-Microbe Interface. *J Chem Ecol*. 2013;39(7):810-825. doi:10.1007/s10886-013-0325-9
200. Pérez J, Jiménez-Zurdo JI, Martínez-Abarca F, Millán V, Shimkets LJ, Muñoz-Dorado J. Rhizobial galactoglucan determines the predatory pattern of *Myxococcus xanthus* and protects *Sinorhizobium meliloti* from predation. *Environ Microbiol*. 2014;16(7):2341-2350. doi:10.1111/1462-2920.12477
201. Zhou XW, Li SG, Li W, Jiang DM, Han K, Wu ZH, Li YZ. Myxobacterial community is a predominant and highly diverse bacterial group in soil niches. *Environ Microbiol Rep*. 2014;6(1):45-56. doi:10.1111/1758-2229.12107
202. Li F, Chen L, Zhang J, Yin J, Huang S. Bacterial community structure after long-term organic and inorganic fertilization reveals important associations between soil nutrients and specific taxa involved in nutrient transformations. *Front Microbiol*. 2017;8:187. doi:10.3389/fmicb.2017.00187

203. Lin W, Lin M, Zhou H, Wu H, Li Z, Lin W. The effects of chemical and organic fertilizer usage on rhizosphere soil in tea orchards. *PLoS One*. 2019;14(5) e0217018. doi:10.1371/journal.pone.0217018
204. Lueders T, Kindler R, Miltner A, Friedrich MW, Kaestner M. Identification of bacterial micropredators distinctively active in a soil microbial food web. *Appl Environ Microbiol*. 2006;72(8):5342-5348. doi:10.1128/AEM.00400-06
205. Cui X, Zhang Y, Gao J, Peng F, Gao P. Long-term combined application of manure and chemical fertilizer sustained higher nutrient status and rhizospheric bacterial diversity in reddish paddy soil of Central South China. *Sci Rep*. 2018;8(1):16554. doi:10.1038/s41598-018-34685-0
206. Bretl DJ, Kirby JR. Molecular Mechanisms of Signaling in *Myxococcus xanthus* Development. *J Mol Biol*. 2016;428(19):3805-3830. doi:10.1016/j.jmb.2016.07.008
207. Landwehr W, Wolf C, Wink J. Actinobacteria and myxobacteria-two of the most important bacterial resources for novel antibiotics. *Curr Top Microbiol Immunol*. 2016;398:273-302. doi:10.1007/82\_2016\_503
208. Schumacher D, Sogaard-Andersen L. Regulation of Cell Polarity in Motility and Cell Division in *Myxococcus xanthus*. *Annu Rev Microbiol*. 2017;71(1):61-78. doi:10.1146/annurev-micro-102215-095415
209. Mueller MJ, Brodschelm W, Spannagl E, Zenk MH. Signaling in the elicitation process is mediated through the octadecanoid pathway leading to jasmonic acid. *Proc Natl Acad Sci U S A*. 1993;90(16):7490-7494. doi:10.1073/pnas.90.16.7490
210. Blechert S, Brodschelm W, Hölder S, Kammerer L, Kutchan TM, Mueller MJ, Xia ZQ, Zenk MH. The octadecanoic pathway: Signal molecules for the regulation of secondary pathways. *Proc Natl Acad Sci U S A*. 1995;92(10):4099-4105. doi:10.1073/pnas.92.10.4099
211. Vijayan P, Shockey J, Lévesque CA, Cook RJ, Browse J. A role for jasmonate in pathogen defense of Arabidopsis. *Proc Natl Acad Sci U S A*. 1998;95(12):7209-7214. doi:10.1073/pnas.95.12.7209
212. Livingstone PG, Morphew RM, Whitworth DE. Genome Sequencing and Pan-Genome Analysis of 23 *Coralloccoccus* spp. Strains Reveal Unexpected Diversity, With Particular Plasticity of Predatory Gene Sets. *Front Microbiol*. 2018;9. doi:10.3389/fmicb.2018.03187
213. Jung SK, Lindenmuth BE, McDonald KA, Hwang MS, Bui MQN, Falk BW, Uratsu SL, Phu ML, Dandekar AM. *Agrobacterium tumefaciens* mediated transient expression of plant cell wall-degrading enzymes in detached sunflower leaves. *Biotechnol Prog*. 2014;30(4):905-915. doi:10.1002/btpr.1888
214. Shannon P, Markiel A, Ozier O, Baliga NS, Wang JT, Ramage D, Amin N, Schwikowski BB, Ideker T. Cytoscape: A Software Environment for Integrated Models of Biomolecular Interaction Networks. *Genome Res*. 2003;13(11):2498-2504. doi:10.1101/gr.1239303

215. Forsberg EM, Huan T, Rinehart D, Benton HP, Warth B, Hilmers B, Siuzdak G. Data processing, multi-omic pathway mapping, and metabolite activity analysis using XCMS Online. *Nat Protoc.* 2018;13(4):633-651. doi:10.1038/nprot.2017.151
216. Domingo-Almenara X, Montenegro-Burke JR, Ivanisevic J, Thomas A, Sidibé J, Teav T, Guijas C, Aisporna AE, Rinehart D, Hoang L, Nordström A, Gómez-Romero M, Whiley L, Lewis MR, Nicholson JK, Benton HP, Siuzdak G. XCMS-MRM and METLIN-MRM: a cloud library and public resource for targeted analysis of small molecules. *Nat Methods.* 2018;15(9):681-684. doi:10.1038/s41592-018-0110-3
217. Patkar RN, Naqvi NI. Fungal manipulation of hormone-regulated plant defense. *PLoS Pathog.* 2017;13(6). doi:10.1371/journal.ppat.1006334
218. da Silva RR, Wang M, Nothias LF, van der Hooft JJJ, Caraballo-Rodríguez AM, Fox E, Balunas MJ, Klassen JL, Lopes NP, Dorrestein PC. Propagating annotations of molecular networks using in silico fragmentation. *PLoS Comput Biol.* 2018;14(4). doi:10.1371/journal.pcbi.1006089
219. Kaiser R, Lamparsky D. Neue inhaltsstoffe des jasminbluetenabsolues mit cyclopentangeruest. *Tetrahedron Lett.* 1974;15(38):3413-3416. doi:10.1016/S0040-4039(01)91921-5
220. Kiyota H, Yoneta Y, Oritani T. Synthesis and biological activities of methyl 3,7- and 4,5- didehydrojasmonates. *Phytochemistry.* 1997;46(6):983-986. doi:10.1016/S0031-9422(97)00374-9
221. McBride MJ, Kohler T, Zusman DR. Methylation of FrzCD, a methyl-accepting taxis protein of *Myxococcus xanthus*, is correlated with factors affecting cell behavior. *J Bacteriol.* 1992;174(13):4246-4257. doi:10.1128/jb.174.13.4246-4257.1992
222. Zhou T, Nan B. Exopolysaccharides promote *Myxococcus xanthus* social motility by inhibiting cellular reversals. *Mol Microbiol.* 2017;103(4):729-743. doi:10.1111/mmi.13585
223. Bateman A, Rawlings ND. The CHAP domain: A large family of amidases including GSP amidase and peptidoglycan hydrolases. *Trends Biochem Sci.* 2003;28(5):234-237. doi:10.1016/S0968-0004(03)00061-6
224. Becker SC, Dong S, Baker JR, Foster-Frey J, Pritchard DG, Donovan DM. LysK CHAP endopeptidase domain is required for lysis of live staphylococcal cells. *FEMS Microbiol Lett.* 2009;294(1):52-60. doi:10.1111/j.1574-6968.2009.01541.x
225. John M, Rohrig H, Schmidt J, Wieneke U, Schell J. Rhizobium NodB protein involved in nodulation signal synthesis is a chitooligosaccharide deacetylase. *Proc Natl Acad Sci U S A.* 1993;90(2):625-629. doi:10.1073/pnas.90.2.625
226. Begley TP, Downs DM, Ealick SE, McLafferty FW, Van Loon APGM, Taylor S, Campobasso N, Chiu HJ, Kinsland C, Reddick JJ, Xi J. Thiamin biosynthesis in prokaryotes. *Arch Microbiol.* 1999;171(5):293-300. doi:10.1007/s002030050713
227. Schulz H, Fabianek RA, Pelliccioli EC, Hennecke H, Thöny-Meyer L. Heme transfer to the heme chaperone CcmE during cytochrome c maturation requires the CcmC protein,



- which may function independently of the ABC-transporter CcmAB. *Proc Natl Acad Sci U S A*. 1999;96(11):6462-6467. doi:10.1073/pnas.96.11.6462
228. Leonardi R, Roach PL. Thiamine biosynthesis in *Escherichia coli*: In vitro reconstitution of the thiazole synthase activity. *J Biol Chem*. 2004;279(17):17054-17062. doi:10.1074/jbc.M312714200
229. Dunn G, Montgomery MG, Mohammed F, Coker A, Cooper JB, Robertson T, Garcia JL, Bugg TDH, Wood SP. The structure of the C-C bond hydrolase MhpC provides insights into its catalytic mechanism. *J Mol Biol*. 2005;346(1):253-265. doi:10.1016/j.jmb.2004.11.033
230. Shisler KA, Broderick JB. Glycyl radical activating enzymes: Structure, mechanism, and substrate interactions. *Arch Biochem Biophys*. 2014;546:64-71. doi:10.1016/j.abb.2014.01.020
231. Schneider R, Razungles A, Augier C, Baumes R. Monoterpenic and norisoprenoidic glycoconjugates of *Vitis vinifera* L. cv. Melon B. as precursors of odorants in Muscadet wines. *J Chromatogr A*. 2001;936(1-2):145-157. doi:10.1016/S0021-9673(01)01150-5
232. Zhang M, Liu M, Pan S, Pan C, Li Y, Tian J. Perillaldehyde controls postharvest black rot caused by *Ceratocystis fimbriata* in sweet potatoes. *Front Microbiol*. 2018;9:1102. doi:10.3389/fmicb.2018.01102
233. Muangphrom P, Misaki M, Suzuki M, Shimomura M, Suzuki H, Seki H, Muranaka T. Identification and characterization of (+)- $\alpha$ -bisabolol and 7-*epi*-silphiperfol-5-ene synthases from *Artemisia abrotanum*. *Phytochemistry*. 2019;164:144-153. doi:10.1016/j.phytochem.2019.05.010
234. Nakano C, Kudo F, Eguchi T, Ohnishi Y. Genome mining reveals two novel bacterial sesquiterpene cyclases: (-)-germacradien-4-ol and (-)-*epi*- $\alpha$ -bisabolol synthases from *Streptomyces citricolor*. *ChemBioChem*. 2011;12(15):2271-2275. doi:10.1002/cbic.201100418
235. Bustamante VH, Martínez-Flores I, Vlamakis HC, Zusman DR. Analysis of the Frz signal transduction system of *Myxococcus xanthus* shows the importance of the conserved C-terminal region of the cytoplasmic chemoreceptor FrzCD in sensing signals. *Mol Microbiol*. 2004;53(5):1501-1513. doi:10.1111/j.1365-2958.2004.04221.x
236. Goyer A. Thiamine in plants: Aspects of its metabolism and functions. *Phytochemistry*. 2010;71(14-15):1615-1624. doi:10.1016/j.phytochem.2010.06.022
237. Nagae M, Parniske M, Kawaguchi M, Takeda N. The thiamine biosynthesis gene TH11 promotes nodule growth and seed maturation. *Plant Physiol*. 2016;172(3):2033-2043. doi:10.1104/pp.16.01254
238. Nagae M, Parniske M, Kawaguchi M, Takeda N. The relationship between thiamine and two symbioses: Root nodule symbiosis and arbuscular mycorrhiza. *Plant Signal Behav*. 2016;11(12). doi:10.1080/15592324.2016.1265723

239. Buhian WP, Bensmihen S. Mini-review: nod factor regulation of phytohormone signaling and homeostasis during rhizobia-legume symbiosis. *Front Plant Sci.* 2018;9. doi:10.3389/fpls.2018.01247
240. Sharma G, Khatri I, Subramanian S. Complete Genome of the Starch-Degrading Myxobacteria *Sandaracinus amylolyticus* DSM 53668T. *Genome Biol Evol.* 2016;8(8):2520-2529. doi:10.1093/gbe/evw151
241. Sharma G, Subramanian S. Unravelling the complete genome of *Archangium gephyra* DSM 2261T and evolutionary insights into myxobacterial chitinases. *Genome Biol Evol.* 2017;9(5):1304-1311. doi:10.1093/gbe/evx066
242. Silakowski B, Pospiech A, Neumann B, Schairer HU. *Stigmatella aurantiaca* fruiting body formation is dependent on the *fbfA* gene encoding a polypeptide homologous to chitin synthases. *J Bacteriol.* 1996;178(23):6706-6713. doi:10.1128/jb.178.23.6706-6713.1996
243. De Tender C, Mesuere B, Van der Jeugt F, Haegeman A, Ruttink T, Vandecasteele B, Dawyndt P, Debode J, Kuramae EE. Peat substrate amended with chitin modulates the N-cycle, siderophore and chitinase responses in the lettuce rhizobiome. *Sci Rep.* 2019;9(1):1-11. doi:10.1038/s41598-019-46106-x
244. Atilho RM, Arachchilage GM, Greenlee EB, Knecht KM, Breaker RR. A bacterial riboswitch class for the thiamin precursor HMP-PP employs a terminator-embedded aptamer. *Elife.* 2019;8:1-19. doi:10.7554/eLife.45210
245. Melby JO, Nard NJ, Mitchell DA. Thiazole/oxazole-modified microcins: Complex natural products from ribosomal templates. *Curr Opin Chem Biol.* 2011;15(3):369-378. doi:10.1016/j.cbpa.2011.02.027
246. Adaikpoh BI, Akbar S, Albatineh H, Misra SK, Sharp JS, Stevens DC. Myxobacterial Response to Methyljasmonate Exposure Indicates Contribution to Plant Recruitment of Micropredators. *Front Microbiol.* 2020;11:34. doi:10.3389/fmicb.2020.00034
247. Lee ZH, Hirakawa T, Yamaguchi N, Ito T. The roles of plant hormones and their interactions with regulatory genes in determining meristem activity. *Int J Mol Sci.* 2019;20(16). doi:10.3390/ijms20164065
248. Gimenez-Ibanez S, Boter M, Fernández-Barbero G, Chini A, Rathjen JP, Solano R. The Bacterial Effector HopX1 Targets JAZ Transcriptional Repressors to Activate Jasmonate Signaling and Promote Infection in Arabidopsis. *PLoS Biol.* 2014;12(2). doi:10.1371/journal.pbio.1001792
249. Zhang C, Lv M, Yin W, Dong T, Chang C, Miao Y, Jia Y, Deng Y. *Xanthomonas campestris* promotes diffusible signal factor biosynthesis and pathogenicity by utilizing glucose and sucrose from host plants. *Mol Plant-Microbe Interact.* 2019;32(2):157-166. doi:10.1094/MPMI-07-18-0187-R
250. Deng Y, Liu X, Wu J, Lee J, Chen S, Cheng Y, Zhang C, Zhang LH. The host plant metabolite glucose is the precursor of diffusible signal factor (DSF) family signals in *Xanthomonas campestris*. *Appl Environ Microbiol.* 2015;81(8):2861-2868. doi:10.1128/AEM.03813-14

251. Islam T, Ghosh A. Genome-wide dissection and expression profiling of unique glyoxalase III genes in soybean reveal the differential pattern of transcriptional regulation. *Sci Rep*. 2018;8(1). doi:10.1038/s41598-018-23124-9
252. Proietti S, Falconieri GS, Bertini L, Baccelli I, Paccosi E, Belardo A, Timperio AM, Caruso C. GLYI4 Plays A Role in Methylglyoxal Detoxification and Jasmonate-Mediated Stress Responses in *Arabidopsis thaliana*. *Biomolecules*. 2019;9(10):635. doi:10.3390/biom9100635
253. Ghosh A, Kushwaha HR, Hasan MR, Pareek A, Sopory SK, Singla-Pareek SL. Presence of unique glyoxalase III proteins in plants indicates the existence of shorter route for methylglyoxal detoxification. *Sci Rep*. 2016;6(1):1-15. doi:10.1038/srep18358
254. Kilaru A, Bailey BA, Hasenstein KH. *Moniliophthora perniciosa* produces hormones and alters endogenous auxin and salicylic acid in infected cocoa leaves. *FEMS Microbiol Lett*. 2007;274(2):238-244. doi:10.1111/j.1574-6968.2007.00837.x
255. Audenaert K, De Meyer GB, Höfte MM. Abscisic Acid Determines Basal Susceptibility of Tomato to *Botrytis cinerea* and Suppresses Salicylic Acid-Dependent Signaling Mechanisms. *Plant Physiol*. 2002;128(2):491-501. doi:10.1104/pp.010605
256. Wang XM, Yang B, Ren CG, Wang HW, Wang JY, Dai CC. Involvement of abscisic acid and salicylic acid in signal cascade regulating bacterial endophyte-induced volatile oil biosynthesis in plantlets of *Atractylodes lancea*. *Physiol Plant*. 2015;153:30-42. doi:10.1111/ppl.12236
257. Buhrow LM, Cram D, Tulpan D, Foroud NA, Loewen MC. Exogenous abscisic acid and gibberellic acid elicit opposing effects on *Fusarium graminearum* infection in wheat. *Phytopathology*. 2016;106(9):986-996. doi:10.1094/PHYTO-01-16-0033-R
258. Park C, Yeo H, Park Y, Morgan A, Valan Arasu M, Al-Dhabi Naif, Park S. Influence of Indole-3-Acetic Acid and Gibberellic Acid on Phenylpropanoid Accumulation in Common Buckwheat (*Fagopyrum esculentum* Moench) Sprouts. *Molecules*. 2017;22(3):374. doi:10.3390/molecules22030374
259. Christeller JT, Galis I.  $\alpha$ -Linolenic acid concentration and not wounding per se is the keyregulator of octadecanoid (oxylipin) pathway activity in rice (*Oryza sativa* L.) leaves. *Plant Physiol Biochem*. 2014;83:117-125. doi:10.1016/j.plaphy.2014.07.013
260. Zhao L, Hu Z, Li S, Zhou X, Li J, Su X, Zhang L, Zhang Z, Dong J. Diterpenoid compounds from *Wedelia trilobata* induce resistance to Tomato spotted wilt virus via the JA signal pathway in tobacco plants. *Sci Rep*. 2019;9(1). doi:10.1038/s41598-019-39247-6
261. Herrera-Medina MJ, Steinkellner S, Vierheilig H, Ocampo Bote JA, García Garrido JM. Abscisic acid determines arbuscule development and functionality in the tomato arbuscular mycorrhiza. *New Phytol*. 2007;175(3):554-564. doi:10.1111/j.1469-8137.2007.02107.x
262. Khare E, Mishra J, Arora NK. Multifaceted interactions between endophytes and plant: Developments and Prospects. *Front Microbiol*. 2018;9:2732. doi:10.3389/fmicb.2018.02732

263. Mark GL, Dow JM, Kiely PD, Higgins H, Haynes J, Baysse C, Abbas A, Foley T, Franks A, Morrissey J, O'Gara F. Transcriptome profiling of bacterial responses to root exudates identifies genes involved in microbe-plant interactions. *Proc Natl Acad Sci U S A*. 2005;102(48):17454-17459. doi:10.1073/pnas.0506407102
264. Kravchenko LV, Azarova TS, Leonova-Erko E.I, Shaposhnikov AI, Makarova NM, I.A T. Root Exudates of Tomato Plants and Their Effect on the Growth and Antifungal Activity of *Pseudomonas* Strains. *Microbiology*. 2003;72(1):48-53.
265. Georgakopoulos DG, Henderson M, Panopoulos NJ, Schroth MN. Cloning of a Phenazine Biosynthetic Locus of *Pseudomonas Aureofaciens* PGS12 and Analysis of Its Expression In Vitro with the Ice Nucleation Reporter Gene. *Appl. Environ. Microbiol* 60.; 1994.
266. Castro-moretti FR, Gentzel IN, Mackey D, Alonso AP. Metabolomics as an emerging tool for the study of plant–pathogen interactions. *Metabolites*. 2020;10(2):1-23. doi:10.3390/metabo10020052
267. Clinical and Laboratory Standards Institute (CLSI). M07-A10 Methods for Dilution Antimicrobial Susceptibility Tests for Bacteria That Grow Aerobically; Approved Standard—Tenth Edition. *Clin Infect Dis*. 2015;35(2). doi:10.1093/cid/ciw353
268. Zaroubi L, Ozugergin I, Mastronardi K, Imfeld A, Law C, Gélinas Y, Findlay BL. The ubiquitous terpene geosmin is a warning chemical. *bioRxiv*. March 2021:2021.03.09.434661. doi:10.1101/2021.03.09.434661
269. Dickschat JS, Nawrath T, Thiel V, Kunze B, Müller R, Schulz S. Biosynthesis of the off-flavor 2-methylisoborneol by the myxobacterium *Nannocystis exedens*. *Angew Chemie - Int Ed*. 2007;46(43):8287-8290. doi:10.1002/anie.200702496

## LIST OF APPENDICES

Appendix A. Antibiotic resistant target seeker (ARTS) rendered analysis of *Archangium* sp. genome

Table A.1. Hits to fifty-three known resistance models (targets) observed in the *A.* sp. genome

<b>Model number</b>	<b>Description</b>	<b>Sequenc e id</b>	<b>E-value</b>	<b>Bitscore</b>	<b>Sequence description</b>
RF0002	AAC3	4897	8.3e-60	201.3	lcl 4897 scaffold_8 source scaffold_8 loc 225454_226231_1
RF0003	AAC3-I	1136	3.8e-18	65.4	lcl 1136 scaffold_1 source scaffold_1 loc 1397111_1397555_-1
RF0007	ABC_efflux	10136	4.1e-93	311.9	lcl 10136 scaffold_32 source scaffold_32 loc 21944_23732_-1
RF0007	ABC_efflux	8640	1.5e-92	310.1	lcl 8640 scaffold_18 source scaffold_18 loc 186091_187867_1
RF0007	ABC_efflux	8421	1.6e-89	300.0	lcl 8421 scaffold_17 source scaffold_17 loc 218484_220230_-1
RF0007	ABC_efflux	10135	2.5e-89	299.4	lcl 10135 scaffold_32 source scaffold_32 loc 20145_21948_-1
RF0007	ABC_efflux	8265	5.8e-79	265.2	lcl 8265 scaffold_17 source scaffold_17 loc 20994_22776_-1
RF0007	ABC_efflux	2398	1.1e-78	264.3	lcl 2398 scaffold_3 source scaffold_3 loc 473951_475715_1
RF0051	Chlor_Efflux_Pu mp	2032	5.2e-123	410.2	lcl 2032 scaffold_2 source scaffold_2 loc 956129_957374_-1
RF0053	ClassA	2655	1e-25	89.5	lcl 2655 scaffold_4 source scaffold_4 loc 46594_47467_1
RF0054	ClassB	7236	2.5e-55	186.8	lcl 7236 scaffold_14 source scaffold_14 loc 63399_64290_-1
RF0056	ClassD	7147	5.3e-70	234.7	lcl 7147 scaffold_13 source scaffold_13 loc 425263_426082_-1
RF0100	MexW-MexI	2286	3.3e-237	788.9	lcl 2286 scaffold_3 source scaffold_3 loc 277371_280542_1
RF0100	MexW-MexI	4218	7.5e-226	751.3	lcl 4218 scaffold_7 source scaffold_7 loc 22393_25540_1
RF0104	MFS_efflux	5591	1.4e-82	276.9	lcl 5591 scaffold_9 source scaffold_9 loc 560792_562052_1

RF0115	RND_efflux	678	0	1052.2	lcl 678 scaffold_1 source scaffold_1 loc 835389_838524_-1
RF0115	RND_efflux	5087	2.4e-296	985.1	lcl 5087 scaffold_8 source scaffold_8 loc 491488_494626_-1
RF0115	RND_efflux	2076	6.3e-296	983.7	lcl 2076 scaffold_3 source scaffold_3 loc 19926_23046_-1
RF0115	RND_efflux	5480	3.5e-285	948.1	lcl 5480 scaffold_9 source scaffold_9 loc 420172_423367_-1
RF0123	SubclassB1	5039	2.3e-13	49.1	lcl 5039 scaffold_8 source scaffold_8 loc 433919_434873_-1
RF0123	SubclassB1	9426	2.2e-12	45.9	lcl 9426 scaffold_22 source scaffold_22 loc 121275_122217_-1
RF0134	tet_MFS_efflux	6133	1.2e-76	257.3	lcl 6133 scaffold_11 source scaffold_11 loc 166200_167418_1
RF0134	tet_MFS_efflux	8750	9.2e-61	205.0	lcl 8750 scaffold_19 source scaffold_19 loc 26547_27774_-1
PF00044.19	Gp_dh_N	6107	1.7e-58	196.3	lcl 6107 scaffold_11 source scaffold_11 loc 134427_135438_-1
PF00183.13	HSP90	1157	6.4e-140	466.5	lcl 1157 scaffold_1 source scaffold_1 loc 1423589_1425563_1
PF00183.13	HSP90	3279	1.4e-07	29.8	lcl 3279 scaffold_5 source scaffold_5 loc 115301_117119_-1
PF00185.19	OTCace	4963	1.3e-49	167.5	lcl 4963 scaffold_8 source scaffold_8 loc 306156_307062_-1
PF00185.19	OTCace	8852	2.1e-37	127.9	lcl 8852 scaffold_19 source scaffold_19 loc 194254_195148_1
PF00204.20	DNA_gyraseB	7684	4.1e-60	201.4	lcl 7684 scaffold_15 source scaffold_15 loc 87858_90201_1
PF00204.20	DNA_gyraseB	9123	1.5e-46	157.1	lcl 9123 scaffold_20 source scaffold_20 loc 212075_214013_1
PF00204.20	DNA_gyraseB	2659	6.5e-10	37.9	lcl 2659 scaffold_4 source scaffold_4 loc 52736_53798_-1
PF00227.21	Proteasome	6460	3.8e-27	94.2	lcl 6460 scaffold_12 source scaffold_12 loc 49776_50304_-1
PF00364.17	Biotin_lipoyl	6338	5.3e-42	140.8	lcl 6338 scaffold_11 source scaffold_11 loc 427791_429399_-1
PF00364.17	Biotin_lipoyl	1014	7.4e-25	85.8	lcl 1014 scaffold_1 source scaffold_1 loc 1236837_1237443_-1
PF00364.17	Biotin_lipoyl	4484	5.2e-22	76.7	lcl 4484 scaffold_7 source scaffold_7 loc 359505_360780_-1
PF00364.17	Biotin_lipoyl	598	1e-20	72.6	lcl 598 scaffold_1 source scaffold_1 loc 736162_737368_-1

PF00364.17	Biotin_lipoyl	8594	4.3e-20	70.6	lcl 8594 scaffold_18 source scaffold_18 loc 120966_121476_1
PF00364.17	Biotin_lipoyl	716	1.4e-19	68.9	lcl 716 scaffold_1 source scaffold_1 loc 883432_883645_-1
PF00364.17	Biotin_lipoyl	2000	1.5e-14	52.8	lcl 2000 scaffold_2 source scaffold_2 loc 903736_905740_1
PF00521.15	DNA_topoisoIV	2361	2.9e-150	500.2	lcl 2361 scaffold_3 source scaffold_3 loc 375460_378229_-1
PF00521.15	DNA_topoisoIV	9122	1.5e-146	488.0	lcl 9122 scaffold_20 source scaffold_20 loc 209672_212063_1
PF01039.17	Carboxyl_trans	8591	1.6e-207	689.1	lcl 8591 scaffold_18 source scaffold_18 loc 117031_118594_1
PF01039.17	Carboxyl_trans	2837	4.6e-155	516.1	lcl 2837 scaffold_4 source scaffold_4 loc 240005_241535_-1
PF01039.17	Carboxyl_trans	1999	8.9e-128	426.1	lcl 1999 scaffold_2 source scaffold_2 loc 902109_903726_1
PF01039.17	Carboxyl_trans	4317	1.6e-20	72.3	lcl 4317 scaffold_7 source scaffold_7 loc 140865_141837_-1
PF01039.17	Carboxyl_trans	6209	2.8e-20	71.6	lcl 6209 scaffold_11 source scaffold_11 loc 262473_263319_-1
PF13599.1	Pentapeptide_4	7021	5.5e-27	92.8	lcl 7021 scaffold_13 source scaffold_13 loc 285217_285853_-1
PF13599.1	Pentapeptide_4	6845	3.6e-24	83.8	lcl 6845 scaffold_13 source scaffold_13 loc 83527_84259_1
PF13599.1	Pentapeptide_4	6844	3.2e-23	80.7	lcl 6844 scaffold_13 source scaffold_13 loc 82715_83447_1
PF13599.1	Pentapeptide_4	647	1.1e-16	59.8	lcl 647 scaffold_1 source scaffold_1 loc 796821_797313_1
PF13599.1	Pentapeptide_4	9621	2.2e-12	46.0	lcl 9621 scaffold_23 source scaffold_23 loc 164585_166067_-1
TIGR02013	TIGR02013	9	0	1899.3	lcl 9 scaffold_1 source scaffold_1 loc 4992_9222_1
TIGR00663	TIGR00663	7612	7.6e-99	330.2	lcl 7612 scaffold_15 source scaffold_15 loc 8198_9305_1



Table A.2. Twenty-two biosynthetic gene clusters with proximity to housekeeping (core) genes, duplicated genes and resistant models.

Cluster number	Type	Source	Location	Core hits	Other hits	Gene list
cluster-2_4	terpene	scaffold _2	369972 - 391007	1	0	[[1549, TIGR00357, 378231, 378672, Core, TIGR00357: methionine-R-sulfoxide reductase, Protein fate]]
cluster-2_5	amglyccycl	scaffold _2	767895 - 789074	1	0	[[1905, TIGR00871, 781064, 782594, Core, zwf: glucose-6-phosphate dehydrogenase, Energy metabolism]]
cluster-3_2	lanthipeptide	scaffold _3	254542 - 277791	0	1	[[2286, RF0115, 277371, 280542, ResModel, RND_efflux: resistance-nodulation-cell division (RND) antibiotic efflux pump [ARO:0010004], N/A]]
cluster-3_3	NRPS, T1PKS	scaffold _3	387410 - 488811	2	1	[[2370, TIGR00055, 388407, 389205, Core, uppS: di-trans,poly-cis-decaprenylcistransferase, Cell envelope], [2396, TIGR02349, 472091, 473222, Core, DnaJ_bact: chaperone protein DnaJ, Unclassified], [2398, RF0007, 473951, 475715, ResModel, ABC_efflux: ATP-binding cassette (ABC) antibiotic efflux pump [ARO:0010001], N/A]]
cluster-4_3	NRPS, T1PKS	scaffold _4	623926 - 726982	5	0	[[3159, TIGR01032, 715969, 716317, Core, rplT_bact: ribosomal protein bL20, Protein synthesis], [3157, TIGR00472, 712352, 714764, Core, pheT_bact: phenylalanine--tRNA ligase, beta subunit, Protein synthesis], [3158, TIGR00468, 714763, 715813, Core, pheS: phenylalanine--tRNA ligase, alpha subunit, Protein synthesis], [3160, TIGR00001, 716405, 716615, Core, rpmI_bact: ribosomal protein bL35, Protein synthesis], [3161, TIGR00418, 716881, 718810, Core, thrS: threonine--tRNA ligase, Protein synthesis]]

cluster-7_1	bacteriocin, NRPS-like	scaffold _7	225399 - 277684	1	0	[[4424, TIGR00401, 268814, 269474, Core, msrA: peptide-methionine (S)-S-oxide reductase, Protein fate]]
cluster-8_1	NRPS, T1PKS	scaffold _8	309513 - 386194	2	0	[[4989, TIGR00763, 367220, 369689, Core, lon: endopeptidase La, Protein fate], [4966, TIGR00120, 309010, 311089, Core, ArgJ: glutamate N-acetyltransferase/amino-acid acetyltransferase, Amino acid biosynthesis]]
cluster-9_2	NRPS	scaffold _9	172427 - 217062	1	0	[[5278, TIGR01023, 179289, 179454, Core, rpmG_bact: ribosomal protein bL33, Protein synthesis]]
cluster-10_1	T1PKS, NRPS	scaffold _10	18783 - 88033	1	0	[[5619, TIGR00521, 27614, 28838, Core, coaBC_dfp: phosphopantothenoylcysteine decarboxylase / phosphopantothenate--cysteine ligase, Biosynthesis of cofactors, prosthetic groups, and carriers]]
cluster-10_2	NRPS, T1PKS	scaffold _10	145995 - 236252	4	0	[[5709, GrpE, 161375, 161945, Core, PF01025.15: GrpE, Unclassified], [5704, TIGR02348, 156050, 157691, Core, GroEL: chaperonin GroL, Protein fate], [5697, TIGR00078, 145619, 146363, Core, nadC: nicotinate-nucleotide diphosphorylase (carboxylating), Biosynthesis of cofactors, prosthetic groups, and carriers], [5698, TIGR00422, 146485, 150064, Core, valS: valine-tRNA ligase, Protein synthesis]]
cluster-10_3	terpene	scaffold _10	452641 - 473652	1	0	[[5906, TIGR02082, 463822, 467338, Core, methH: methionine synthase, Amino acid biosynthesis]]
cluster-11_3	T1PKS	scaffold _11	478766 - 524055	1	0	[[6412, TIGR00416, 523524, 524886, Core, sms: DNA repair protein RadA, DNA metabolism]]
cluster-13_1	NRPS, T1PKS	scaffold _13	41163 - 93514	0	2	[[6845, PF13599.1, 83527, 84259, ResModel, Pentapeptide_4: Pentapeptide repeats (9 copies), N/A], [6844, PF13599.1, 82715,

						83447, ResModel, Pentapeptide_4: Pentapeptide repeats (9 copies), N/A]]
cluster-13_2	T3PKS	scaffold_13	276511 - 331711	0	1	[[7021, PF13599.1, 285217, 285853, ResModel, Pentapeptide_4: Pentapeptide repeats (9 copies), N/A]]
cluster-13_3	NRPS, T1PKS	scaffold_13	419025 - 486153	3	1	[[7145, TIGR00936, 422507, 423764, Core, ahcY: adenosylhomocysteinase, Energy metabolism], [7144, TIGR01034, 421182, 422364, Core, metK: methionine adenosyltransferase, Central intermediary metabolism], [7153, TIGR00753, 433976, 434870, Core, undec_PP_bacA: undecaprenyl-diphosphatase UppP, Cell envelope], [7147, RF0056, 425263, 426082, ResModel, ClassD: Class D beta-lactamases [ARO:3000075;ARO:3000017], N/A]]
cluster-16_2	NRPS-like	scaffold_16	215662 - 257939	2	0	[[8118, TIGR01430, 222598, 223759, Core, aden_deam: adenosine deaminase, Unclassified], [8140, TIGR00109, 254421, 255501, Core, hemH: ferrochelatase, Biosynthesis of cofactors, prosthetic groups, and carriers]]
cluster-17_1	NRPS, arylpolyene, T1PKS	scaffold_17	154502 - 238295	1	1	[[8427, TIGR00959, 226071, 227715, Core, ffh: signal recognition particle protein, Protein fate], [8421, RF0007, 218484, 220230, ResModel, ABC_efflux: ATP-binding cassette (ABC) antibiotic efflux pump [ARO:0010001], N/A]]
cluster-1_3	PKS-like	scaffold_1	1035610 - 1076687	1	0	[[866, TIGR02960, 1067677, 1068631, Core, SigX5: RNA polymerase sigma-70 factor, TIGR02960 family, Unclassified]]
cluster-19_1	NRPS, T1PKS	scaffold_19	95089 - 193242	3	0	[[8849, TIGR01393, 190709, 192521, Core, lepA: elongation factor 4, Unknown function], [8844, TIGR00218, 186551, 187751, Core, manA: mannose-6-phosphate isomerase, class I,

						Energy metabolism], [8850, TIGR02227, 192524, 193769, Core, sigpep_I_bact: signal peptidase I, Protein fate]]
cluster-19_2	bacteriocin	scaffold_19	241483 - 252341	1	0	[[8902, TIGR01695, 248071, 249685, Core, murJ_mviN: murein biosynthesis integral membrane protein MurJ, Cell envelope]]
cluster-21_1	terpene	scaffold_21	113333 - 134383	3	0	[[9272, TIGR01146, 130821, 131730, Core, ATPsyn_F1gamma: ATP synthase F1, gamma subunit, Energy metabolism], [9273, TIGR01039, 131845, 133291, Core, atpD: ATP synthase F1, beta subunit, Energy metabolism], [9275, TIGR01216, 133895, 134300, Core, ATP_synt_epsilon: ATP synthase F1, epsilon subunit, Energy metabolism]]
cluster-1_4	T1PKS, NRPS	scaffold_1	1116703 - 1168144	2	0	[[948, TIGR00418, 1165077, 1166274, Core, thrS: threonine--tRNA ligase, Protein synthesis], [949, TIGR01771, 1166360, 1167311, Core, L-LDH-NAD: L-lactate dehydrogenase, Energy metabolism]]

Table A.3. Thirty-six housekeeping (core) genes observed to be duplicated

Core_gene	Count	Ref_median	Ref_stdev	Ref_RSD	Ref_ubiquity	Description
TIGR00763	2.0	1.0	0.1213	0.3474	0.3526	lon: endopeptidase La
TIGR03156	2.0	1.0	0.1451	0.9579	0.9789	GTP_HflX: GTP-binding protein HflX
TIGR02350	2.0	1.0	0.5448	0.8579	1.0	prok_dnaK: chaperone protein DnaK
TIGR00009	2.0	1.0	0.5021	0.6421	0.9895	L28: ribosomal protein bL28
TIGR01035	2.0	1.0	0.1183	0.7316	0.7421	hemA: glutamyl-tRNA reductase
TIGR00392	2.0	1.0	0.1439	0.9737	0.9947	ileS: isoleucine--tRNA ligase
TIGR00396	2.0	1.0	0.0756	0.9105	0.9158	leuS_bact: leucine--tRNA ligase
GrpE	3.0	1.0	0.521	0.8368	1.0	PF01025.15: GrpE
TIGR00157	2.0	1.0	0.529	0.5737	0.8684	TIGR00157: ribosome small subunit-dependent GTPase A
TIGR02227	3.0	1.0	1.1572	0.5579	0.9789	sigpep_I_bact: signal peptidase I
TIGR00575	2.0	1.0	0.3226	0.8263	0.9368	dnlj: DNA ligase, NAD-dependent
Ribosomal_S14	2.0	1.0	0.5099	0.6105	0.9895	PF00253.17: Ribosomal protein S14p/S29e
TIGR01023	3.0	1.0	0.6482	0.5737	0.9895	rpmG_bact: ribosomal protein bL33
TIGR00382	2.0	1.0	0.125	0.9789	0.9947	clpX: ATP-dependent Clp protease, ATP-binding subunit ClpX
TIGR00630	3.0	1.0	0.2244	0.9368	0.9895	uvra: excinuclease ABC subunit A
TIGR00149	2.0	1.0	0.1324	0.2895	0.2947	TIGR00149_YjbQ: secondary thiamine-phosphate synthase enzyme
TIGR00430	2.0	1.0	0.0	0.5579	0.5579	Q_tRNA_tgt: tRNA-guanine transglycosylase
TIGR01017	2.0	1.0	0.3	0.9	1.0	rpsD_bact: ribosomal protein uS4
TIGR01417	2.0	1.0	0.4095	0.5947	0.6737	PTS_I_fam: phosphoenolpyruvate-protein phosphotransferase
TIGR00079	3.0	2.0	0.7097	0.3579	0.9421	pept_deformyl: peptide deformylase
TIGR00077	3.0	1.0	0.4968	0.7105	0.8	lspA: signal peptidase II
TIGR00401	2.0	1.0	0.2605	0.8368	0.8842	msrA: peptide-methionine (S)-S-oxide reductase
TIGR00484	3.0	1.0	0.2697	0.9211	1.0	EF-G: translation elongation factor G

TIGR03705	2.0	1.0	0.0	0.8	0.8	poly_P_kin: polyphosphate kinase 1
TIGR00431	2.0	1.0	0.0	0.9737	0.9737	TruB: tRNA pseudouridine(55) synthase
TIGR00485	2.0	1.0	0.4065	0.8316	0.9947	EF-Tu: translation elongation factor Tu
TIGR00165	2.0	1.0	0.4663	0.7421	1.0	S18: ribosomal protein bS18
TIGR01083	2.0	1.0	0.0	0.9	0.9	nth: endonuclease III
TIGR00418	2.0	1.0	0.3889	0.8316	0.9947	thrS: threonine--tRNA ligase
TIGR00057	2.0	1.0	0.6181	0.5842	0.9316	TIGR00057: tRNA threonylcarbamoyl adenosine modification protein, Sua5/YciO/YrdC/YwIC family
TIGR00936	2.0	1.0	0.456	0.6368	0.7579	ahcY: adenosylhomocysteinase
TIGR00357	3.0	1.0	0.3523	0.8579	0.9211	TIGR00357: methionine-R-sulfoxide reductase
TIGR01064	3.0	1.0	0.3924	0.8421	0.9684	pyruv_kin: pyruvate kinase
TIGR02012	2.0	1.0	0.1023	0.9842	0.9947	tigrfam_recA: protein RecA
TIGR02866	2.0	1.0	0.2503	0.4737	0.4895	CoxB: cytochrome c oxidase, subunit II
TIGR00871	3.0	1.0	0.7244	0.6526	0.9316	zwf: glucose-6-phosphate dehydrogenase

Appendix B. Links to Global Natural Products Social Molecular Networking (GNPS) jobs

1. Phytohormone exposure group in Chapter 3.3:

<http://gnps.ucsd.edu/ProteoSAFe/status.jsp?task=0e48a49876684364bb49d81758b60cc1>

2. Other exposure group in Chapter 3.3:

<http://gnps.ucsd.edu/ProteoSAFe/status.jsp?task=85a8ba2eca344aaa87d640c4825084e5>

3. Fractions run in Chapter 4:

<http://gnps.ucsd.edu/ProteoSAFe/status.jsp?task=3202c12903aa4210880cc3f971b00a67>

## Appendix C. Antimicrobial assays

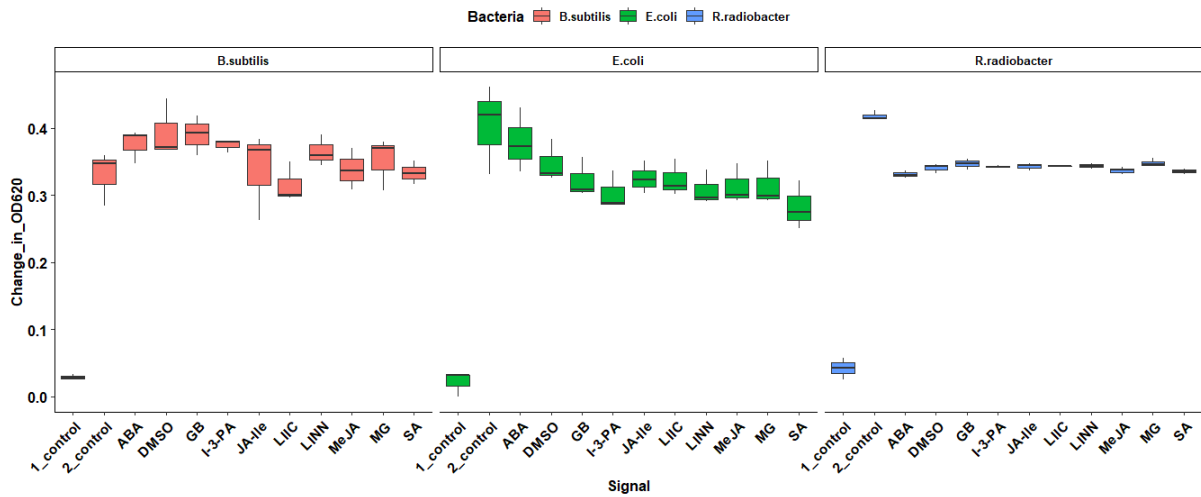


Figure C-1. Antibacterial effects of phytohormones and plant-related signals used in the study shows no growth inhibiting activities. 1\_control = media control (no bacteria) and 2\_control = bacteria control (no signal).



## VITA

### EDUCATION

**M.Sc, Pharmacognosy • September, 2015**

University College London, London, UK

**Pharm.D • May, 2009**

University of Benin, Benin city, Nigeria

### PROFESSIONAL EMPLOYMENT

**Graduate Research Assistant (2016 – 2021)**, Department of BioMolecular Sciences,  
School of Pharmacy, University of Mississippi, University, MS, USA

**Graduate teaching assistant (Fall, 2019)**, School of Pharmacy, University of  
Mississippi, University, MS, USA

- P2 modules (PHCY 502: Integrated systems – Cardiovascular, PHCY 503: Integrated systems - Respiratory, PHCY 504: Integrated systems - Renal and PHCY 505: Integrated systems – Musculoskeletal/Neuro)

**Graduate teaching assistant (Fall, 2018)**, Department of BioMolecular Sciences,  
School of Pharmacy, University of Mississippi, University, MS, USA

- PHCG 321 – Pathogenesis of Infectious Diseases

**Lecturer II (2013 – 2016)**, Department of Pharmacognosy and Traditional Medicine,  
Faculty of Pharmacy, Delta State University, Abraka, Nigeria

- Instructor of multiple assigned courses

### PUBLICATIONS

<https://www.ncbi.nlm.nih.gov/sites/myncbi/1ZunJwjuZoqAm/bibliography/48052866/public/?sortby=pubDate&sdirection=descending>

4. **Adaikpoh BI**, Dowd SE, Stevens DC (2021). Draft Genome Sequence of *Aneurinibacillus* sp. strain BA2021 isolated as a contaminant of a laboratory cultivated predatory myxobacterium. (in press) *Microbiology Resource Announcements*.
3. **Adaikpoh BI**, Akbar S, Albataineh H, Misra SK, Sharp JS and Stevens DC (2020). Myxobacterial Response to Methyljasmonate Exposure Indicates Contribution to Plant Recruitment of Micropredators. *Frontiers in Microbiology* 11:34.
2. Gregory K, Salvador LA, Akbar S, **Adaikpoh BI**, Stevens DC (2019). Survey of Biosynthetic Gene Clusters from Sequenced Myxobacteria Reveals Unexplored Biosynthetic Potential. *Microorganisms* 7(6).
1. **Adaikpoh BI**, Dowd SE, Stevens DC (2017). Draft Genome Sequence of *Archangium* sp. Strain Cb G35. *Genome Announcements* 5(8).

## AWARDS, FUNDING AND HONORS

- 2019-Present **Graduate Student Representative** – Research and Graduate Affairs committee, School of Pharmacy
- Fall, 2019 **Teaching Assistanship** – BioMolecular Sciences, School of Pharmacy, University of Mississippi
- 2019-2020 **Senator** – Graduate Student Council, University of Mississippi
- 2018 **Outstanding Graduate Student Award** – Pharmacognosy Division, BioMolecular Sciences, School of Pharmacy, University of Mississippi
- 2018 **Second Place Chemistry and Chemical Engineering Division poster Award** – Mississippi Academy of Sciences (MAS)
- 2018 **Honorable Mention INBRE Graduate Symposium** – Mississippi Academy of Sciences (MAS)
- 2018 **Second Place Pharmacy Poster Award** – Graduate School Council (GSC) Annual Research Symposium, University of Mississippi

Fall, 2018 **Teaching Assistanship** – BioMolecular Sciences, School of Pharmacy,  
University of Mississippi

2018-2019 **Treasurer** - BioMolecular Sciences Student Advocates, University o  
Mississippi

2018 **Rho Chi**

2016-Present **Research Assistantship** – BioMolecular Sciences, School of Pharmacy,  
University of Mississippi

## **PROFESSIONAL MEMBERSHIPS**

American Society for Pharmacognosy (ASP)

Rho Chi

## **PRESENTATIONS AND TALKS**

### **Poster presentations**

- Adaikpoh BI & Stevens DC “Myxobacterial Response to Methyljasmonate Exposure Indicates Contribution to Plant Recruitment of Micropredators”. Presented at the 2019 American Society for Microbiology South Central Branch Meeting, University of Mississippi, Oxford, MS, USA. **November, 2019.**
- Adaikpoh BI & Stevens DC “Myxobacterial perception and transformation of exogenous environmental quorum signals (QS)”. Presented at the 2019 American society of Pharmacognosy Annual meeting, Maddison, WI, USA. **July, 2019.**
- Adaikpoh BI & Stevens DC “Production of cryptic metabolites from predatory Archangiaceae in response to quorum sensing signal interception”. Presented at the Graduate School Council (GSC) Annual Research Symposium, University of Mississippi, Oxford, MS, USA. **March, 2018.**

- Adaikpoh BI & Stevens DC “Accessing Cryptic Space in Myxobacteria: Production of cryptic metabolites from predatory Archangiaceae in response to quorum sensing signal interception”. Presented at the Mississippi Academy of Sciences (MAS), Hattiesburg, MS, USA. **February, 2018.**

### **Podium presentations**

- Adaikpoh BI “Response of Myxobacteria to Plant-related Chemosignals suggests their Roles in the Rhizobiome”. Presented at the Graduate School Council (GSC) Annual Research Symposium, University of Mississippi, Oxford, MS, USA. **March, 2021.**
- Adaikpoh BI & Stevens DC “Myxobacterial perception, degradation and transformation of exogenous environmental quorum signals”. Presented at the 46<sup>th</sup> Annual MALTO Medicinal Chemistry & Pharmacognosy Meeting-in-Minature, University of Tennessee Health Science Center, Memphis, TN, USA. **May, 2019.**
- Adaikpoh BI & Stevens DC “Myxobacterial perception, degradation and transformation of exogenous environmental quorum signals”. Presented at the Graduate School Council (GSC) Annual Research Symposium, University of Mississippi, Oxford, MS, USA. **March, 2019.**

### **LABORATORY SKILLS**

- Bacteria Cultivation
- Antimicrobial Screening
- RNA/DNA Isolation and Quantification; PCR
- Cloning; Protein Expression and Extraction
- *In-vitro* Enzymatic Reactions
- Chromatographic Techniques including High Performance Liquid Chromatography (HPLC), Thin Layer Chromatography (TLC), Flash Silica Gel Column Chromatography

- Bruker 400 MHz and 500 MHz NMRs
- Bioinformatics Tools including antibiotics & Secondary Metabolite Analysis Shell (antiSMASH), Biosynthetic Gene Similarity Clustering and Prospecting Engine (BiG-SCAPE), Antibiotic Resistant Target Seeker (ARTS), Type (Strain) Genome Server (TYGS)
- Metabolomics Tools including Global Natural Products Social Molecular Networking (GNPS), XCMS-Multiple Reaction Monitoring, Small Molecule Accurate Recognition Technology (SMART-NMR), MZmine.
  - Statistical Computing and Data Visualization with R